

INFORMATION TO USERS

This reproduction was made from a copy of a document sent to us for microfilming. While the most advanced technology has been used to photograph and reproduce this document, the quality of the reproduction is heavily dependent upon the quality of the material submitted.

The following explanation of techniques is provided to help clarify markings or notations which may appear on this reproduction.

1. The sign or "target" for pages apparently lacking from the document photographed is "Missing Page(s)". If it was possible to obtain the missing page(s) or section, they are spliced into the film along with adjacent pages. This may have necessitated cutting through an image and duplicating adjacent pages to assure complete continuity.
2. When an image on the film is obliterated with a round black mark, it is an indication of either blurred copy because of movement during exposure, duplicate copy, or copyrighted materials that should not have been filmed. For blurred pages, a good image of the page can be found in the adjacent frame. If copyrighted materials were deleted, a target note will appear listing the pages in the adjacent frame.
3. When a map, drawing or chart, etc., is part of the material being photographed, a definite method of "sectioning" the material has been followed. It is customary to begin filming at the upper left hand corner of a large sheet and to continue from left to right in equal sections with small overlaps. If necessary, sectioning is continued again—beginning below the first row and continuing on until complete.
4. For illustrations that cannot be satisfactorily reproduced by xerographic means, photographic prints can be purchased at additional cost and inserted into your xerographic copy. These prints are available upon request from the Dissertations Customer Services Department.
5. Some pages in any document may have indistinct print. In all cases the best available copy has been filmed.

**University
Microfilms
International**

300 N. Zeeb Road
Ann Arbor, MI 48106

8401888

Anderes, Berta

INHIBITION OF THERMAL ELECTRON TRANSFER REACTIONS BY SHORT
SATURATED BARRIERS.

City University of New York

PH.D. 1983

University
Microfilms
International 300 N. Zeeb Road, Ann Arbor, MI 48106

PLEASE NOTE:

In all cases this material has been filmed in the best possible way from the available copy. Problems encountered with this document have been identified here with a check mark .

1. Glossy photographs or pages _____
2. Colored illustrations, paper or print _____
3. Photographs with dark background _____
4. Illustrations are poor copy
5. Pages with black marks, not original copy _____
6. Print shows through as there is text on both sides of page _____
7. Indistinct, broken or small print on several pages
8. Print exceeds margin requirements _____
9. Tightly bound copy with print lost in spine _____
10. Computer printout pages with indistinct print _____
11. Page(s) _____ lacking when material received, and not available from school or author.
12. Page(s) _____ seem to be missing in numbering only as text follows.
13. Two pages numbered _____. Text follows.
14. Curling and wrinkled pages _____
15. Other _____

University
Microfilms
International

Inhibition of Thermal Electron Transfer Reactions by Short Saturated Barriers

by

Berta Anderes

A dissertation submitted to the Graduate Faculty
in Chemistry in partial fulfillment of the
requirements for the degree of Doctor of Philosophy,
The City University of New York.

1983

This manuscript has been read and accepted for the Graduate Faculty in Chemistry in satisfaction of the dissertation requirement for the degree of Doctor of Philosophy.

August 25, 1983 David K. Laska
Date Chairman of the Examining Committee

30 August 83 David C. Lork
Date Executive Officer

David L. Beveridge
Harry D. Gaffney
Supervisory Committee

TABLE OF CONTENTS

	<u>Page</u>
Abstract	i
Acknowledgements	iii.
List of Tables	iv
List of Figures	v
PREFACE	1
CHAPTER 1	
A. Introduction	
1. Biological Electron Transfer Reactions	3
2. Theories of Electron Transfer Reactions	5
3. Characteristics of the Model System	13
B. Description of the Kinetics Experiments	26
C. Results and Discussion	28
CHAPTER 2	
A. Introduction	54
B. Experimental	
1. Materials	58
2. Synthesis	59
3. Kinetics of Complex Formation	109
4. Kinetics of Complex Hydrolysis	111
5. Instrumentation	112
6. Apparatus	113
C. Results and Discussion	
1. Synthesis	115
2. Formation Kinetics	117
3. Kinetics of Nitrile Hydrolysis	128
LITERATURE CITED	138

Abstract

Inhibition of Thermal Electron Transfer by Short Saturated Barriers

by

Berta Anderes

Advisor: David K. Lavalley

Numerous studies have determined the general adequacy of the theories of Marcus and Hush for rationalizing trends in rates of adiabatic outer-sphere electron transfer reactions. However, it is likely that the sizes of biological molecules often preclude the adiabatic mechanism that is typical of smaller molecules. Reactions in biological systems for which a tunneling mechanism has been discussed include photosynthesis and the conversion of oxygen to water. The latter electron transfer reactions involve a series of membrane-bound proteins, the cytochromes. The objective of this project is to try to understand how the separation of the cytochromes would affect the rate at which the electron is transferred from one site to the next. In order to study the electron transfer reactions, I synthesized model molecules which had to satisfy several criteria: 1) inert metal atoms, and 2) a rigid ligand so that the metal ions would be separated by a known distance and, 3) the reduction potentials for the reactions should be of the same order of magnitude as those of biological reactions, about 0.5V or less. One of the ligands I used was 1,4-dicyano-

[2.2.2]-bicyclooctane. This ligand is rigid, providing a well-defined separation of the metal atoms. The inert metals used were Co(III) and Ru(III). The bimetallic complexes were synthesized by mixing the ligand with a chloro complex of Co(III) in the presence of $(CF_3SO_2)_2O$ to form the corresponding Co(III)-nitrile complex, followed by a second reaction in which the Ru(III) moiety was added using $[Ru(NH_3)_5(CF_3SO_3)](CF_3SO_3)_2$. The relatively inert solvent sulfolane was used throughout. The reactions are rapid and the products stable for months. The Ru(III)-CN group does undergo acid-independent hydrolysis, but very slowly ($t_{1/2} > 5$ h at 25° C). The Ru(III) site was rapidly reduced using $Ru(NH_3)_6^{2+}$. Intramolecular reduction of Co(III) is very slow ($< 10\%$ after 10 h at 25° C). The inhibition of the electron transfer rate by the 4 \AA barrier is estimated to be at least a factor of 10^4 .

ACKNOWLEDGMENTS

I especially like to thank professor Dr. David Lavallee for his excellent direction, assistance, advice and patience throughout this project. Dr. D. Lavallee's encouragement provided incentive and satisfaction throughout the course of this work.

Appreciation is also expressed to the other members of my Ph.D. committee, Dr. Harry Gafney and Dr. David Beveridge. I wish to thank two undergraduates for their help, Cathy Magliozzo and Sally Collins.

Finally, I would like to thank my mother for her continuing love and encouragement throughout my studies.

LIST OF TABLES

<u>Table</u>	<u>Page</u>
I Rate Constants for Formation of Complexes From $[\text{Ru}(\text{NH}_3)_5(\text{CF}_3\text{SO}_3)](\text{CF}_3\text{SO}_3)_2$ in Sulfolane.	124
II Kinetic Results for the Acid Hydrolysis of Organonitrile Complexes of Ru(III) in 0.005 M Aqueous Trifluoro- methanesulfonic Acid.	134
III Absorption Maxima and Extinction Coefficients for Amido Complexes of Pentaammineruthenium(III).	135
IV Kinetic Results for Acid Hydrolysis of $[\text{Ru}(\text{NH}_3)_5\text{NCCH}_3]^{3+}$ at Various Acid Concentrations and Ionic Strengths.	136
V Activation Parameters for the Acid Hydrolysis of Pentaammineruthenium(III) Organonitrile Complexes.	137

LIST OF FIGURES

<u>Figure</u>		<u>Page</u>
1	The differential pulse polarogram of 1,4-dicyano-[2.2.2]-bicyclooctanepentaamineruthenium(III)trifluoromethanesulfonate.	17
2	The differential pulse polarogram of μ -1,4-dicyano-[2.2.2]-bicyclooctane-bis(pentaamineruthenium(III) trifluoromethanesulfonate).	19
3	The cyclic voltammograms of 1,4-dicyano-[2.2.2]-bicyclooctanepentaamineruthenium(III)trifluoromethanesulfonate at various scan rates.	21
4	The cyclic voltammograms of μ -1,4-dicyano-[2.2.2]-bicyclooctanebis(pentaamineruthenium(III))trifluoromethanesulfonate at various scan rates.	23
5	Structures of diended steroids.	30
6	A plot of absorbance data (as 1/concentration) vs. time for the reaction of 1-cyanoadamantylpentaamineruthenium(II) with diaquotriamminecobalt(III) in aqueous trifluoromethanesulfonic acid solution.	43
7	Cyclic voltammograms of μ -1,4-dicyano-[2.2.2]-pentaamineruthenium(III) aquotetraamminecobalt(III) before and after the addition of pentaamineruthenium(II).	45
8	The visible absorption spectrum of trifluoromethanesulfonato-pentaamineruthenium(III)trifluoromethanesulfonate in sulfolane.	67

<u>Figure</u>		<u>Page</u>
9	The cyclic voltammogram of 1-cyanoadamantylpentaamine-ruthenium(III)trifluoromethanesulfonate.	70
10	The visible absorption spectrum of 1-cyanoadamantyl-pentaamineruthenium(III)trifluoromethanesulfonate.	73
11	The visible absorption spectrum of the supernatant liquid in the synthesis of 1-adamantylcarbonitrilopentaamine-ruthenium(III)trifluoromethanesulfonate.	75
12	The infrared spectrum of 1-adamantylcarbonitrilopentaamine-ruthenium(III)trifluoromethanesulfonate in a KBr pellet, from 4000 to 1800 cm^{-1} .	77
13	The infrared spectrum of 1-adamantylcarbonitrilopentaamine-ruthenium(III)trifluoromethanesulfonate in a KBr pellet, from 1800 to 400 cm^{-1} .	77
14	The cyclic voltammogram of μ -1,4-dicyano- [2.2.2] - bicyclooctane-pentaamineruthenium(III)diaquotriamine-cobalt(III)trifluoromethanesulfonate.	83
15	The cyclic voltammogram of μ -1,4- dicyano-[2.2.2] - bicyclooctanepentaamineruthenium(III) aquotetraamine-cobalt(III)trifluoromethanesulfonate.	85
16	The visible absorption spectrum of 1,4-dicyano- [2.2.2] - bicyclooctanediaquotriaminecobalt(III)trifluoromethane-sulfonate.	87
17	The infrared spectrum of 1,4-dicyano- [2.2.2] -bicyclo-octanediaquotriaminecobalt(III)trifluoromethanesulfonate from 4000 to 1800 cm^{-1} .	91.

<u>Figure</u>		<u>Page</u>
18	The infrared spectrum of 1,4-dicyano- [2.2.2] -bicyclo-octanediaquotriamminecobalt(III)trifluoromethanesulfonate from 1800 to 400 cm^{-1} .	93
19	The visible absorption spectrum of 1,4-dicyano- [2.2.2] -bicyclooctaneaquotetraamminecobalt(III)trifluoromethanesulfonate.	97
20	The visible absorption spectrum of μ -1,4-dicyano- [2.2.2] -bicyclooctane-bis(pentaammineruthenium(III))trifluoromethanesulfonate.	102
21	The infrared spectrum of μ -1,4-dicyano- [2.2.2] -bicyclooctane-bis(pentaammineruthenium(III))trifluoromethanesulfonate from 4000 to 1900 cm^{-1} .	104
22	The infrared spectrum of 1,4-dicyano- [2.2.2] -bicyclooctane-bis(pentaammineruthenium(III))trifluoromethanesulfonate from 1300 to 400 cm^{-1} .	106
23	The cyclic voltammogram of 1,4-dicyano-[2.2.2] -bicyclooctane-bis(pentaammineruthenium(III))trifluoromethanesulfonate.	108
24a	The fit for a typical kinetics run for the formation of acetonitrilopentaammineruthenium(III) from trifluoromethanesulfonatopentaammineruthenium(III) and acetonitrile.	119
24b	A table of parameters generated by the PROPHEET computing system for the fit of kinetics data.	121
25	A plot of the observed first-order rate constants for the formation of 1-adamantylcarbonitrilopentaammineruthenium(III) trifluoromethanesulfonate as a function of temperature.	123

Figure

Page

- 26 A typical plot of absorbance vs. time for the acid hydrolysis reaction of acetonitrilopentammineruthenium(III) trifluoromethanesulfonate.

PREFACE

The main objective of this project has been to learn how the rate of electron transfer between donor and acceptor sites is affected by their separation distance. Numerous studies have tested current theories of electron transfer reactions which occur between metal complexes that are free to approach each other in solution. These theories have been shown to give consistent predictions of trends in the rates of such adiabatic outer-sphere reactions which occur when the nature of the metal atom, ligands and the solvent environment are varied.

Relatively few results are available, however, which bear on the question of the change in rate as the metal atoms are separated. Current theories of such reactions center on the role of electron tunneling as a possible mechanism. While theoreticians are generally agreed that the functional form of the relationship between distance and rate will be an inverse exponential one, there were no rate data available for thermal electron transfer reactions between isolated metal ions before this project was undertaken.

The effect of separation of metal ions on electron transfer reactions is of importance with respect to biological processes involving metallo-proteins. It is likely that steric restrictions of biological molecules may preclude the adiabatic mechanism that is typical of smaller molecules. In order to understand which properties of molecules such as the cytochromes determine their electron transfer rates, the variables such as the nature of the ligands around the metal, the medium between the donor and acceptor sites, and the distance between the sites must be separately investigated.

To determine the effect of distance, in this project complexes were synthesized which would fulfill several criteria: The metal atoms are inert so that the ligands around the metal atom are known with certainty and the ligand which binds the two metal atoms must be rigid to give a well-defined separation distance and saturated to isolate the donor and acceptor orbitals. These criteria had not been met by any previously-reported studies.

In this thesis, the first chapter begins with a discussion of the significance of this project, other studies which have been done and theories of electron transfer. My experiments and results are then described and compared with theoretical predictions. In order to obtain these results, new synthetic techniques had to be developed and the formation and decomposition rates for the complexes had to be determined. These studies were crucial in order to establish the effect of the saturated barrier, but they were also of interest in their own right. As a result, these aspects are discussed in the second chapter, separately from the electron transfer reactions.

CHAPTER 1

A. Introduction

1. Discussion of Biological Electron Transfer Reactions

A question of current interest is: How far apart can the donor and the acceptor in an electron transfer reaction be and what other special requirements are there for electron transfer to occur? There is a lot of interest in the role that tunneling may play in electron transfer reactions in biological systems. (1,2,3). There are a number of cases in which the distances between oxidant and reductant sites in biological systems are likely to be large (close to or greater than 10 \AA). The actual distances between the prosthetic groups of interacting electron transfer proteins in biological systems proposed to date vary from 8 to 50 \AA . By using first-approximation estimates of tunneling probabilities, tunneling distances have been estimated to be tens of \AA . Hopfield (3), however, taking into account interactions due to nuclear motion, and estimating probabilities from bond-resonance integrals, declares the distance must be less than 10 \AA . James Chien has shown good correlation to the Hopfield theory prediction of electron tunneling with a series of cytochrome c metal derivatives, where he estimates the distance of interaction to be 4 \AA (4). Miller (5) has studied the tunneling of trapped electrons to scavenger ions in cold, organic glasses. He estimates distances in the range of 30 to 50 \AA . Mary Vanderkooa (6) performed a fluorescence experiment derivatives of cytochromes c to study the distances predicted in the cytochrome c-cytochrome oxidase redox pair using tin and applying Forster theory. She estimated the distance of interaction to be between 20 - 40 \AA . The tunneling of electron through planar sandwiches of metal-insulator-metal has been measured out to 100 \AA (7,8). On the other hand, the measurements

of Weissman (9) and of Voevodski and others (10) indicate that the electron exchange rate between anionic benzene rings falls below 10 sec^{-1} if the distance is more than 3 to 5 Å.

In many of the biological systems the reductant is either so large or so well fixed in position that direct collision of coordination spheres of the metal atoms or channelling through a cleft to reach the oxidant and reductant sites in electron transfer proteins is often sufficiently large to preclude the inner-sphere model of electron transfer, in which one ligand is simultaneously bound to both the oxidant and reductant sites at the instant of electron transfer. Instead the electron must pass from one molecule to another without the aid of a direct "bridge" by what is called an outer-sphere mechanism (11, 12). In this project we are trying to understand what properties of the cytochromes affect the rate at which the electron is transferred from one site to the next. We are trying to learn about how this rate is related to the geometric arrangements of metal ions. The object is to determine how the cytochromes are bound to the membrane with respect to one another and whether or not any conformational changes of the protein might be required. Electron transfer reactions involving metalloproteins are essential to biological energy transfer processes such as oxidative phosphorylation and photosynthesis. Well designed model systems for the testing of alternative theories are an important component in developing reasonable mechanism for these reactions. We have used a model system to deduce fundamental information about electron transfer reactions. Our system involving intramolecular electron transfer reactions that occur between portions of the same molecules (such as the 2(4Fe-4S)ferredoxins and cytochrome c oxidase), those which form long-lived complexes that undergo electron transfer internally (some

hydrogenases and nitrogenase), and membrane-bound proteins such as those involved in mitochondrial oxidative phosphorylation.

In the next section theories of electron transfer reactions which are relevant to my studies of electron transfer reactions will be discussed.

2. Theories of Electron Transfer

Sutin and coworkers have applied Marcus theory for predicting the rates for outer-sphere electron transfer reactions in which the coordination sphere about the oxidant and reductant metal atoms remain intact during electron transfer, with no single ligand acting as a bridge. Outer-sphere electron transfer reactions for simple inorganic systems are now well understood in terms of theory of Marcus and Hush (13,14,15,16). In such reactions, the electron is transferred adiabatically by means of a molecular orbital of the donor-acceptor complex. The matrix element of electron exchange which mixes the donor and acceptor wave functions can be estimated theoretically and can sometimes be determined from the energy of optical electron transfer (17,16). Such outer-sphere electron transfer reactions of moderate driving force have rates determined by: 1) the inner-sphere reorganization energy, such as the Franck-Condon barrier, which tends to be larger the greater the structural change for each reactant as it is converted to product, 2) the outer-sphere reorganization energy, which for charged complexes consists chiefly of the changes in electrostatic interactions of solutes and solvents in the formation of the activated complex, 3) the work term for bringing the reactants together and separating the products of the activated complex, 4) the effect of the driving force itself, which is predicted to be a linear free energy relationship giving a slope of 0.5 for a plot of ΔG^\ddagger vs. ΔG_o .

Theory then predicts the following dependence for the rate constant:

$$k = \kappa \frac{k_B T}{h} \frac{Q^\ddagger}{iQ_i} e^{-E_a/RT} \quad (1)$$

where κ is a thermally averaged transmission factor being equal to one for purely adiabatic behavior, Q_i are the partition functions, and E_a is the activation energy. By converting equation (1) in terms of free energy this expression becomes:

$$k = \frac{k_B T}{h} e^{-\Delta G^\ddagger / RT} \quad (2)$$

Marcus type behavior now appears in terms of ΔG^\ddagger .

$$\Delta G^\ddagger = \Delta G_{\text{trans}}^\ddagger + \Delta G_{\text{in}}^\ddagger + \Delta G_{\text{out}}^\ddagger + w_r + G_0/2 \quad (3)$$

where $\Delta G_{\text{trans}}^\ddagger$ is the free energy of formation of the transition state:

$$\Delta G_{\text{trans}}^\ddagger = -RT \ln(hZ/k_B T) \quad (4)$$

where Z is the collision frequency. For a series with very similar inner-sphere reorganization energies the ratio of rates due to different outer-sphere reorganization energies as a function of distance can be determined from G values given by:

$$\Delta G_0 = m^2 \lambda = \frac{1}{4} |Z|^2 e^2 \left[\frac{1}{2r_1} + \frac{1}{2r_2} + \frac{1}{r^\ddagger} \right] \left[\frac{1}{\epsilon_{\text{op}}} + \frac{1}{\epsilon} \right] \quad (5)$$

where m measures the extent to which the electron is transferred from the reductant in the activated complex, λ is the outer-sphere reorganization term, ΔZ is the number of electrons transferred in the overall reaction, e is the electronic charge, r_1 and r_2 are the radii of each reactant and $r^\ddagger = r_1 + r_2$ is the radius of the activated complex. ϵ_{op} is the optical dielectric and ϵ is the static dielectric. In addition, there will be some

variation in the coulombic work term that will depend on ionic strength (Reynolds, 1966):

$$\Delta G_o = 4.22 Z_1 Z_2 (10^{-1.43 r^\ddagger \mu}) / r^\ddagger \quad (6)$$

This term also leads to a rate increase with increasing size (assuming strong coupling) if the reactants are each positively charged.

The term ΔG_{in}^\ddagger in equation (3) is the reorganization energy of the inner coordination shell as shown in equation (7).

$$\Delta G_{in}^\ddagger = 3 f_1 f_2 (a_1 - a_2)^2 / (f_1 + f_2) \quad (7)$$

where a_1 , and a_2 are radii of the two reactants with f_1 and f_2 the reactants force constants.

The w_r in equation (3) is the work required to bring the reactants together, being calculated by Debye-Huckel treatment:

$$w_r = q_1 q_2 / D_s d (1 - \beta d \sqrt{\mu}) \quad (8)$$

$$\text{where: } \beta = (8 \pi \mu^2 e^2 / 1000 D_s RT)^{1/2} \quad (9)$$

There are extensive compilation of kinetic studies of electron transfer reactions which have been discussed in terms of the Marcus theory for adiabatic electron transfer (18,19,20,11,21). But few experiments bear directly on the question of the effect of insulating (saturated) barriers. Comparison of electron transfer rates of electron transfer for a pair of small complexes such as $\text{Fe}(\text{H}_2\text{O})_6^{2+}$ and $\text{Fe}(\text{H}_2\text{O})_6^{3+}$ with a pair of complexes which is larger due to unsaturated ligands such as $\text{Fe}(\text{phen})_3^{2+}$ and $\text{Fe}(\text{phen})_3^{3+}$

(where phen=1,10-phenanthroline) have been made. With unsaturated ligands such as phenanthroline, the orbitals involved in electron transfer are significantly delocalized from the metal center onto the ligand; significant overlap is attained and tunneling is unnecessary. In these cases, the experimental results are those expected based only on the electrostatic terms of Marcus' theory. If, however, a saturated ligand sphere is involved, the orbitals involved in electron transfer will remain localized on the metal. Then as the size of the sphere increases, so will the distance between donor and acceptor orbitals and at some point adiabatic electron transfer will become unfavorable relative to a tunneling process.

The theoretical model of Hopfield's rate equation is based on electron transfer between two sites in a fixed geometry. The electron to be transferred is initially in a wave function a , eventually to be transferred to site b in b . The matrix element, T_{ab} , represents the Hamiltonian of these two, one-particle states resulting from the overlap between these wave functions. The closer together sites a and b are, the greater the orbital overlap and the larger T_{ab} will be.

According to Hopfield's theory, electron transfer occurs by a process analogous to the Forster mechanism of resonance energy transfer (3). For transfer of an electron, from site a to b the rate is given by (10):

$$k_{ab}^{\mu} = \frac{2\pi}{\hbar} |T_{ab}(r)| \int_{-\infty}^{\infty} D_a(E) D_b(E) dE \quad (10)$$

with T_{ab} a function of the distance, r , of separation between sites a and b .

The term $D_a(E)$ and $D_b(E)$ are the electron removal and electron insertion spectral distribution functions, respectively, which are Gaussian line shape functions that derive their form from vibronic components of the wave functions.

Hopfield derived an explicit form for $D_a(E)$ and $D_b(E)$ assuming that the curvature of the wave functions (k_a and k_b) were the same either with or without the electron:

$$k_{ab} = (2\pi / h) |T_{ab}(r)|^2 (2\pi h)^{\frac{1}{2}} e^{-\frac{(E_a - E_b - \Delta)^2}{2\sigma^2}} \quad (11)$$

$$\text{where: } \sigma^2 = (k_a q_a^2 / 2) k_B T \coth(T_a / 2T) + (k_b q_b^2 / 2) k_B T \coth(T_b / 2T) \quad (12)$$

$$\text{and } \Delta = k_a q_a^2 / 2 + k_b q_b^2 / 2 \quad (13)$$

with q_a and q_b being the nuclear coordinates and k_B is the Boltzmann constant. The vibronic coupling parameter is defined by Δ , and T is the temperature in degrees Kelvin, with $k_B T_a$ ($k_B T_b$) being the energy separation between nuclear harmonic oscillator states for site a(b). From this theory, the activation energy should have the common Arrhenius dependence on temperature at high temperatures and should become temperature independent at low temperatures. At high temperature this rate becomes:

$$k_{ab} = (2\pi / h) |T_{ab}(r)|^2 (4\pi k_B T \Delta)^{-\frac{1}{2}} e^{-\frac{(E_a - E_b - \Delta)^2}{4k_B T}} \quad (14)$$

In such a treatment, the electron transfer occurs from one vibronic state of a to another state of b, the vibrational form being that of a harmonic oscillator. The vibrational potential energy, $\frac{1}{2}kq^2$, relates k and q as the force constant and displacement from equilibrium nuclear position, respectively. The tunneling matrix element is further approximated by:

$$T_{ab} = 2.7 e^{-0.72 r} \quad (15)$$

which is the resonance integral for carbon atoms, each in an aromatic

molecule, with $(N_a N_b)^{-1/2}$ being a normalization factor of N_a and N_b atoms in contact through one "edge". The separation between edge atoms is then r .

According to Hopfield's theory, in the high temperature region T_{ab} should decrease exponentially as the oxidant-reductant separation increases. For similar systems, the exponential distance dependence suggested by Jortner, et al. (23).

$$d \ln T_{ab} / dr = 1.3 \text{ \AA}^{-1} \quad (16)$$

For metal atoms connected by a saturated ligand system, the barrier is expected to be about one half the $\sigma \rightarrow \sigma^*$ band gap for an organic insulator, about 3eV, giving a sharper decline in T_{ab} with R . At this time direct calculations for T_{ab} are difficult because they are determined by the behavior of the "tails" of the molecular wavefunction (24). Experimentally determined values, therefore, are essential in establishing typical exponential factors for saturated barriers.

Previously, most correlations have been based solely on theoretical calculations. James Chien just recently completed an electron transfer study involving biological molecules in solution (4). In this treatment, experimentally obtained kinetic data were found to be in good agreement with the theoretical rate constants predicted by Hopfield theory. By using metal substituted hemoproteins, the oxidoreductions of an iron heme and a metal substituted heme were followed. Treatment of such a system was extended to describe bimolecular electron transfer in solution. The rate of transfer is calculated by averaging the rate as a function of distance over probability distribution of geometries, where the relative location of donor and acceptor varies with time. Neglecting a particular

geometry for electron transfer, the bimolecular rate becomes (17):

$$k_{ab}^b = 6.023 \times 10^{-4} k_{ab}^u (2 \pi \lambda^3 r / R p) \quad (17)$$

$$\text{and } \Delta H^\ddagger = (E_a + E_b - \Delta)^2 / 4 - 3RT / 2 \quad (18)$$

$$\Delta S^\ddagger = R \ln[(0.0238/k_B T) (2\pi\lambda^3 r / R p) + (1 + 4k_B T)^{\frac{1}{2}} T_{ab}] - 3R/2 \quad (19)$$

The tunneling theory of Jortner takes into account low-frequency phonon modes as well as high-frequency molecular vibrational modes. In the high temperature region, his results match those of Hopfield's theory while at low temperatures, Jortner's development yields results closer to those observed experimentally for light-induced oxidation of cytochrome in Chromatium (23). From the temperature at which low-temperature behavior is observed in the Chromatium experiments, we do not expect to reach the low-temperature region in our reactions in common liquid solvents. The lower limit to the intramolecular electron transfer rate which can be measured in homogeneous solution is the rate at which intermolecular electron transfer becomes predominant. From a consideration of the statistics of molecular packing in liquids (25) and the dependence of the work term for bringing charged reactants together in solution (which is avoided preassembly of the reactants for an intramolecular reaction), one can calculate the concentration factor that would be equivalent for comparison of intermolecular and intramolecular rates. For complexes the size of Ru(III), Ru(II) and Co(III) amines, this factor is about 3M. Thus, if two species of charge 2+ and 3+ at a concentration of $1.0 \times 10^{-3} M$ react with a half-life of, for example, 3000 seconds, the same two reactants placed adjacent to one another in a preassembled bimetallic complex should react with a half-life of about

1 second (all calculations for complexes in H₂O at 25° with I=0.10M). Thus, an intramolecular reaction will have a measureably competitive rate even if there is a substantial barrier to electron transfer in the preassembled bimetallic complex. The ability to set a limit on the barrier depends on slowing the intramolecular process by dilution (the intramolecular rate being concentration independent).

In order to be able to use these theories of electron transfer for comparison, my model system must satisfy several criteria which I will discuss in the next section.

3. Characteristics of the Model System

The system chosen for this investigation had to meet the following criteria in order to obtain interpretable information that is relevant to the biological reactions:

a. The ligand system must be saturated, rigid, and bind two metal atoms at a well defined distance. This distance must be synthetically variable. Saturation guarantees localization of donor-acceptor orbitals on the metal atoms. The rigidity requirement prevents the two metal-containing portions of the molecule from approaching each other.

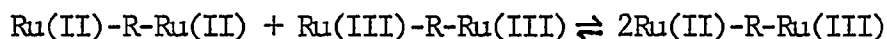
b. The metal atoms must be substitution inert so that only an outer-sphere electron transfer is possible.

c. To allow sufficient time for synthesis and characterization of the reactant complex, it is necessary that the complex not undergo electron transfer until the reaction can be initiated and properly monitored. In order to meet this requirement; there must be a method of initially reducing the site which is thermodynamically less stable in the reduced state.

The system so chosen to meet these requirements are composed of a reducing center, a difunctional saturated ring system and oxidizing center. For this specific project, we have used $(\text{NH}_3)_5\text{Ru}^{2+}$ as the reducing center. The bifunctional ligands used were 1,4-dicyano-(2.2.2)-bicyclooctane and trans-1,4 dicyanocyclohexane and $(\text{NH}_3)_n(\text{H}_2\text{O})_{5-n}\text{Co}^{3+}$ as the oxidizing center.

In order to demonstrate that the ligands which we chose do prevent substantial mixing of the donor and acceptor orbitals, I synthesized

complexes of 1,4-dicyano-[2.2.2]-bicyclooctane with only one pentaammine-ruthenium(III) moiety attached and with two pentaammineruthenium(III) moieties bound. Richardson and Taube have shown that the extent of mixing of the ruthenium orbitals at either end of a complex can be determined using differential pulse polarography and cyclic voltammetry. These methods provide an accurate means of assessing the value of the comproportionation constant K_C , which is the equilibrium constant for the reaction:



If there is no mixing, which would stabilize the mixed valence state species, the comproportionation constant has a value of 4. If there is mixing of the donor-acceptor orbitals, the full width at half-height of the peak in the differential pulse polarogram will be greater for the bimetallic complex than for the corresponding monometallic complex (the increase in width is 36mV for $K_C = 4$ and a greater value for $K_C > 4$). In the case of the two complexes of 1,4-dicyano-2.2.2-bicyclooctane, the width increase (Figures 1 and 2) is $15 \pm 20\text{mV}$, consistent with a K_C of 4 and no mixing. In the cyclic voltammetry of mixed valence species, the slope is less for a bimetallic species with mixing than for the corresponding monometallic species. If the mixing is great ($K_C > 120\text{mV}$) two peaks are actually observed. In the case of the mono(pentaammineruthenium(III)) and bis(pentaammineruthenium(III)) complexes of 1,4-dicyano-[2.2.2]-bicyclooctane, as shown in figures 3 and 4, and there is no discernable differences in slope. In both of these complexes, the cyclic voltammograms

show that the redox processes are reversible and they show the correct dependence on scan rate. Thus, our model satisfies criterion(a).

Figure 1. The differential pulse polarogram of 1,4-dicyano-[2.2.2]-bicyclooctanepentaamineruthenium(III) trifluoromethanesulfonate taken in dimethylformamide with 0.10M tetraethylammonium perchlorate using a platinum coil working electrode, Ag/AgCl reference electrode and a platinum wire auxiliary electrode. The pulse width and scan rate were 25mV and 2mV/sec, respectively. The full width at half height is 107mV.

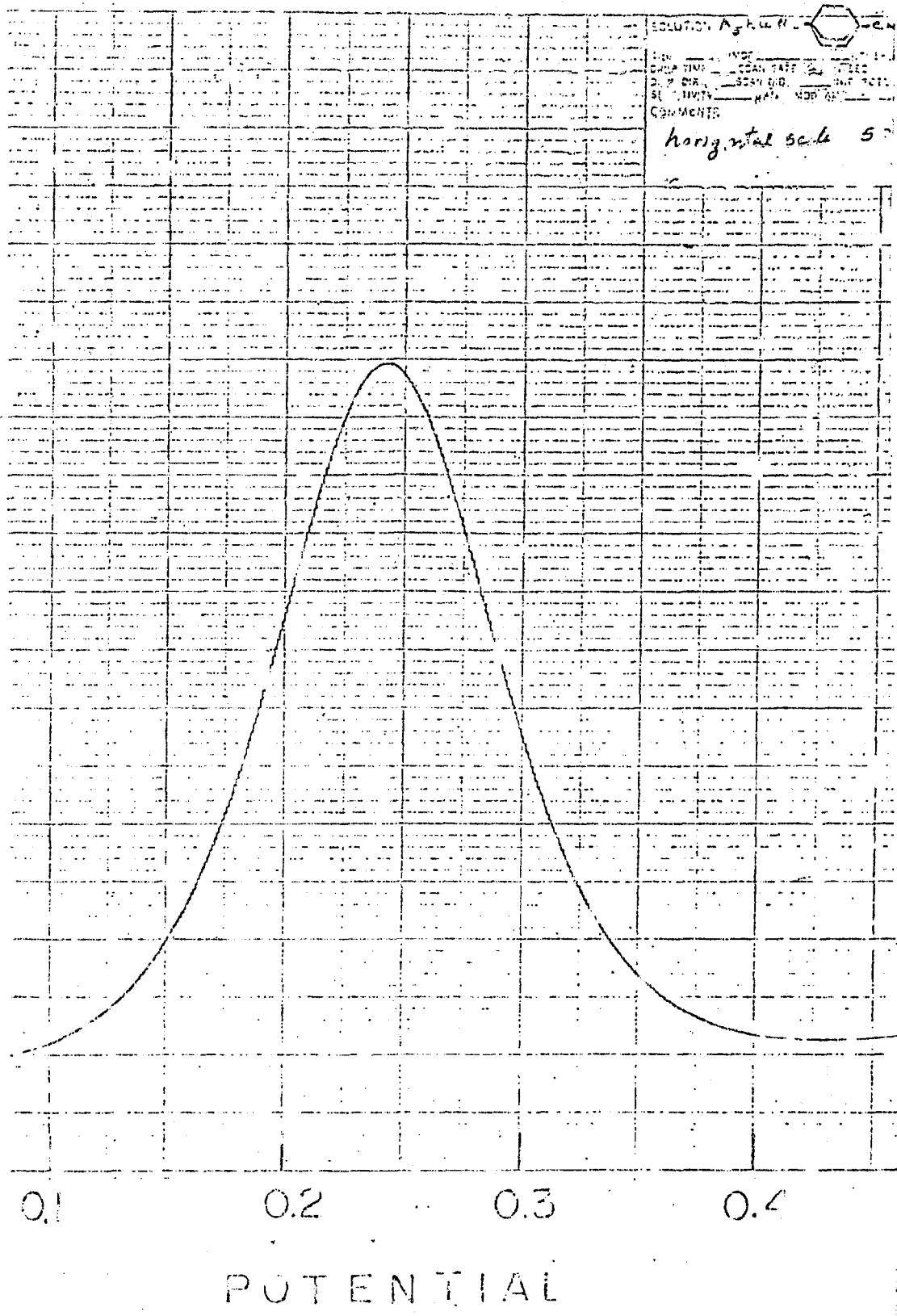
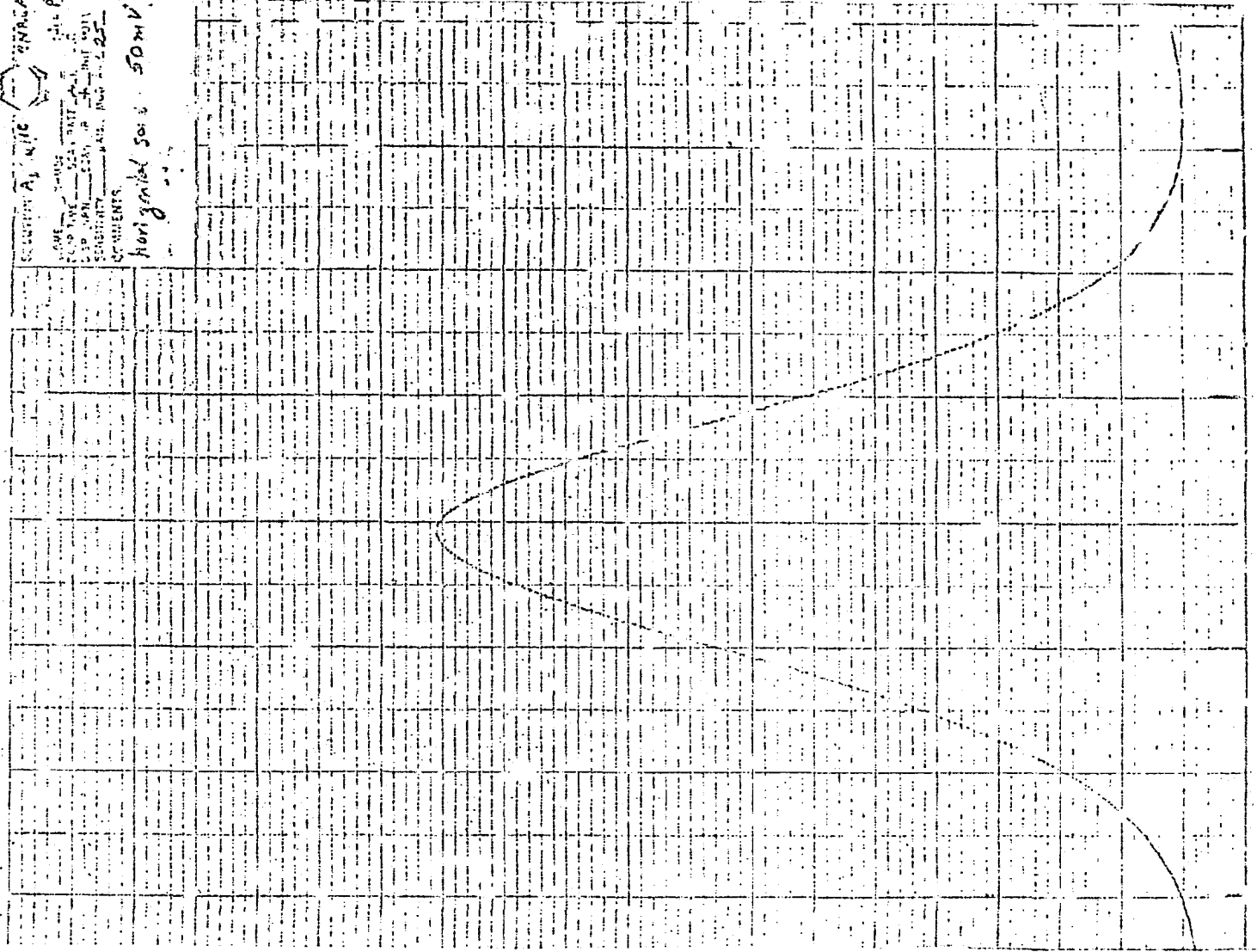


Figure 2. The differential pulse polarogram of μ -1,4-dicyano-[2.2.2]-bicyclooctane-bis (pentaammineruthenium(III)trifluoromethanesulfonate taken in dimethylformamide with 0.10M tetraethylammonium perchlorate using a platinum coil working electrode, Ag/AgCl reference electrode and platinum wire auxiliary electrode. The pulse width and scan rate were 25mV and 2mV/sec, respectively. The full width of half height is 112mV. The full width at half weight for 1-cyanoadamantylpentaammineruthenium(III) is 105mV and the full width at half height for the polarogram of cyanobenzylpentaammineruthenium(III) is 97mV.

SOLUTION $AgNO_3$ 0.1M
SOME 2-USE
200 TIVE 200 TIVE
500 1000 2000 4000 8000 16000 32000
SENSITIVITY 1000 2000 4000 8000 16000 32000
COMMENTS
Horizontal Scale 50 mV



0.1 0.2 0.3 0.4

POTENTIAL

Figure 3. The cyclic voltammograms of 1,4-dicyano- [2:2.2] - bicyclooctanepentaammineruthenium(III)trifluoromethanesulfonate at various scan rates (1, 250mV/sec; 2, 200mV/sec; 3, 150mV/sec; 4, 100mV/sec and 5, 50mV/sec); taken in dimethylformamide with 0.10M tetraethylammonium perchlorate. The working and reference electrode were platinum wires and the reference electrode was Ag/AgCl.

21

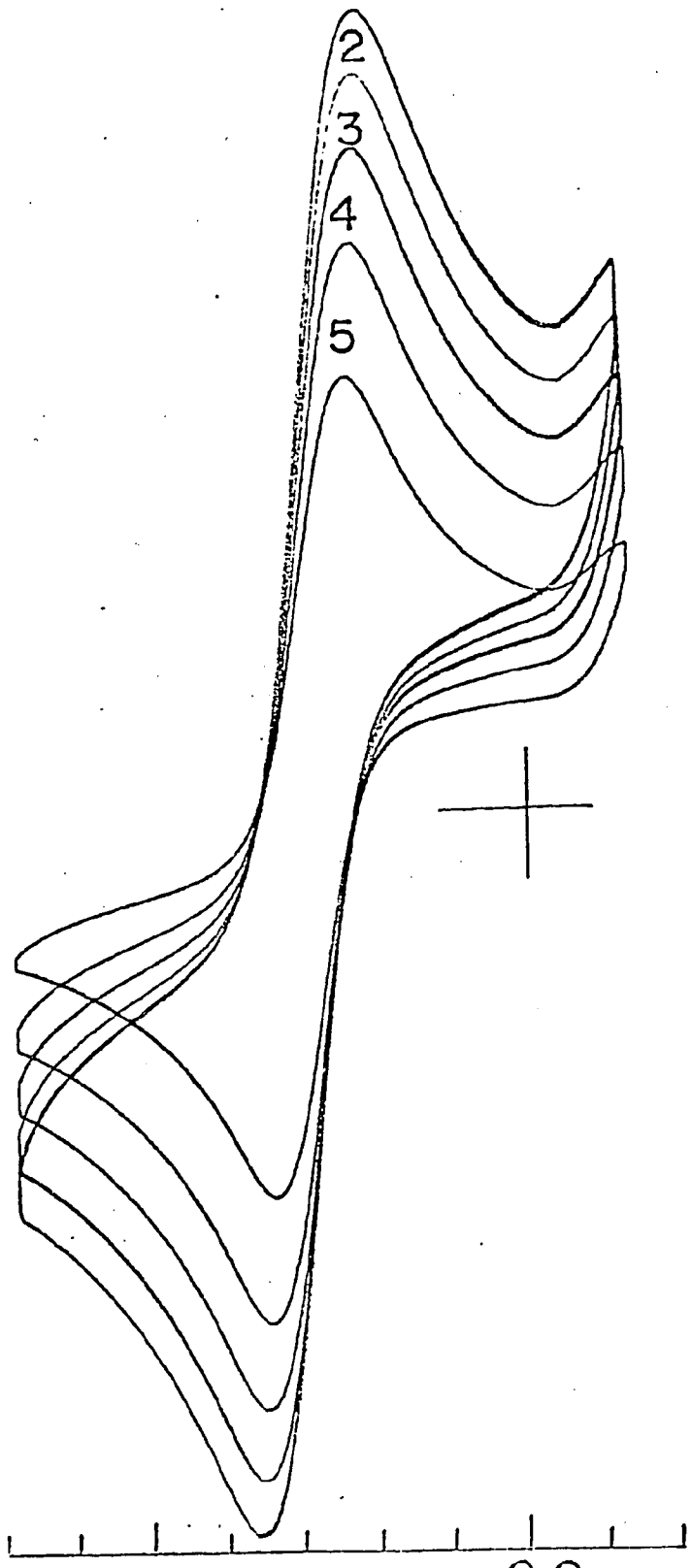
1

2

3

4

5

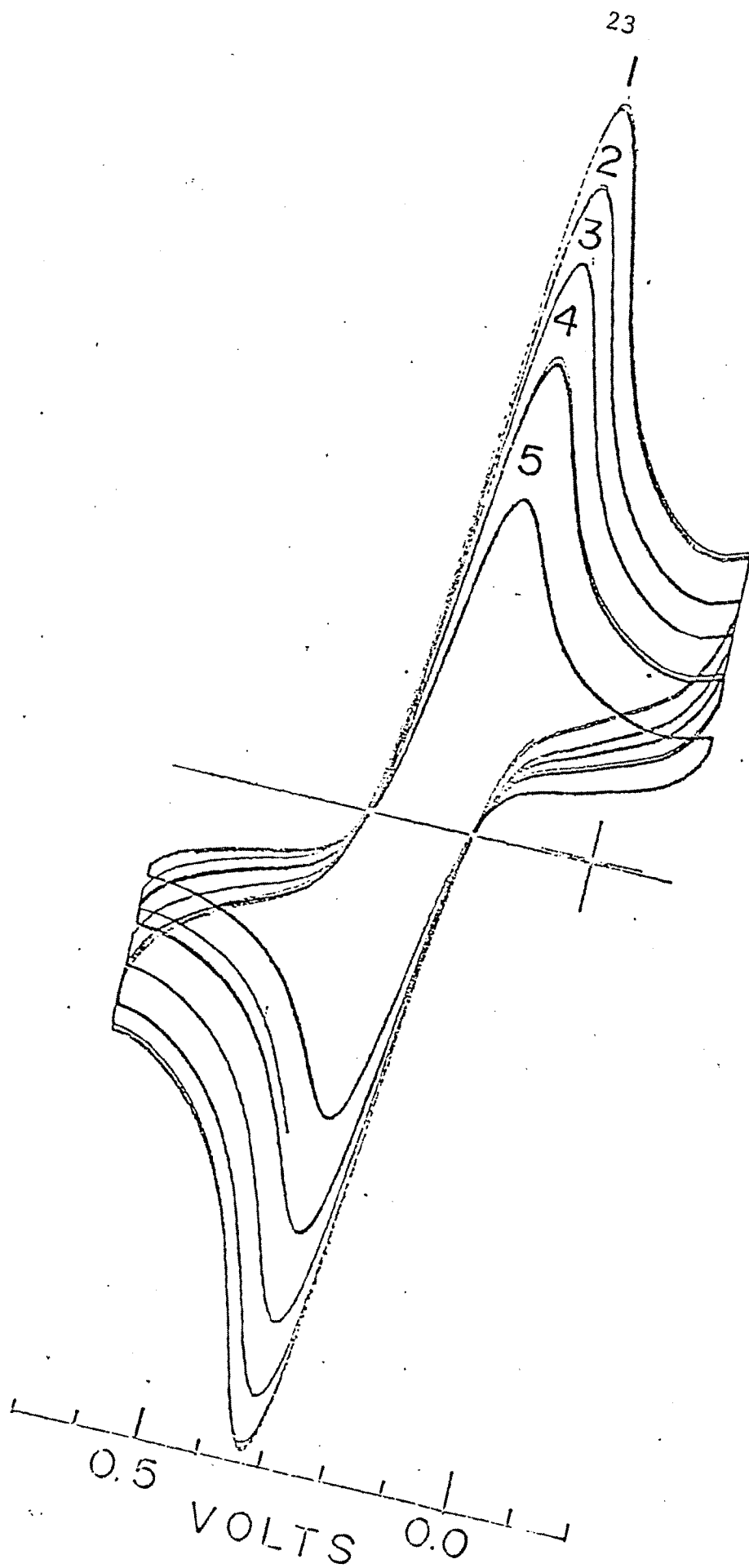


0.5

0.0

VOLTS

Figure 4. The cyclic voltammograms of μ -1,4-dicyano- [2.2.2] - bicyclooctanebis (pentaammineruthenium(III))trifluoromethanesulfonate at various scan rates (1, 350mV/sec; 2, 200mV/sec; 3, 170mV/sec; 4, 100mV/sec and 5, 50mV/sec), taken in dimethylformamide with 0.10M tetraethylammonium perchlorate. The working and reference electrodes were platinum wires and the reference electrode was Ag/AgCl.



Because both of the oxidation states of ruthenium that we have employed, Ru(II) and Ru(III), are substitution inert, as is Co(III), so that the inner sphere electron transfer is precluded as a possible mechanism. The bimetallic complex was synthesized with Ru(III) and Co(III), both the oxidized states of the metal atoms, thus satisfying criterion (b). Concerning criterion (c), when we desired to initiate electron transfer within the complex, the Ru(III) site was reduced by $\text{Ru}(\text{NH}_3)_6^{2+}$, which reduces Ru(III) much faster than Co(III) even when the more thermodynamically favorable reaction is that with the Co(III) (26). The high Franck-Condon barrier of Co(III) for inner sphere rearrangement provides the kinetic advantage to the Ru(III) site (27,28). This initial reduction is driven by the more favorable reduction potential of Ru(III) bound to a nitrile than to amines (29,30). The Ru(II) site, which contains a nitrile in the coordination sphere, can then reduce the Co(III) site intramolecularly. The potential for the Co(III) reduction is close to that of the ruthenium site and the next reaction is aided by the irreversible release of labile Co(II) upon electron transfer. The $\text{Co}(\text{H}_2\text{O})_6^{2+}$ which is produced is very resistant to oxidation and will not reduce the Ru(III) site. This scheme for taking advantage of the kinetic and thermodynamic properties of Ru(III) and Co(III) has been utilized by Isied and Taube who studied intramolecular electron transfer across ligands such as isonicotinate and 4-pyridylacetate (26). The potential

difference for the electron transfer reaction (which contributes to ΔG as $\frac{nFe}{2}$ according to Marcus' theory) can be modified by using different Co(III) moieties. We have monitored reactions of $\text{Ru}(\text{NH}_3)_6^{2+}$ with $\text{Co}(\text{NH}_3)_6^{3+}$ and $\text{Co}(\text{NH}_3)_5(\text{H}_2\text{O})^{3+}$ (as had Endicott and Taube (1964) and also $\text{Co}(\text{NH}_3)_4(\text{H}_2\text{O})_2^{3+}$. We have also monitored reactions of $\text{Ru}(\text{NH}_3)_5\text{NCR}^{2+}$ with $\text{Co}(\text{NH}_3)_4(\text{H}_2\text{O})\text{NCR}^{3+}$ and $\text{Co}(\text{NH}_3)_3(\text{H}_2\text{O})_2\text{NCR}^{3+}$ (where R= adamantane). We find that each successive replacement of NH_3 by H_2O leads to a increase of 200 - 300 mV in the second order rate constant, equivalent to change in ΔE of $\approx 250\text{mV}$. It should be noted that direct polarographic determination of $\text{Co}^{3+/2+}$ potentials is not currently feasible due to slow electrode reactions.

The details of the kinetic experiments are presented in the following section.

B. Description of the Kinetic Experiments

The synthesis of the bimetallic complexes used for the electron transfer kinetics, is described in chapter II. The bimetallic complexes used for the kinetic studies of electron transfer reactions, were the following: μ -1,4-dicyano-[2.2.2]-bicyclooctanepentaammineruthenium(III) aquotetraamminecobalt(III); μ -1,4-dicyano-[2.2.2]-bicyclooctanepentaammineruthenium(III) diaquotriamminecobalt(III); trans-1,4-dicyanocyclohexanepentaammineruthenium(III) aquotetraamminecobalt(III); trans-1,4-dicyanocyclohexanepentaammineruthenium(III) diaquotriamminecobalt(III).

Concentrations of the bimetallic complexes were typically for kinetics experiments about 10^{-4} M. The complexes were dissolved in 0.010M aqueous trifluoromethanesulfonic acid solution. The bimetallic complexes were weighed and dissolved directly into the cell to be used for kinetics. The cells were closed with rubber septums and fastened tightly with copper wire. The cell was transferred to the cuvette holder where argon was bubbled through one septum needle and vented by another. This purging was continued for 20 to 30 minutes, at which time the bleeder needle is first withdrawn, followed immediately by the input needle. Immediately after the withdrawal of both needles, the septum is coated with Apiezon grease type H. This purging was done in the Peltier thermo-regulated cuvette holder inside a Beckman DU-8 spectrophotometer. The reductive solution of $\text{Ru}(\text{NH}_3)_6^{2+}$ was purged at the same time in the argon line, which is described in details in

chapter II. After the cell has equilibrated, a kinetic run is initiated with the reductive solution. A gas tight syringe is first purged of air by withdrawing the atmosphere within the erylenmeyer bubbler and ejecting outside the flask. This procedure is repeated 5 or 6 times. The syringe is dipped into the solution and filled with a quarter volume of liquid. Bubbles are purged from the syringe and the solution is discarded. This procedure is once more repeated. The third sample is adjusted to the desired volume. The reaction is initiated with this addition. Once the injection has been made, the timer is started using the other hand. The cell is immediately removed from the thermostated compartment by holding the rubber septum portion of the cell system. This is transferred to a vortex mixer briefly and replaced back into the compartment and within 10 seconds the Beckman DU-8 is turned on to monitor the reaction.

The electron transfer reactions can be monitored conveniently with conventional or stopped flow spectrophotometers. Changes occur due to the oxidation of the Ru(II)-nitrile site (for peaks in the region of $350 - 380 \text{ nm}^{-1}$ and near 230 nm^{-1}) and due to the reduction of the Co(III)-nitrile site (for peaks in the region of $320 - 340 \text{ nm}^{-1}$ and $470 - 510 \text{ nm}^{-1}$). Data were treated with statistics programs available on the PROPHEET computing system (9).

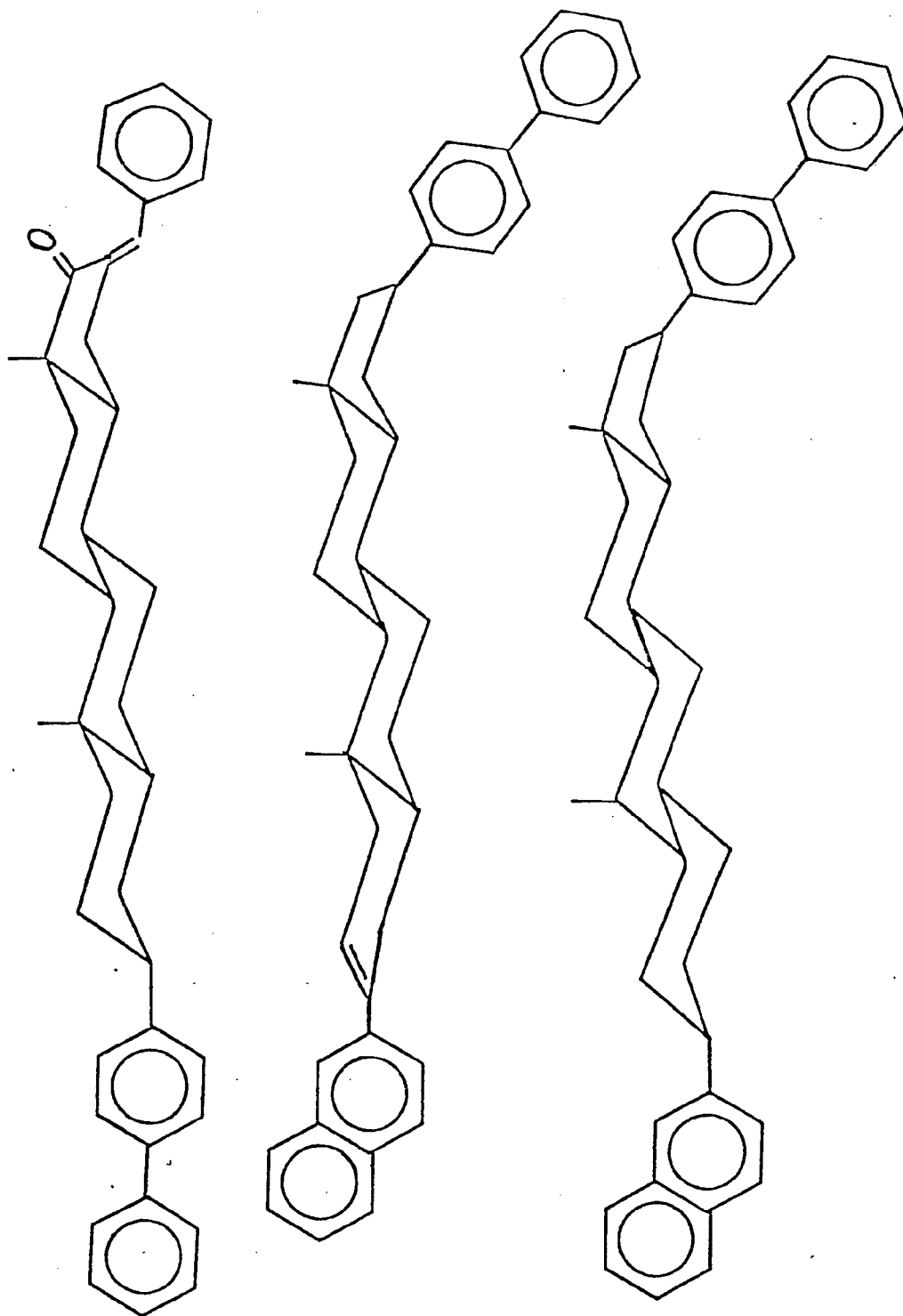
C. Results and Discussion

In order to understand photosynthesis or to design efficient molecular systems for photochemical energy storage and to understand mechanisms involved in the electron transfer reactions of the oxidative phosphorylation process, it is important to understand how distance, energy differences and molecular structure control rates of long-distance electron transfer.

Several recent reports have shown that electron transfer can occur when oxidizing and reducing centers are separated by long distances. While each of those cases are of interest, none of them satisfy all of the criteria I have discussed in the introduction, i.e. a system with a rigid saturated barrier of well-defined length containing two substitution inert metal ions capable of undergoing thermal electron transfer.

Using a system with donor and acceptor groups linked by a relatively rigid spacer consisting of steroid derivatives (Figure 5), Calcaterra and coworkers (31) have found that relatively rapid electron transfer occurs over long distances (about 15\AA). Their model system is made up of a donor that is the negative ion of the biphenyl moiety which can donate an electron to any of the three different acceptors that have used (cinnamoyl, 2-vinylnaphthyl and 2-naphthyl groups). The system is reduced by use of an electron pulse from a linear accelerator. The electron capture can occur at either end of the molecules with almost equal probability due to the

Figure 5. Structures of diended steroids studied by Calcaterra, Closs and Miller (Journal of the American Chemical Society, 1983, 105, 670-671). The half-lives for electron transfer and free energy changes are 0.5ns, -1.1eV (top molecule), 25ns, -0.32eV (center of molecule) and 1 s, -0.05eV (bottom molecule).



and his coworkers have used the crystal structure of the oxidized and reduced forms of tuna cytochrome c to estimate the distance between the donor and acceptor groups. The distance has been estimated to be $10-16\text{\AA}$. They have shown that electron transfer within proteins can take place rapidly at long distance given a driving force of 0.1eV . At present Isied and coworkers are trying to monitor intramolecular electron transfer from the ruthenium atom to the ion (heme) in the modified cytochrome as well as the measurement of the electron transfer from the ion (heme) to the ruthenium atom. These experiments will tell them the effect of driving force on the rate of electron transfer between a donor and acceptor held at long distances. Their assumption on this work is that the two metal atom sites on the protein are held apart and that the protein is relatively inflexible.

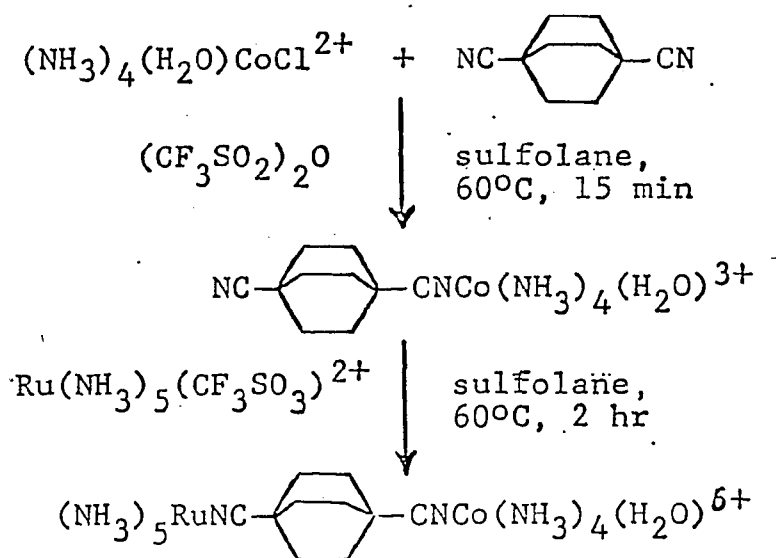
Zawacky and Taube (33) have reported rates of intramolecular electron transfer in binuclear complexes containing ruthenium (II) and cobalt(III) with pyrazine, 4,4'-bipyridine and selected pyridinecarboxylate anions as bridging ligands. Their results indicate that electron transfer in the pyridinecarboxylate complexes approaches the adiabatic regime, *i.e.* there is no need to involve tunneling to account for the electron transfer rates. In all cases they report, the ligands which have been used are either unsaturated or sufficiently flexible for the two metal sites to approach each other closely so that the electron could avoid crossing a saturated barrier.

The system which Taube and Isied have used exploit two general patterns of metal ion reactivity: 1) The inertness to ligand exchange of metal atoms that have highly populated bonding and nonbonding orbitals and empty antibonding orbitals (low spin d^5 and d^6 ions, Ru(III) and Co(III) and 2) the sluggishness of reactions which involve a high Franck-Condon barrier (i.e. those of Co(III) Co(II) relative to Ru(III) Ru(II), since electron transfer in the case of cobalt results in population of an antibonding orbital and a large change in cobalt-ligand bond lengths while addition to ruthenium results in population of a relatively nonbonding orbital and very little change in ruthenium-ligand bond lengths). Thus, a bimetallic complex with Co(III) and Ru(III) can remain intact in solution and the addition of a suitable reducing agent will cause the Ru(III) atom to be reduced before the Co(III) atom even if the overall potential favors the Co(III) reduction. An additional advantage of this scheme is that the subsequent reduction of the Co(III) site by the newly generated Ru(II) site produces $\text{Co}(\text{H}_2\text{O})_6^{2+}$, which is very difficult to oxidize, so the reaction is made irreversible. Thus, even a reaction with an unfavorable free energy difference can be accomplished. In the applications of this scheme such as those discussed above, a major difficulty has been encountered-saturated ligands are generally flexible and the first order reactions which have been observed quite possibly result from the reaction of the metal atom at one end of the bimetallic complex

with the metal atom at the other end when the ligand bends enough for them to come into close proximity. My study has involved the use of this scheme developed by Taube and coworkers but applied to the rigid ligand, 1,4-dicyano-[2.2.2]-bicyclooctane and to a more flexible ligand which still prevents contact of the first coordination spheres of the metal atoms, trans-1,4-dicyanocyclohexane. Results have been obtained with the aquotetraamminecobalt(III) moiety bound to each of these species and, in more preliminary form with the diaquotriamminecobalt(III) moiety bound to each. The latter species provides a more favorable potential for the reaction and much faster rates.

The bimetallic complexes are synthesized as discussed in chapter 2. Scheme 1 illustrates this sequence for the aquotetraamminecobalt(III)-pentaammineruthenium(III) complex of 1,4-dicyano-[2.2.2]-bicyclooctane. The visible-uv spectrum (498nm, $\epsilon=62$; 383nm, shoulder; 283nm, $\epsilon=613$) is characteristic of Co(III)N₅O and Ru(III) (NH₃)₅NCR coordination spheres (where R is a bridgehead nitrile (34); the cyclic voltammogram ($E_{1/2}$ vs. n.h.e.=0.467V) is characteristic of Ru(NH₃)₅NCR^{3+/2+} (35), and the infrared spectrum shows Ru(III) and Co(III) coordination of NCR groups (34c) CN shifts from 2240 cm⁻¹ for the ligand to 2310 cm⁻¹ and 2240 cm⁻¹ when only Co(III) is bound to a single peak at 2300 cm⁻¹ when both Co(III) and Ru(III) are bound). Any free ligand present after the first step in the synthesis is removed by extraction so no bis(ruthenium

Scheme 1. The sequence of reactions used for the synthesis of bimetallic complexes of Co(III) and Ru(III) with dicyano ligands.



species should be formed. The elemental analysis is in excellent agreement with the proposed structures.

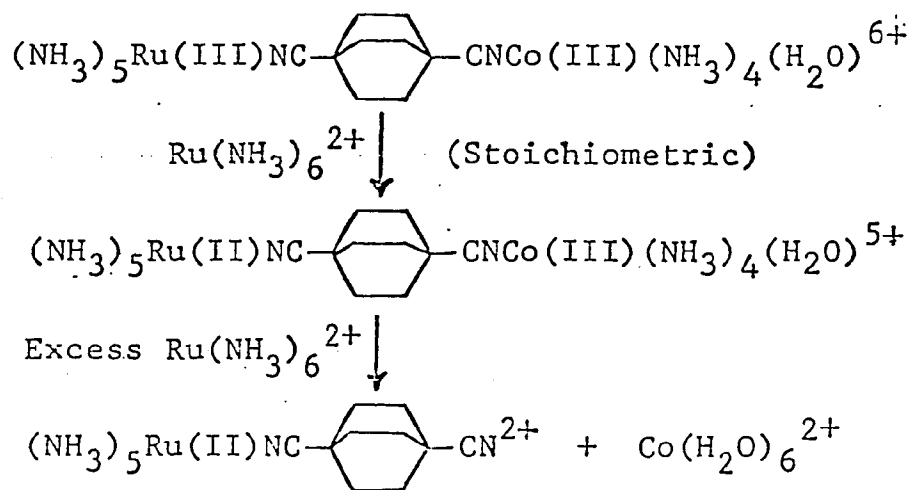
When excess $\text{Ru}(\text{NH}_3)_6^{2+}$ is added to the bimetallic complex, as shown in Scheme 2, the Ru(III) atom is reduced and the remainder of the $\text{Ru}(\text{NH}_3)_6^{2+}$ then proceeds to reduce the Co(III) site with a rate constant of $0.54\text{M}^{-1}\text{s}^{-1}$, consistent with rates obtained by Endicott and Taube for the reduction of Co(III) ammine complexes (i.e. the rate constant they obtained for the reaction of $\text{Ru}(\text{NH}_3)_6^{2+}$ with a Co(III) N_2O species, $\text{Co}(\text{NH}_3)_5(\text{H}_2\text{O})^{3+}$, is $3\text{M}^{-1}\text{s}^{-1}$, at an ionic strength of 0.22 rather than 0.10 which should measure the rate by a factor of about $(2+)(3+)(\frac{0.22}{0.10})^{\frac{1}{2}}$ or 9). When less than a stoichiometric amount of $\text{Ru}(\text{NH}_3)_6^{2+}$ is added, the only Ru(II) in solution after mixing is the bimetallic complex (reduction of $\text{Ru}(\text{NH}_3)_5\text{NCR}^{3+}$ is rapid and quantitative). In this case (at 25°C , 0.10M ionic strength with trifluoromethanesulfonic acid and the concentration of the bimetallic complex at about 10^{-4}M) reduction of the Co(III) is very slow: less than 10% after 10 hours.

Since no reaction was observed, an upper limit for the reaction rate constant can be estimated using the integrated rate law for a first order reaction to be $3 \times 10^{-6}\text{s}^{-1}$. To find out what the barrier of the saturated bridge ligand does to the rate of electron transfer, we estimated the rate expected for the same reaction without the bridge. In order to estimate the rate without the bridge, the rate constant for the appro-

priate intermolecular reaction must be obtained and then modified to account for the fact the two metal atom sites would be held fixed in a bimetallic complex. Unfortunately, the direct reaction of a pentaammineruthenium(III) organonitrile complex with an aquotetraamminecobalt(III) complex at the concentrations at which these species are soluble in acidic solution ($\leq 0.01M$) is too slow for good data to be obtained. As a result, I observed the reaction of hexaammineruthenium(II) with 1-adamantylcarbonitriloaquotetraamminecobalt(III) and have used the Marcus cross relation to obtain the expected rate for the reaction involving a pentaammineruthenium(II) organonitrile complex. At $25^{\circ}C$ and an ionic strength of $0.10M$ (the ionic strength must be carefully controlled because the reactants are both charged), I obtained a rate constant of $7.0M^{-1}s^{-1}$. As a check on the application of results for this single step reaction to the two-step sequential reaction series we are using (Scheme 2). I ran reactions which are faster, allowing me to monitor both the direct reaction of hexaammineruthenium(II) and, in a separate experiment, a pentaammineruthenium(II) organonitrile complex with the same cobalt(III) complex, 1-adamantylcarbonitrilodiaquotriamminecobalt(III). The synthesis for these compounds is described in Chapter II. The concentrations of the metal complexes were typically about $10^{-4}M$ for both the ruthenium and the cobalt complexes. The method is described in detail in the experimental section of this chapter. With the exception

Scheme 2. The electron transfer sequence.

In the first reaction, the ruthenium(III) site of the bimetallic complex is reduced rapidly. The subsequent slow reduction of Co(III) can occur by intermolecular or intramolecular reactions. Addition of excess pentaammineruthenium(II) leads to relatively rapid reduction of the Co(III).



that in the case of the reaction involving 1-adamantylcarbonitrilopentaammineruthenium(II) and 1-adamantylcarbonitrilodiaquotriamminecobalt(III), I had three solutions to purge. The solution of the cobalt complex was purged inside the cell in the cuvette holder. The solution of $\text{Ru}(\text{NH}_3)_6^{2+}$ and the ruthenium organonitrile complex were purged at the same time on the argon line, which is described in detail in Chapter II. In all cases, the reactions showed second order kinetics behavior. The rate constants were calculated by plotting $1/\text{absorbance}$ against time and obtaining the slope. The rate constants and half-lives obtained from the second order equation, $t_{1/2} = 1/k[\text{concentration}]_0$, were $1.33 \times 10^3 \text{ M}^{-1}\text{s}^{-1}$ with a half-life of 1.25 seconds at concentrations of 6.0×10^{-4} for the reaction of $\text{Ru}(\text{NH}_3)_6^{2+}$ with 1-adamantylcarbonitrilodiaquotriamminecobalt(III) and $3 \text{ M}^{-1}\text{s}^{-1}$ with a half life on the order of 10 minutes for the reaction of $\text{Ru}(\text{1-adamantylcarbonitrilo})(\text{NH}_3)_5^{2+}$ and $\text{Co}(\text{1-adamantylcarbonitrilo})(\text{NH}_3)_3(\text{H}_2\text{O})_2^{3+}$, both at $5.0 \times 10^{-4} \text{ M}$. The much slower rate found in the reaction in which $\text{Ru}(\text{1-adamantylcarbonitrilo})(\text{NH}_3)_5^{2+}$ is present initially demonstrates that the $\text{Ru}(\text{NH}_3)_5^{2+}$ certainly does reduce the $\text{Ru}(\text{NH}_3)_5\text{NCR}^{3+}$ moiety first. The fact that the ruthenium-nitrile bond remains intact is demonstrated by cyclic voltammograms taken before and after addition of $\text{Ru}(\text{NH}_3)_6^{2+}$ (Figure 7). The rate of reduction of the $\text{Co}(\text{III})$ species is much slower in the case of reduction by

$\text{Ru}(\text{NH}_3)_5\text{NCR}^{2+}$ compared with the reaction of Co(III) with $\text{Ru}(\text{NH}_3)_6^{2+}$. This is consistent with the more favorable reduction potential (and, hence, less favorable oxidation) of $\text{Ru}(\text{NH}_3)_5\text{NCR}^{3+/2+}$ compared with $\text{Ru}(\text{NH}_3)_6^{3+/2+}$. This difference in reduction potential is the most important factor needed to obtain the expected rate for the reaction of the pentaammineruthenium(III) organonitrile species with 1-adamantylcarbonitriloaquotetraamminecobalt(III) from the rate obtained for the reaction of hexaammineruthenium(II).

Marcus' cross relation is: $k_{12} = (k_{11}k_{22}K_{12}f)^{\frac{1}{2}}$ (36). To get the rate of one cross reaction ($\text{Ru}(\text{NH}_3)_5\text{NCR}^{2+} + \text{Co}(\text{NH}_3)_4(\text{H}_2\text{O})\text{NCR}^{3+}$) from the rate of another ($\text{Ru}(\text{NH}_3)_6^{2+} + \text{Co}(\text{NH}_3)_4(\text{H}_2\text{O})\text{NCR}^{3+}$), the most important factor will be K_{12} and a significant but less important factor is "f". Other factors that contribute to ΔG^\ddagger can be eliminated as follows. Complexes of the same metal ions with similar metal-ligand bonds (i.e. Co(III) with 5 nitrogen atoms and one oxygen atom bound and Ru(II) with six nitrogen atoms in both reactions) should have similar inner-sphere reorganization energies (the principal component of the Franck-Condon barrier). Complexes of the same charges and sizes have very similar outer-sphere reorganization energies and coulombic work terms. Thus, the only remaining factors that might cause an appreciable difference in rates of two reactions of this type are the overall driving force due to the potential difference and the factor f.

Figure 6. A plot of absorbance data (as $1/\text{concentration}$) vs. time for the reaction of 1-adamantylcarbonitrilo-pentaammineruthenium(II) with diaquotriamminecobalt(III) in aqueous trifluoromethane sulfonic acid solution ($I=0.10M$) at 25 C. The linear plots are consistent with second order behavior. The concentrations of Ru(II) and Co(III) were $4.5 \times 10^{-4}M$ and $4.5 \times 10^{-4}M$, respectively. The rate constants obtained from these plots are $3.1 M^{-1}s^{-1}$ and $3.6 M^{-1}s^{-1}$.

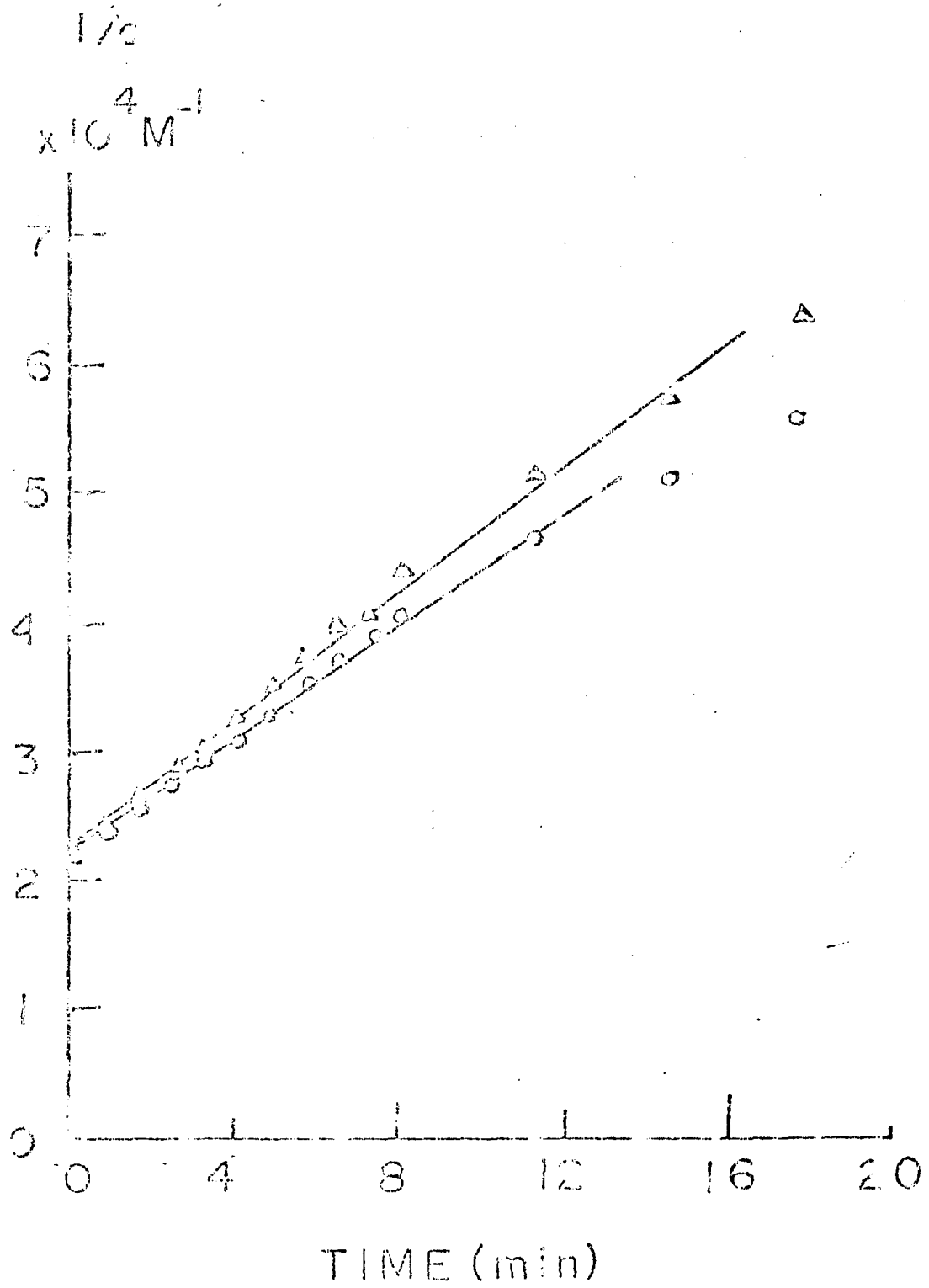
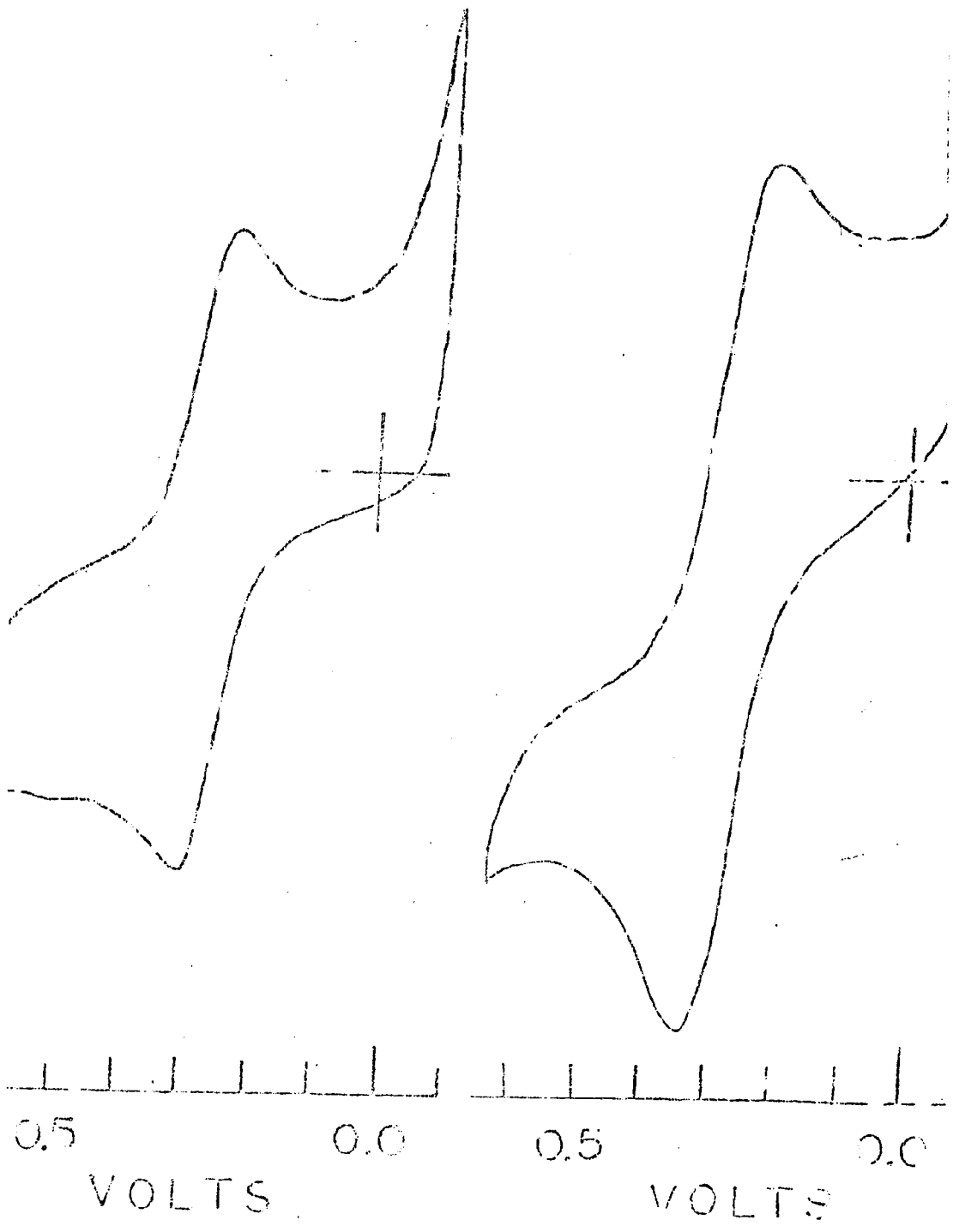


Figure 7. Cyclic voltammograms of μ -1,4-dicyano-[2.2.2]-pentaammineruthenium(III) aquo tetraamminecobalt(III) before (right) and after (left) the addition of an equivalent amount of pentaammineruthenium(II). Both voltammograms were obtained in dimethylformamide (0.10M tetrabutylammonium perchlorate) using platinum wires for working and auxiliary electrodes and a Ag/AgCl reference electrode.



To use the Marcus cross relation, the values of k_{11} and k_{22} (the self exchange rates for the cobalt complex in the 2+ and 3+ states and for the ruthenium complex in the 2+ and 3+ states, respectively) and K_{12} (the overall equilibrium constant for the reaction of a particular Co(III) and Ru(II) complex) must be estimated. The self-exchange rates for the Co(III) complexes I have studied should be very similar to those of other small cobalt(III) ammine complexes. Due to difficulties with the measurement of the $\text{Co}(\text{NH}_3)_6^{3+/2+}$ self-exchange rate (37), the best established self-exchange rate for a cobalt amine complex is that of $\text{Co}(\text{ethylenediamine})_3^{3+/2+}$, which is $5 \times 10^{-5} \text{M}^{-1} \text{s}^{-1}$ at 25°C and an ionic strength of 0.10M (38). Likewise, the self-exchange rates for the ruthenium complexes I have studied should be similar to those of other rutheniumammine complexes. Using the values of the $\text{Ru}(\text{NH}_3)_6^{3+/2+}$ self-exchange rate constants of Meyer and Taube (39) and correcting to an ionic strength using the relationship: $\log k = \log k_0 + (.2Z_1Z_2 \alpha (\mu)^{\frac{1}{2}}) / (1 + \beta(\mu)^{\frac{1}{2}})$ (21) where $\alpha = 0.51$ and $\beta = 0.329$, gives a rate constant of 2×10^3 .

The value for the reduction potentials of cobalt(III) ammine complexes cannot be directly determined because the electron transfer reactions of these complexes at electrode surfaces are too slow. The self-exchange rates discussed above and the reaction rate for the cross reactions of the cobalt(III) and ruthenium(II) complexes can be used in the Marcus cross relation equation, however, to estimate potentials of the

overall reactions. This equation gives $E = 0.317V$ for the observed reaction and $E = -0.100V$ for the desired reaction. With these values in hand, we can now calculate the factor f and the difference in the rate expected by changing K_{12} . It should be kept in mind that the rate depends on f by the relationship: $k'+k(f'/f)^{\frac{1}{2}}$. The factor f for the observed reaction is:

$$\ln f = \frac{(\ln K_{12})^2 / 4}{\ln \frac{k_{11} k_{22}}{z^2}} = \frac{[(\frac{23.06}{0.600})(0.317)]^2}{4} / \ln \frac{(5 \times 10^{-5})(2 \times 10^3)}{(10^{11})^2} \quad (22)$$

or $f=0.509$. The factor f' for the desired reaction is

$$\ln f' = \frac{[(\frac{23.06}{0.600})(-0.100)]^2}{4} / \ln \frac{(5 \times 10^{-5})(2 \times 10^3)}{(10^{11})^2} = -0.067 \quad (23)$$

so $f'=0.935$ and $(f')^{\frac{1}{2}}/(f)^{\frac{1}{2}}=1.36$. The absolute value for the potentials which were used ($0.317v$ and $-0.100V$) are questionable from the Marcus cross relation, but the value of f is quite insensitive to K_{12} unless it is very large (i.e. changing the values of the potentials to $0.217v$ and $0.200v$ gives $(f')^{\frac{1}{2}}/(f)^{\frac{1}{2}}=1.17$ instead of 1.36).

Using the value for ΔE that I have determined for 1,4-dicyano-[2.2.2]-bicyclooctanepentaammineruthenium^{3+/2+}, (which is nearly identical to that of 1-adamantylcarbonitrilo-pentaammineruthenium^{3+/2+}), gives

$$k' = k (f'/f)^{\frac{1}{2}} e^{(n F \Delta E^{\circ} / RT)} \quad (24)$$

$$k' = 7.0 \text{ M}^{-1} \text{ s}^{-1} (1.36) \exp(-0.417) (23.06 \frac{\text{kcal}}{\text{mol}\cdot\text{V}}) / (2) (1.987 \frac{\text{cal}}{\text{mol}\cdot\text{K}}) (298\text{K})$$

$$k' = 2.7 \times 10^{-3} \text{ M}^{-1} \text{ s}^{-1}$$

As expected from the less favorable potential for oxidation of the $\text{Ru}(\text{NH}_3)_5 \text{NCR}^{2+}$ complex, the predicted reaction rate for the intermolecular reaction of the organonitrile ruthenium(II) complex is much slower than that of hexaammineruthenium(II).

Once we have obtained the appropriate intermolecular reaction rate constant, it has to be modified by two factors that differentiate an intramolecular reaction with fixed metal ions from the intermolecular reaction. The first of these factors is the advantage of preassembly of these positively charged metal atom sites in the bimetallic complex. This factor is obtained from the equation for coulombic work, $w_r = \frac{(Z_1 Z_2 e^2)}{D_s \kappa (1 + \kappa)}$. The factor w_r has (25) been calculated for aqueous solutions at 25 C and an ionic strength of 0.10M for $\text{Ru}(\text{NH}_3)_6^{3+/2+}$ by Sutin and coworkers to have a value of 1.8 kcal/mole (21). The second alteration is a statistical factor to account for the effective concentration of two metal complexes at their contact distances. For any second order intermolecular reaction, the rate as a function of concentration would eventually reach a plateau at high concentration when the probability of the two species being in close proximity approaches unity. The statistics of this situation has been

treated by Kreitman and Hamaker (25). In their treatment, they used volumes for the two "impurities" in the close-packed lattices. In our case we are dealing with species which are of quite different size (the Ru(II) and Co(III) complexes) than the solvent. Therefore, we have chosen to use molar volume fractions rather than mole fractions. We are using the close-packed face centered cubic lattice for our model of the liquid state. The radii of the complexes is taken to be approximately 7.2\AA (using a radius of 6.6\AA for $\text{Ru}(\text{NH}_3)_6^{2+}$ and 2\AA additional for the bridge and the equation, $\bar{a} = \frac{1}{2}(d_1 d_2 d_3)^{\frac{1}{2}}$ (23)); giving a molar volume of 0.94 liters or a concentration, if one could make an entire solution consisting only of the metal complex ion, of 1.06M. Kreitman and Hamaker give the following equations for the probability of proximity of the two "impurities", i.e. the Ru(II) and Co(III) inner coordination spheres on our case):

$12 ab (1 - x)^{18} / x$ for mixed double interaction,
 $36 a^2 b (1-x)^{23} 5(1-x) + 2 / x$ for mixed open triple interactions and $48 a^2 b (1-x)^{22} / x$ and $24 ab^2 (1-x)^{22} / x$ for mixed closed triple interactions. At the volume fraction of 1.0×10^{-3} (i.e. $1.06 \times 10^{-3} \text{M}$), the probabilities of a and b being adjacent are, respectively, 5.8×10^{-3} , 0.08×10^{-3} , 0.08×10^{-3} , 0.02×10^{-3} and 0.01×10^{-3} for a total of 6.0×10^{-3} . Thus, the rate for the intermolecular reaction at a given concentration has a probability factor about six times as

great as the magnitude of that concentration ($6.0 \times 10^{-3} / 1.06 \times 10^{-3}$). From this analysis, we take the conversion factor for the effective concentration to be $1/6M$. The expected rate for the intramolecular reaction is, therefore, $2.7 \times 10^{-3} M^{-1} s^{-1} \times \frac{1}{22 \times 6M} = 1.0 \times 10^{-2} s^{-1}$.

The theories most commonly applied to predictions of rates of tunneling reactions are due to Hopfield and Jortner (3,23), Marcus and Siders (40) have discussed the importance of distinguishing cases involving matter between the sites (as in Hopfield's estimation of $e^{-1.4r}$ for cytochromes) (3) and cases involving vacuum (Jortner's estimate of $e^{-2.6r}$) (25). All approaches have resulted in an exponential dependence of the rate on distance, but the value of the exponential factor is difficult to ascertain theoretically. Our observed value of over 10^4 for 4\AA requires a value of at most $e^{-2.3r}$ (41). It is certainly possible for electron transfer reactions to occur over large distances, as recently shown by Calcaterra, Closs and Miller (31), but it appears from this work that further experiments now involving higher driving forces and/or shorter barriers will be necessary to achieve measurable electron transfer reactions with bimetallic complexes of Ru(II) and Co(III).

One approach we have made is to increase the driving force by using a diaquotriamminecobalt(III) moiety. My initial experiments with a bimetallic complex of 1,4-dicyano-[2.2.2]-

bicyclooctane with this moiety and pentaammineruthenium(II) production of $\text{Co}(\text{H}_2\text{O})_6^{2+}$ (i.e. $t_{1/2}$ 1 minute at 10^{-4}M) occurs. To interpret these data, a large number of runs must be made to see if the plot of the second-order rate constant obtained is linear with concentration or if the reaction becomes first order at low concentrations. This study requires much more of the 1,4-dicyano-[2.2.2]-bicyclooctane ligand than is now available and further study is being undertaken by Dr. Kenneth Wilkowski and other members of our group. Dr. Wilkowski and I have also monitored the reaction of the bimetallic complex of trans-1,4-dicyanocyclohexane with diaquotriamminecobalt(III) and pentaammineruthenium(II) attached. This species shows second order reduction of Co(III) that is directly concentration dependent over the concentration range of $2 \times 10^{-4}\text{M}$ to $5 \times 10^{-4}\text{M}$ with a rate constant of $556^{+27} \text{M}^{-1}\text{s}^{-1}$ (correlation coefficients of 0.998 or better for runs at five different concentrations, $I=0.10\text{M}$, $T=25.0^\circ\text{C}$). If the effective concentration for comparison of intramolecular and intermolecular rate constants is taken to be 3.7M and it is assumed that as much as 20% of the reaction could be first-order (intramolecular) the inhibition by the saturated ligand would be a factor of $\frac{5 \times 3.7}{2 \times 10^{-4}} = 9 \times 10^4$.

To extend these studies, the easiest method would involve using the same complexes but using solvents of lower dielectric constant in order to slow down the intermolecular reaction

without greatly affecting the intramolecular reaction. The coulombic work term is inversely dependent on the static dielectric constant:

$$w_r = (Z_1 Z_2 e^2) / D_s \kappa (1 + \kappa) \quad (25)$$

$$\text{where: } \kappa = (8 \pi N^2 e^2 \mu / 1000 D_s R T)^{\frac{1}{2}}$$

reducing a reaction with a rate constant of 1 sec^{-1} in water to $4.2 \times 10^{-3} \text{ s}^{-1}$ in methanol and 3×10^{-5} in acetone. The solvent rearrangement term, ΔG , however, is principally dependent on the optical dielectric constant, which is quite similar for several reasonable solvent systems (e.g. 1.78 for H_2O , 1.77 for MeOH, 1.85 for acetone), so the intramolecular rate would be only slightly affected. Other experiments could involve ligands with shorter distances between the metal atoms or complexes with greater driving forces.

From this work, it is clear that even short saturated barriers such as bicyclooctane or cyclohexane can inhibit electron transfer between metal ions. We have found the inhibition factor to be at least 10^4 to 10^5 for complexes of ruthenium(II) and cobalt(III) in which the separation between the metal atoms is no more than 4\AA beyond the normal radius of the first coordination sphere. This inhibition factor is greater than that predicted by Hopfield and at least as great as that predicted by Jortner. The range of possible separation distances of cytochromes has been wide - from only a few Angstroms to tens of Angstroms. The reactions of cytochromes

in mitochondria are relatively fast - within a few orders of magnitude of their reactions in homogeneous solution (1). The great inhibition at such short distances which we have observed indicates that either the donor and acceptor sites of the cytochromes in mitochondria must be very close to one another (within 5\AA) at the time of electron transfer or that proteins can allow electron transfer to occur more readily than saturated molecules. More experiments will be required in which the type of ligand between the metal ions is changed and in which the metal sites themselves are changed also. At least in the case of cobalt and ruthenium complexes of the saturated ligands, 1,4-dicyano-[2.2.2]-dicyanocyclohexane, thermal electron transfer is greatly inhibited by the saturated barrier.

The following chapter describes the synthesis and the kinetics of formation and decomposition reactions of the complexes described in this chapter. The study of these complexes required the development of new synthetic methods. The complexes had to be well characterized and their stability in solution had to be established. These related studies produced results which are interesting in their own right and which are distinct from the study of electron transfer reactions presented in the first chapter.

CHAPTER 2

A. Introduction

In this chapter, the synthesis, and the kinetics of formation and decomposition of ruthenium(III) nitrile complexes and the synthesis of bimetallic complexes of ruthenium(III) and cobalt(III) will be discussed. The objective for studying formation and decomposition reactions of these complexes is to be able to learn about the stability of these complexes before undertaking the kinetics studies of the electron transfer reactions with the bimetallic complexes.

A very important objective of this project was to develop a synthesis for mixed bimetallic complexes which avoids ruthenium(II) as an intermediate. The bimetallic complexes have been synthesized with the aid of Sargeson's and coworkers' idea of using labile trifluoromethanesulfonate complexes as intermediates (42). The typical procedure that are presently used to make ruthenium(III) complexes involve the use of relatively labile ruthenium(II) intermediates such as $\text{Ru}(\text{NH}_3)_5(\text{H}_2\text{O})^{2+}$ or $\text{Ru}(\text{NH}_3)_4(\text{SO}_3)(\text{H}_2\text{O})$ (43,44). Once the labile ligand on the ruthenium(II) complex gets replaced by the desired ligand, oxidation to ruthenium(III) is accomplished with reagents such as $\text{Ag}(\text{I})$ (45), $\text{Ce}(\text{IV})$ (45), Br_2 (46), H_2O_2 (44). In some cases, these methods are not ideal, and the use of the

trifluoromethanesulfonate complex to avoid the use of ruthenium(II) as an intermediate becomes important. Some of the reasons why the use of ruthenium(II) as an intermediate would be inappropriate in our synthesis of the bimetallic complexes are: one, cobalt(III) is reduceable by ruthenium(II); two, the ligands themselves are oxidizable, therefore strong oxidizing agents should be avoided and; three, these methods require that the ligand compete successfully against the solvent, water, in binding to ruthenium(II).

Some background information concerning the kinetics and mechanism for formation reactions of ruthenium complexes is available in the literature. First, there are considerable data for ruthenium(II) substitution reactions reported especially by Henry Taube's and Peter Ford's groups (43,47). The ruthenium(II) ligand exchange kinetics can generally be interpreted as involving a dissociative-interchange mechanism. Much less data are available for ruthenium(III) reactions. These reactions are considerably slower, often by a factor of a million. Broomhead, Basolo and Pearson have reported rates for the hydrolysis of the halopentaammine-ruthenium(III) complexes (48). The acid hydrolysis rate for chloropentaammine ruthenium(III) is 3.1×10^{-6} /sec at 35°C. In 1969, Eliades, Harris and Reinsalu reported that the rate for acid hydrolysis of the chloropentaammine ruthenium(III)

complex is 3.5×10^{-6} /sec at 37°C and of the bromopentaammine ruthenium(III) complex is 4.0×10^{-6} /sec at 37°C (49). Thus, this reaction has a half-life on the order of a month.

Some studies have been reported of the substitution kinetics for reactions of relatively inert octahedral complexes of the heavier transition metals such as rhodium(III) and iridium(III). Data for volumes of activation of these reactions obtained by Thomas Swaddle indicate that they may follow an associative-interchange mechanism rather than dissociative-interchange mechanism which is characteristic of familiar cobalt(III) reactions (50).

In addition to the synthesis and the formation kinetics of the bimetallic complexes, this chapter also considers the question of stability of Co(III)-Ru(III) complexes. It is important to know how stable the bimetallic complexes are before undertaking the kinetic studies of the intramolecular electron transfer reactions. It is well known from Basolo and Pearson's work that the substitution of NH_3 and H_2O bound to Co(III) are catalyzed by base but in acid the half life is on the order of weeks (48). It is well known from Taube's work that ruthenium(II) and ruthenium(III) amines are stable in acid concentrations of 1.0M or less and here again the half life is on the order of weeks (44,45). The question we needed to answer was the degree of the stability of Co(III) organonitriles and Ru(III) organonitriles. We

have synthesized bimetallic complexes with cobalt(III) and ruthenium(III) amines bound to nitrile groups for the study of intramolecular electron transfer reactions. When such complexes are dissolved in acid solutions, spectral changes consistent with hydrolysis of the nitrile group bound to ruthenium(III) occurs slowly. To understand the nature of these reactions and to determine how well the reaction rate can be predicted for given conditions, we undertook the study of the acid hydrolysis of organonitriles bound to ruthenium(III).

Work done by Buckingham, Keene and Sargeson in 1973 showed that the hydrolysis of acetonitrile in basic aqueous solution is catalyzed by a factor of 2×10^6 on coordination to $\text{Co}(\text{NH}_3)_5^{3+}$ (51). Zanella and Ford reported in Inorganic Chemistry, 1975, that the specific rate of hydrolysis of the ruthenium(III) organonitrile is on the order of $10^2 \text{M}^{-1} \text{sec}^{-1}$ (52), which is about 10^2 times faster than the analogous cobalt(III) complexes at pH7 or below. The predicted half life for hydrolysis of a ruthenium(III) nitrile complex, then, would be 190,000 hours at pH3. In both cases, there was no evidence for a base independent hydrolysis path. In our work we have found there is a base independent hydrolysis path.

B. EXPERIMENTAL

1. MATERIALS

Commercial ChemicalsSupplies

acetone	Fisher
acetonitrile	Fisher
alumina (80-200mesh)	Fisher
anhydrous trifluoromethanesulfonic acid	3M Company
cobalt carbonate	Alfa
cobaltous chloride	Fisher
cuprous chloride	Malinckrodt
1,2-dibromoethane	Aldrich
1,4-dicyanocyclohexane	Aldrich
1,4-dione-2,5-dicarboxylic estes	Aldrich
dimethyl sulfoxide	Fisher
ethanol (95%)	Fisher
ethanol (absolute-Gold Shield)	IMC Chemical Group
ether (anhydrous)	Fisher
methylene chloride	Fisher
propane-1,3-dithiol	Aldrich
ruthenium hexaammine trichloride	Matthey Bishop Inc.
sieves (3 $\overset{\circ}{\text{A}}$)	Davison
sodium hydroxide	Fisher
sodium bicarbonate	Fisher
zinc metal (granular, 20 mesh)	Fisher
zinc metal (mossy)	Baker

Trifluoromethanesulfonate reagents

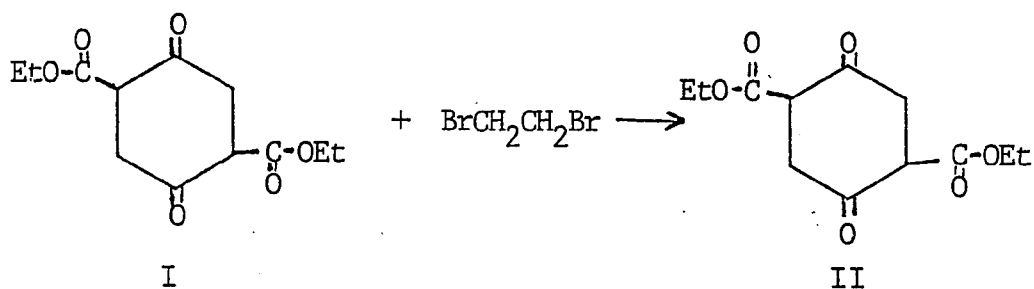
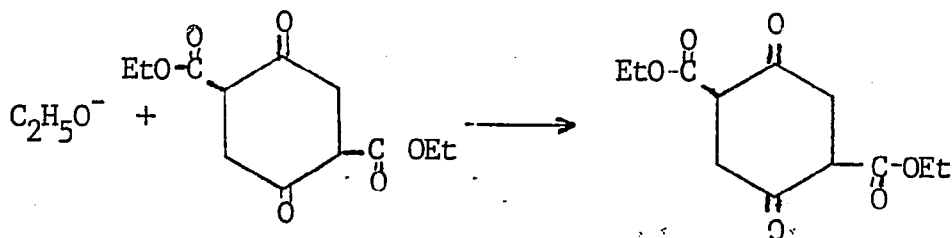
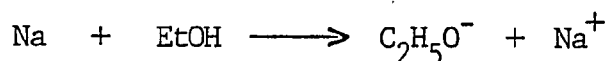
The trifluoromethanesulfonic acid (HTFMS) was obtained from 3M Manufacturing Company as the anhydrous acid. This material was slowly added to an equimolar amount of water and then vacuum distilled twice through on all glass distillation apparatus. The monohydrate contained 5.85mmHg^+ /g and had a density of 1.68g/ml at 25°C . resulting in a calculated molarity at 25°C . of 9.83M .

The lithium salt of trifluoromethanesulfonate, LiCF_3SO_3 was prepared by the addition of dilute $\text{H}_3\text{O}^+\text{CH}_3\text{SO}_3^-$ to recrystallized LiCO_3 .

2. Synthesis

a. Organic compounds

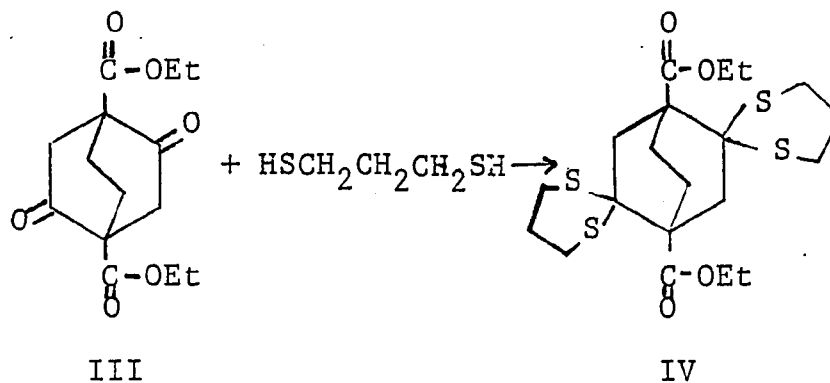
μ -1,4-dicyano-[2.2.2] -bicyclooctane. One approach followed for the synthesis of the -1,4-dicyano-[2.2.2]-bicyclooctane was that reported by Guha in 1972 (17). Initially, 3.6g of Na was dissolved in 200ml of EtOH then 20g of cyclohexane-1,4-dione-2,5-dicarboxylic ester were added after refluxing for 2 hours most of the ethanol was distilled off. The last traces of ethanol was removed with a water aspirator at 150°C . To this sodium compound 100ml of dried 1,2-dibromoethane were added. This mixture was refluxed for 72 hours using an oil bath at 140 - 150°C .



Then steam distillation was done by occasional addition of water until no more dibromoethane comes off. It takes about 10 hours. Product isolation was difficult. The product was filtered and washed three times with H_2O . A semisolid was obtained. This semisolid was transferred to a beaker and 50ml of EtOH were added, which dissolved most of the oil and left the crystals behind. After several hours standing in the refrigerator, the white solid ppt. was filtered from alcohol solution. The white crystals were washed several times with 1% NaOH until the test for FeCl_3 was negative. The way to test the presence of enol is by taking a little bit of starting material and test with FeCl_3 . If a purple color is obtained, the enol test is positive. To recrystallize the product it was dissolved in hot ethanol.

The yield was about 15%. The m.p. reported in the literature is 112°C. and I obtained 107° to 109°C. The infrared spectrum has the characteristic peaks of a ketone, 1735 cm^{-1} and ester, 1722 cm^{-1} as reported in the literature.

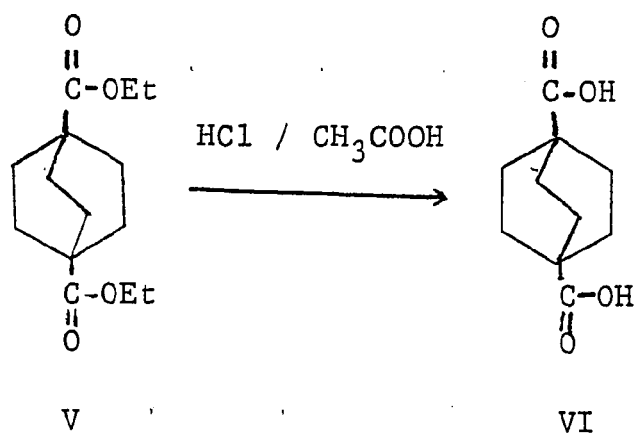
The objective of the next two steps is the removal of the ketone functional groups. 7.0g of the ketoester were dissolved in 20ml of freshly distilled chloroform. 10.88g of propane-1,3 dithiol were added with constant bubbling of HCl for six hours at 0°C. the product was washed with 2N/NaOH two times and with 1N/NaHCO₃ one time. The product was dried using the rotatory evaporator. Then this product was refluxed for 2 hours in hexane and filtered with a slow paper. The yield was about 50% an infrared spectrum shows the disappearance of the ketone peak at 1735 cm^{-1} . This step converted the diketone to the dithioether.



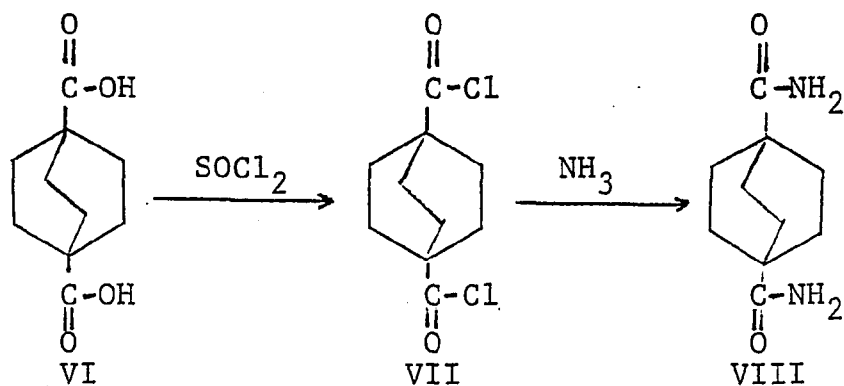
The next step involves the use of Raney Nickel. To a solution containing 380g of NaOH in 1.5l of H₂O in a 3.1 beaker was stirred and cooled in an ice bath to 10°C. then 300g of

Nickel-Aluminum alloy 50%-50% was added to the solution in small portions with continuous stirring at such rate that the temperature did not rise above 25° C. It took about two hours to add all the alloy. The reaction mixture was placed on a steam bath for 12 hours. The water volume was kept constant until there was no more evolution of hydrogen observable after twelve hours. The nickel must be washed many times with water until the pH is neutral. Caution must be observed because it is easy for the nickel to ignite. ($\text{NiAl}_2 + 6\text{NaOH} \rightarrow \text{Ni} + 2\text{Na}_3\text{AlO}_3 + 3\text{H}_2$). The continuation of the synthesis was done by Liangshia Lee and John D. Petersen from Clemon University. In order to remove the thioether groups from here, IV, 20 grams of this compound were refluxed for 48 hours with 250g Raney Nickel in 250 ml of 95% ethanol. The nickel was filtered, the solvent was removed through a 20cm vigreux column and the residue was distilled under reduced pressure. Additional product was obtained by extraction of the filtered nickel for 24 hours with ether in a soxhlet extraction apparatus. The yield was 40%. The yield reported in the literature is 80%.

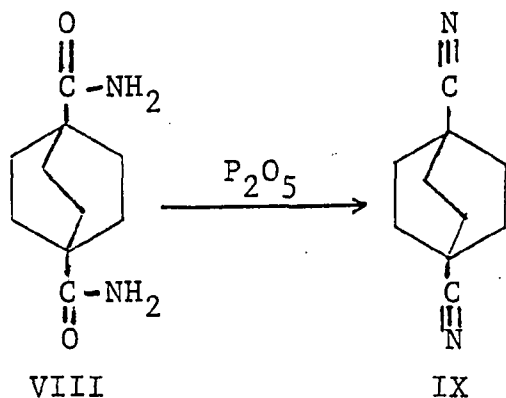
The next step is:



7.4g of diethyl bicyclo[2.2.2]-octane-1,4 dicarboxylate was heated gently in the presence of 50 ml of glacial acetic acid and 25 ml of concentrated HCl, for four hours. The product was filtered with suction and recrystallized from glacial acetic acid. The yield at this step was 90%. Then the dicarboxylic acid was converted to the 1,4-dicarboxamide-[2.2.2]-bicyclooctane by taking 15 grams of the dicarboxylic acid and heating for nine hours in the presence of 100 ml of SOCl_2 , the excess amount of SOCl_2 was distilled off under suction with a water pump. Then



40 ml of aqueous ammonia was added to the residue and refluxed for two hours. The product was collected on a filter. The final step involves the conversion of amide to the dinitrile compound. This was done by taking 300mg of amide and 1.2 grams of P_2O_5 , mixing well in a nitrogen filled



glove bag and placing in a cold finger trap. The mixture was then heated with a direct flame under suction. The white crystals were collected on the cold finger after 30 minutes. The yield was about 69%. The infrared spectrum shows a cyano stretch at 2240cm^{-1} as it was reported in the literature.

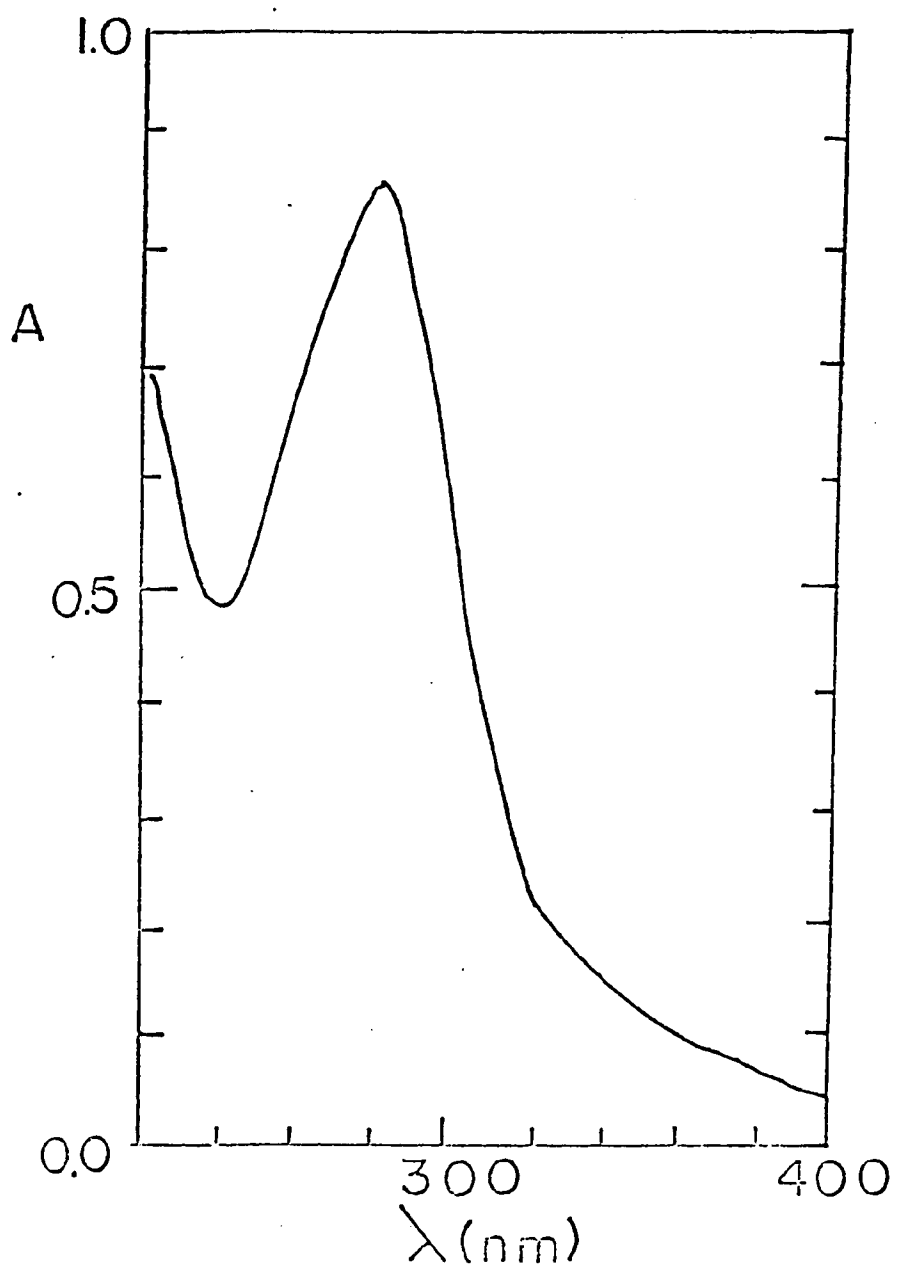
Trans-1,4-dicyanocyclohexane. The material obtained from KNK laboratories required purification. It was crystallized from boiling glacial acetic acid (30g to 50 ml) twice. The white needle-shaped crystals were washed copiously with water and air-dried, giving a yield of 75%. This material had the melting point of the trans isomer and 65°C . for the cis isomer: Liberman, A.L. and Lerman, B.M., Akad. Nauk. SSSR, Doklady, English Ed., 1971, 201, 905).

b. Ruthenium Compounds

Trifluoromethanesulfonatopentaammineruthenium(III)trifluoromethanesulfonate.

The synthesis for the trifluoromethanesulfonatopentaammine-ruthenium(III) proceeds as described by Sargeson and coworkers (42) for the analogous cobalt complex. trifluoromethanesulfonatopentaamminecobalt(III), with the following exceptions: (1) the ruthenium precursor, $\text{Ru}(\text{NH}_3)_5\text{Cl}_2 \cdot 2/3\text{H}_2\text{O}$, was allowed to react for 2 hours at 95°C instead of 1 hour, and (2) the product was filtered by equally dividing the reaction mixture into three medium porosity fitted filter funnels of 2.5cm diameter and 10.5 cm height fitted with a septum cap and under positive pressure of dry nitrogen gas. The most convenient scale for this preparation is 5-10g of product. Visible spectrum (in anhydrous HCF_3SO_3): 285cm^{-1} , $\epsilon=890$; (in sulfolane) 284cm^{-1} , $\epsilon=870$, (Fig 8).

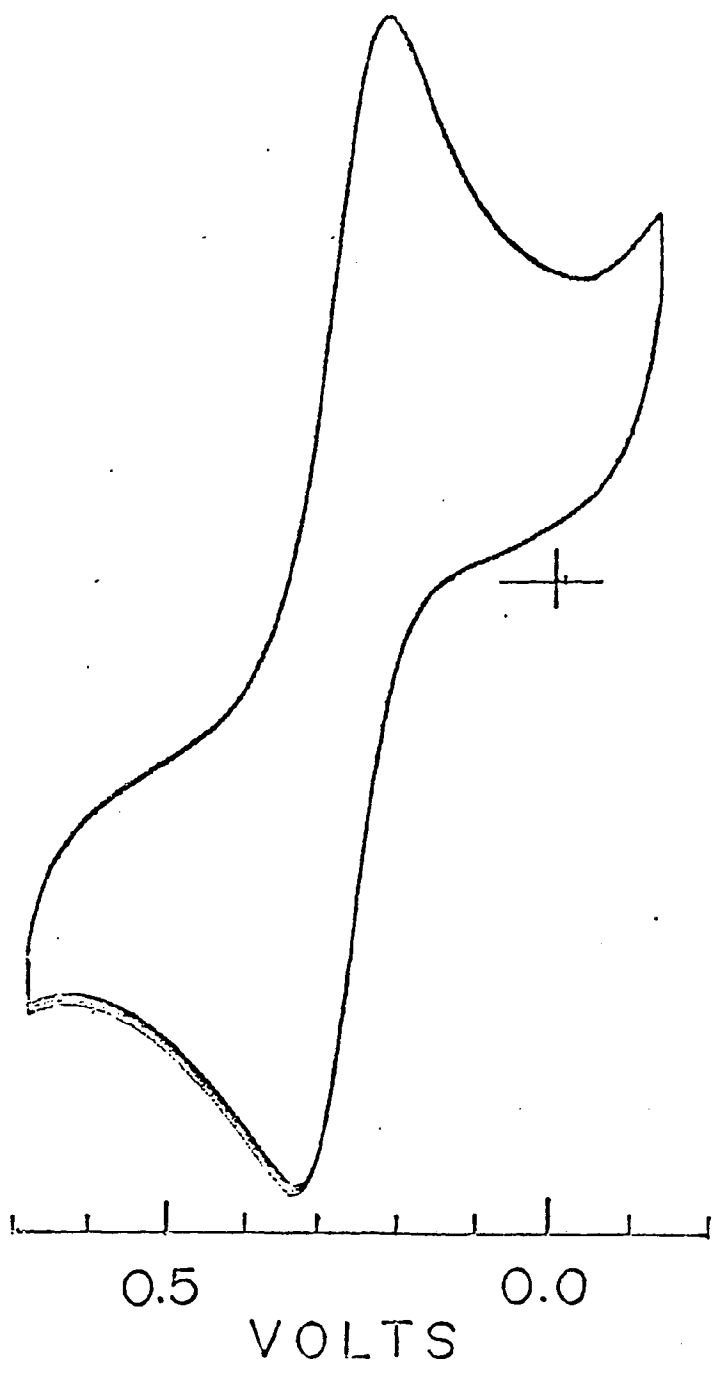
Figure 8. The visible absorption spectrum of
trifluoromethanesulfonatopentaammineruthenium(III)
trifluoromethanesulfonate in anhydrous
trifluoromethanesulfonic acid.



1-adamantylcarbonitrilopentaammineruthenium(III) trifluoromethanesulfonate

A new complex, (1-adamantylcarbonitrile)pentaammine-ruthenium(III), was synthesized using trifluoromethanesulfonato-pentaammineruthenium(III) as the starting material. The synthesis was done by dissolving 500mg of $[\text{Ru}(\text{NH}_3)_5(\text{CF}_3\text{SO}_3)](\text{CF}_3\text{SO}_3)_2$ in 10 ml of tetramethylenesulfone and adding an equal molar amount of the organic ligand, in this case 1-adamantylcarbonitrile. The reaction takes about thirty minutes at 60° C. The way to monitor these reactions is by using cyclic voltammetry. The reason for that is that the half wave potential of these ruthenium complexes are very sensitive to the nature of the ligands. This reaction has a reversible $E_{1/2}$ of 0.467V vs N.H.E. in dimethylformamide, 0.10M tetrabutylammonium perchlorate (Fig 9). The product was isolated by adding an equal volume of acetane followed by addition of diethyl ether approximately ten times the original volume. The crude product was recrystallized in a minimum amount of water and adding 5 M aqueous trifluoromethanesulfonic acid drop by drop until the acid concentration is approximately 1 M. For initial isolation of a complex, it is useful to periodically centrifuge the mixture and observe the visible-uv spectrum of the supernatant. The principal by-product appears from its spectrum to be $[\text{Ru}(\text{NH}_3)_5(\text{H}_2\text{O})](\text{CF}_3\text{SO}_3)_3$. The anhydride, $(\text{CF}_3\text{SO}_2)_2\text{O}$, may

Figure 9. The cyclic voltammogram of 1-adamantylcarbonitrilo-pentaammineruthenium(III)trifluoromethanesulfonate in dimethylformamide with 0.10M tetrabutylammonium perchlorate using platinum wire working and auxiliary electrodes and a Ag/AgCl reference electrodes.



be added to the initial reaction mixture to reduce the amount of this by-product. Visible- u.v. spectrum: 299 cm^{-1} ; $\epsilon = 626$; ($0.1\text{M H}_3\text{O}^+\text{CF}_3\text{SO}_3^-$) (Figure 10) and infrared spectrum: CN stretch 2290 cm^{-1} (Figures 12 and 13).

Figure 10. The visible absorption spectrum of
1-adamantylcarbonitrilopentaammineruthenium(III)-
trifluoromethanesulfonate in aqueous trifluoro-
methanesulfonic acid (0.1M).

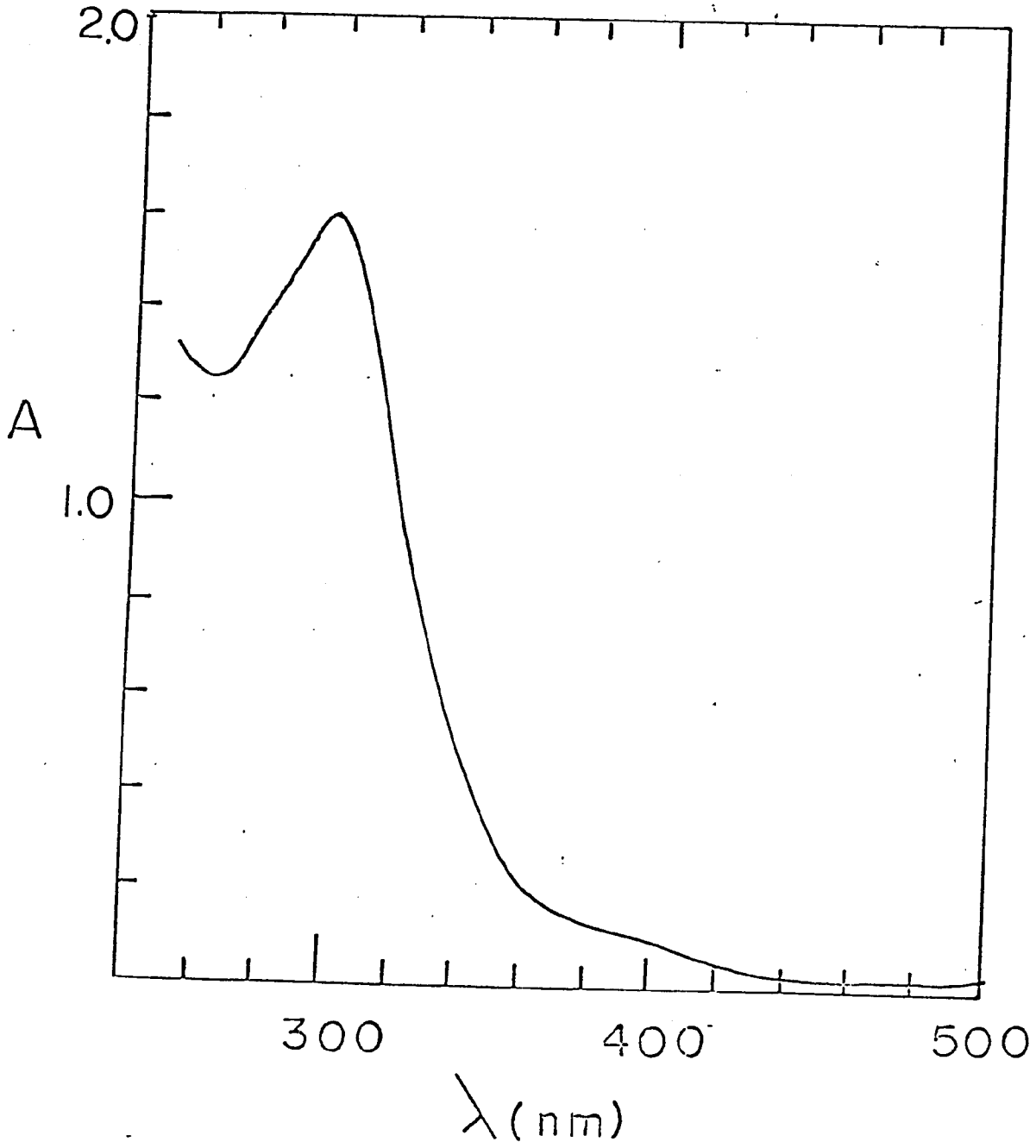


Figure 11. The visible absorption spectrum of the supernatant liquid in the synthesis of 1-adamantylcarbonitrilopentaammineruthenium(III) trifluoromethanesulfonate. This spectrum closely resembles that of an authentic sample of aquopentaammineruthenium(III) trifluoromethanesulfonate.

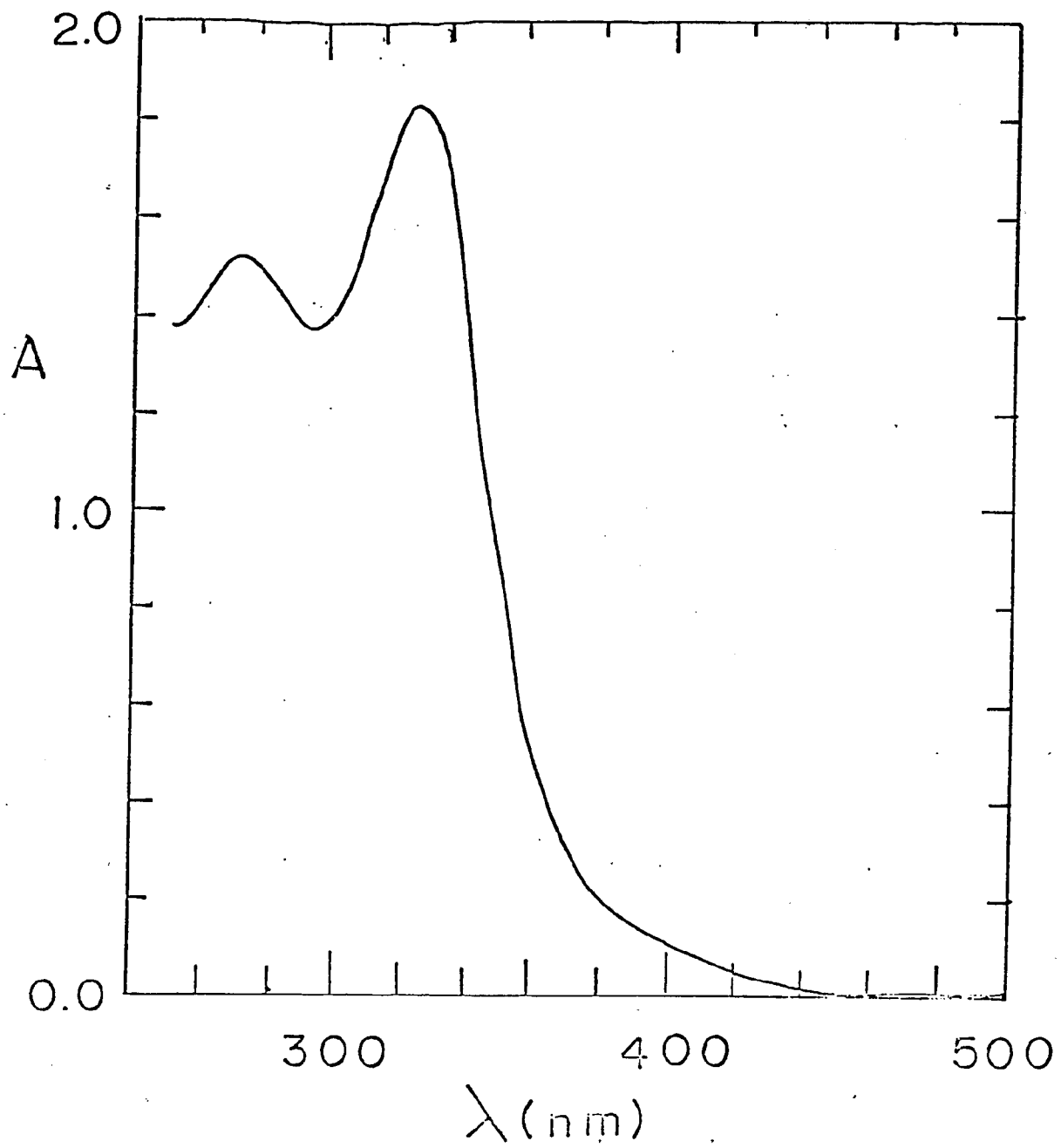


Figure 12. The infrared spectrum of 1-adamantylcarbo-
nitrilopentaammineruthenium(III) trifluoro-
methane sulfonate in a KBr pellet from 4000
to 1800 cm^{-1} . The peak assigned to the CN
stretch is at 2280 cm^{-1} .

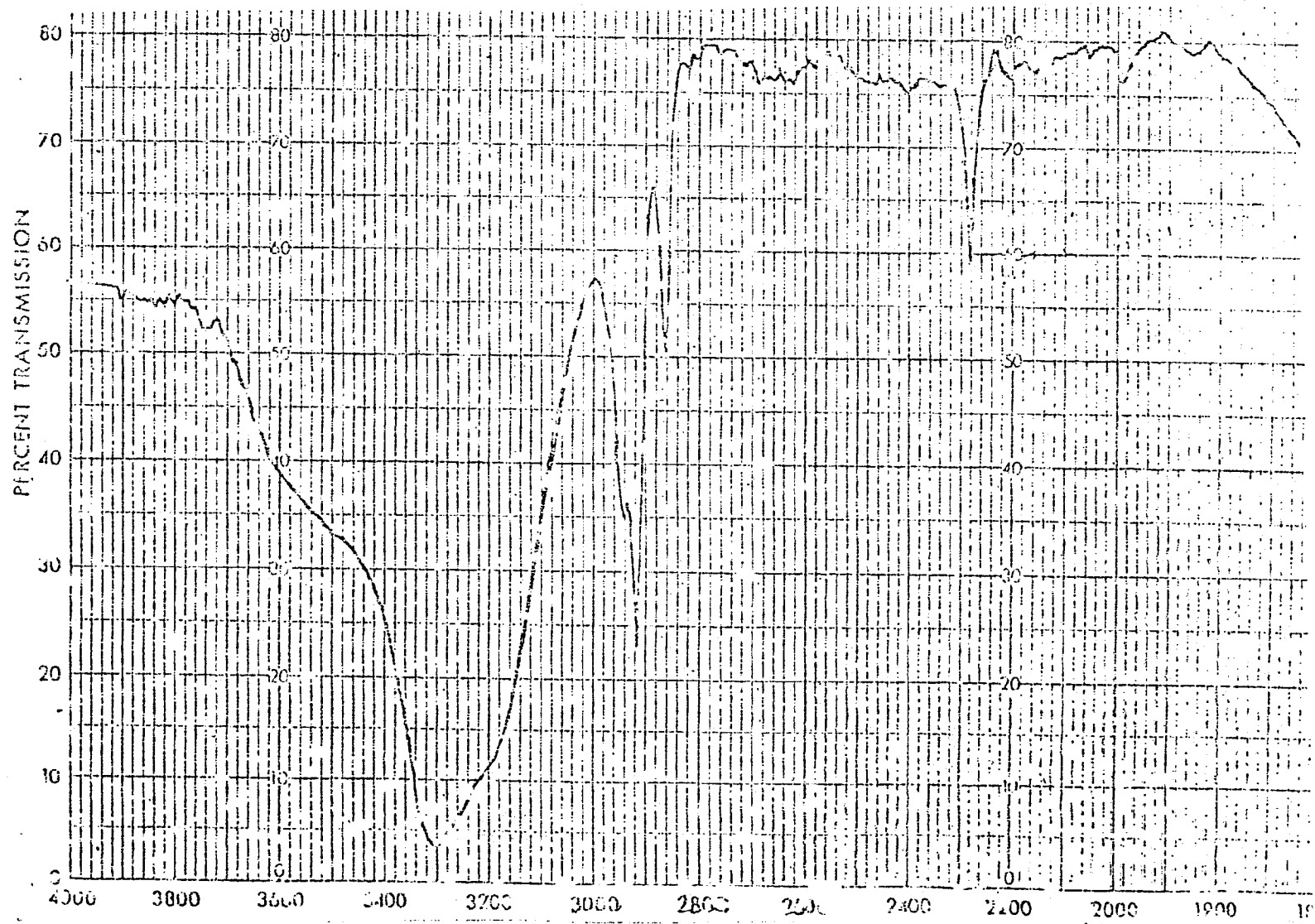
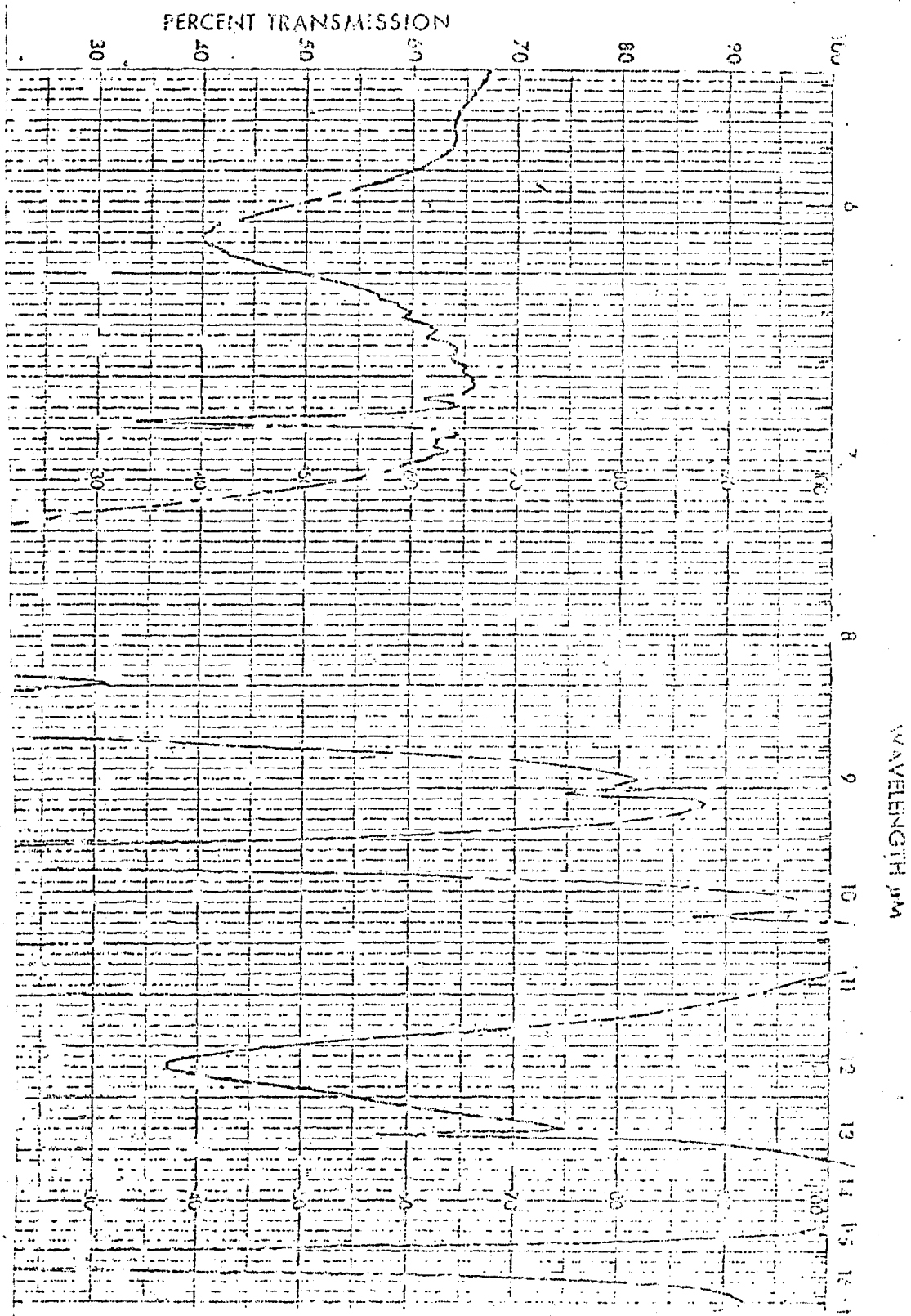


Figure 13. The infrared spectrum of 1-adamantylcarbonitrilo-
pentaammineruthenium(III) trifluoromethanesulfon-
ate in a KBr pellet from 1800 to 300 cm^{-1} .



C. Bimetallic Compounds

General Procedure

The synthesis of the bimetallic compounds involves first reacting chloroaquoamminecobalt(III) trifluoromethanesulfonate (obtained from the corresponding sulfate salt prepared by Schlessinger's method, followed by ion exchange chromatography) with the desired organic ligand in the presence of 10% excess trifluoromethane sulfonic anhydride using dried sulfolane as a solvent. In this reaction the anhydride removes the chloride and this is replaced by cyano group from the organonitrile ligand. The reaction mixture is heated for 15 minutes at 75^oC. The reaction is monitored with the aid of visible absorption spectroscopy. The complex is then isolated by extracting with methylene chloride and further characterization is done with the aid of an infrared spectrum. Once the cobalt is bound to one end of the ligand an equal molar amount of the trifluoromethanesulfonatopentaammine-ruthenium(III) in the presence of trifluoromethanesulfonic anhydride (using 10% excess of the anhydride). The reaction is carried out in dried double distilled sulfone. The reaction is carried out in dried distilled sulfone. The reaction mixture is heated up for 2 hours at 65^oC. The reaction is monitored with the aid of cyclic voltammetry. Figure 14 is a voltammogram for the 1,4-dicyano[2.2.2]-bicyclooctanepentaammineruthenium(III)-diaquotriamminecobalt(III) complex and Figure 15 is the

voltammogram for the μ -1,4-dicyano-[2.2.2]-bicyclooctane-pentaammineruthenium(III)-aquotetraamminecobalt(III) complex. The half-wave potential for the ruthenium complexes is generally very sensitive to the nature of the ligand. In this case the half wave potential shifted from -0.013v vs the neutral hydrogen electrode when the sulfone was bound to 0.467v when the 1,4-dicyano[2.2.2]bicyclooctane became bound to the ruthenium complex. Cyclic voltammetry is a better method by which to monitor the ruthenium reactions than is visible absorption spectra are quite similar in this region. After two hours the product is cooled to room temperature and isolated by addition of an equal volume of acetone and a ten-fold volume of diethyl ether. The bimetallic product is recrystallized by dissolution in a minimum amount of 0.01 molar trifluoromethanesulfonic acid, filtration to remove pentaammineruthenium(III) impurities, and addition of 10M aqueous trifluoromethanesulfonic acid until the total acid concentration is about 4M. The analytical results are found to be in good agreement with the calculated ones. The different bimetallic complexes I have synthesized using this method are: one, μ -1,4-dicyano[2.2.2]bicyclooctanepentaammineruthenium(III)aquotetraamminecobalt(III); two, μ -1,4-dicyano[2.2.2]-bicyclooctanepentaammineruthenium(III)diaquotriamminecobalt(III); three, 1,4-dicyanocyclohexanepentaammineruthenium(III)-aquotetraamminecobalt(III); four, 1,4-dicyanocyclohexanepentaammineruthenium(III)diaquotriamminecobalt(III);

Figure 14. The cyclic voltammogram of μ -1,4-dicyano-[2.2.2]-bicyclooctane-pentaammineruthenium(III)diaquotriamminecobalt(III)trifluoromethanesulfonate in dimethylformamide with 0.10M tetrabutylammonium perchlorate. The working and auxiliary electrodes were platinum wires and the reference electrode was Ag/AgCl.

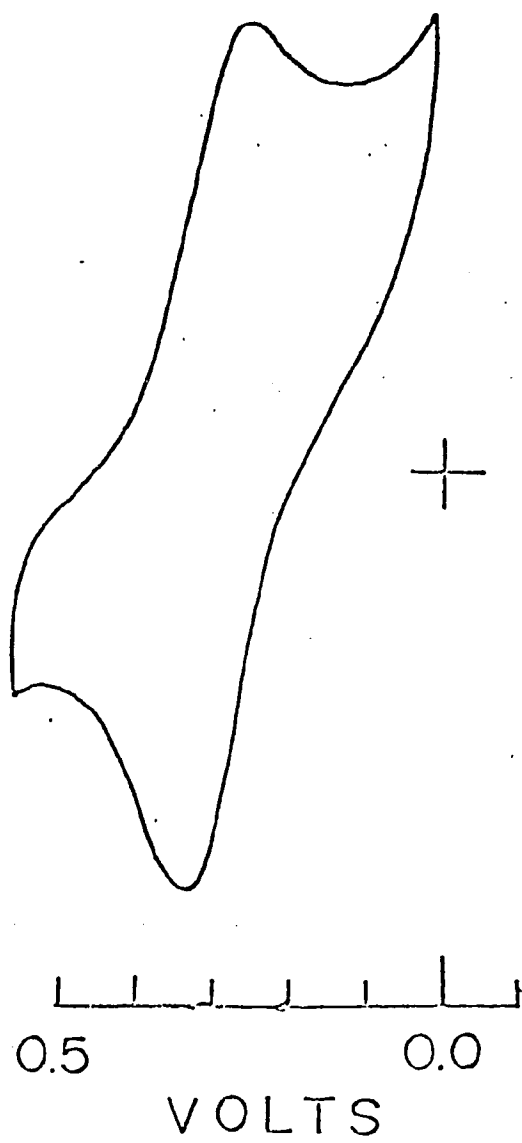
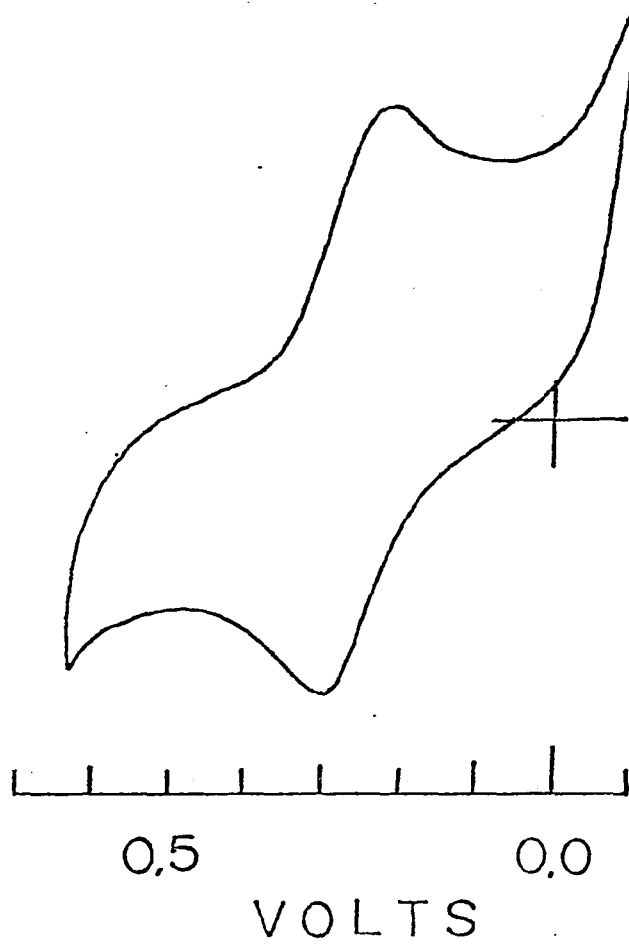


Figure 15. The cyclic voltammogram of μ -1,4-dicyano-[2.2.2]-bicyclooctanepentaammineruthenium(III) aquotetraamminecobalt(III) trifluoromethanesulfonate in dimethylformamide with 0.10M tetrabutylammonium perchlorate. The working and auxiliary electrodes were platinum wires and the reference electrode was Ag/AgCl.



five, μ -1,4-dicyano-[2.2.2]bicyclooctanebis(pentaammine-ruthenium(III)).

μ -1,4-dicyanobicyclo-[2.2.2]-octanepentaammineruthenium(III)-
diaquotriamminecobalt(III) trifluoromethanesulfonate

The procedure for the synthesis of μ -1,4-dicyano[2.2.2]-bicyclooctanepentaammineruthenium(III)diaquotriamminecobalt(III)-trifluoromethanesulfonate involved reacting 0.200g of the chlorodiaquotriammine with 0.668g of 1,4-dicyano[2.2.2]-bicyclooctane in two ml of dried double distilled sulfolane in the presence of 80 λ of trifluoromethane sulfonic anhydride. This reaction takes 10 to 15 minutes at 80 $^{\circ}$ C. In order to keep the temperature constant an oil bath was used in top of a hot plate. This reaction is monitored with the aid of a visible absorption spectra. The peak shifts from 523 cm^{-1} initially to 506 cm^{-1} (Figure 16) at the end of 15 minutes. The material was allowed to come to room temperature and then the product was isolated by extracting with methylene chloride. For each ml of sulfane, 10 ml of water and 50 ml of CH_2Cl_2 are added. The 10 ml of water which retains the complex is extracted 8 to 10 times with 50 ml portions of methylene chloride. The water layer is dried using the rotatory evaporator. Further characterization is done with the aid of an infrared spectrum (Figure 17 and 18) an average yield at this step is between 75-80%. Once the cobalt complex is bound at one end of the ligand then the ruthenium complex is added to the other end. To 0.100g of diaquotriamminecobalt(III) trifluoromethanesulfonate in 2 ml of double distilled sulfolane and 25 λ of trifluoro-

Figure 16. The visible absorption spectrum of μ -1,4-dicyano-[2.2.2]-bicyclooctanediaquatriamminecobalt(III)-trifluoromethanesulfonate in acidic aqueous solution.

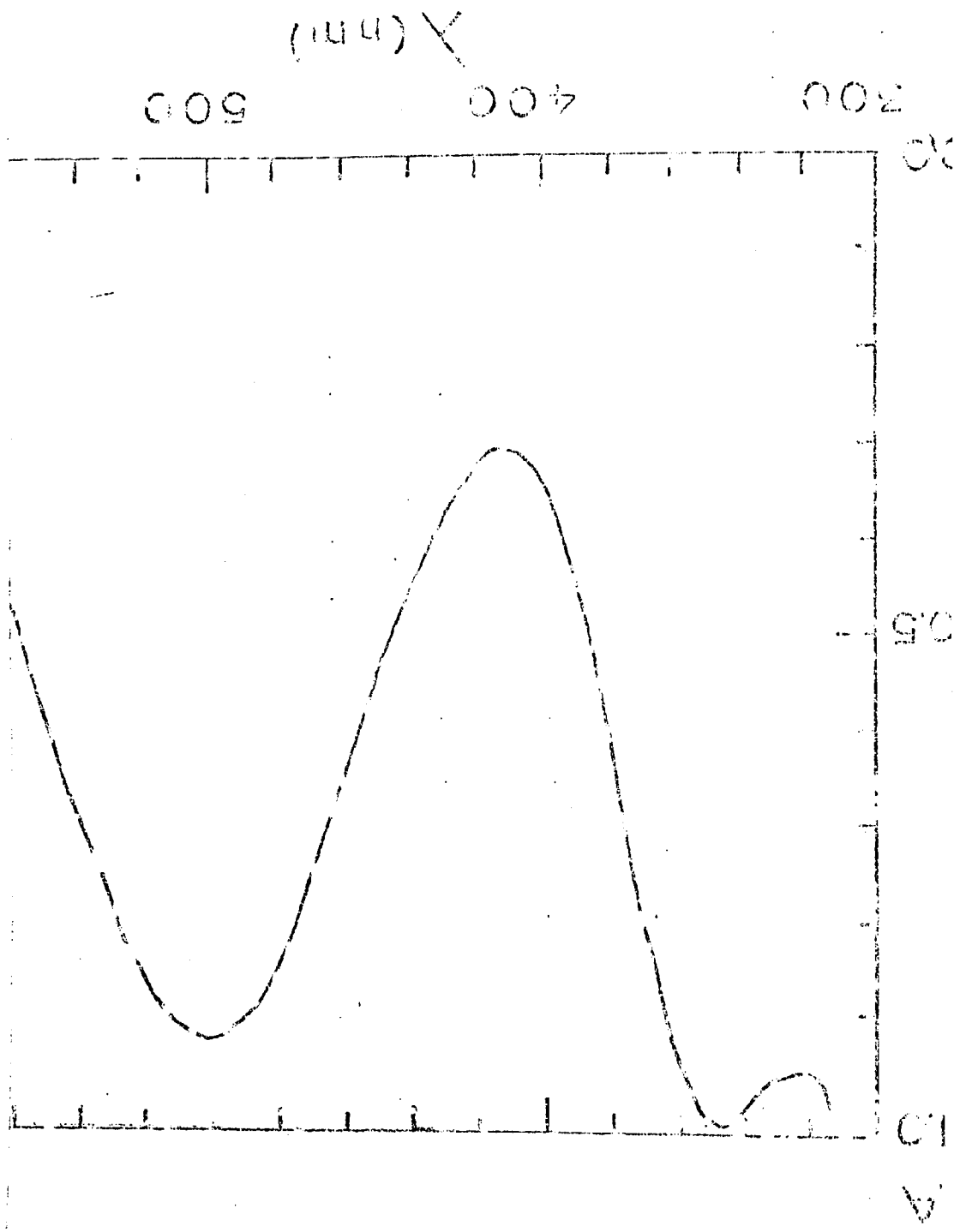


Figure 17. The infrared spectrum of 1,4-dicyano-[2.2.2]-bicyclooctanediaquotriamminecobalt(III)trifluoromethanesulfonate in a KBr pellet, from 4000 to 1800 cm^{-1} . The peak assigned to the free CN group is at 2240 cm^{-1} .

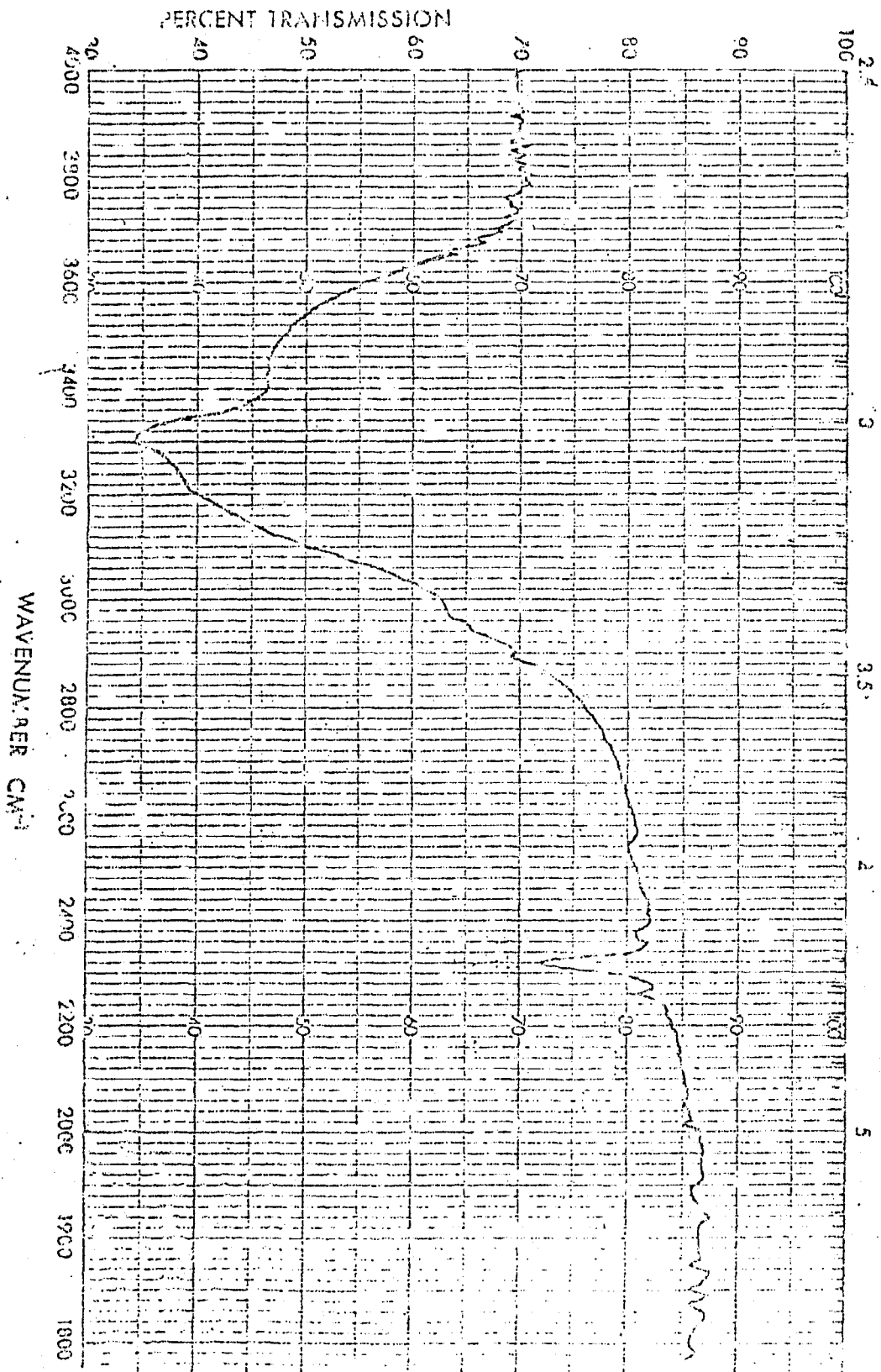
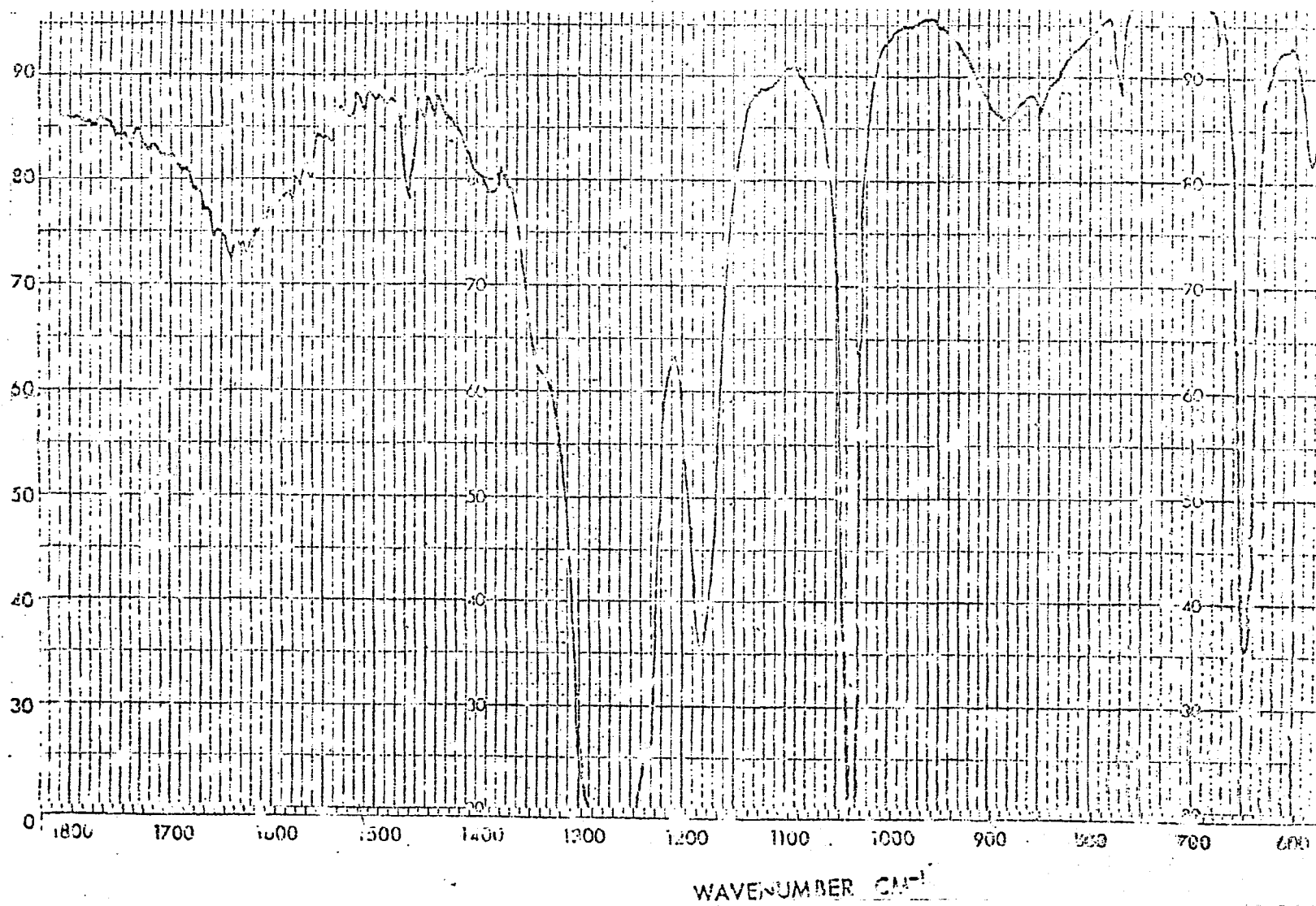


Figure 18. The infrared spectrum of μ -1,4-dicyano-[2.2.2]-bicyclooctanediaquotriamminecobalt(III)trifluoromethanesulfonate in a KBr pellet, from 1800 to 400 cm^{-1} .

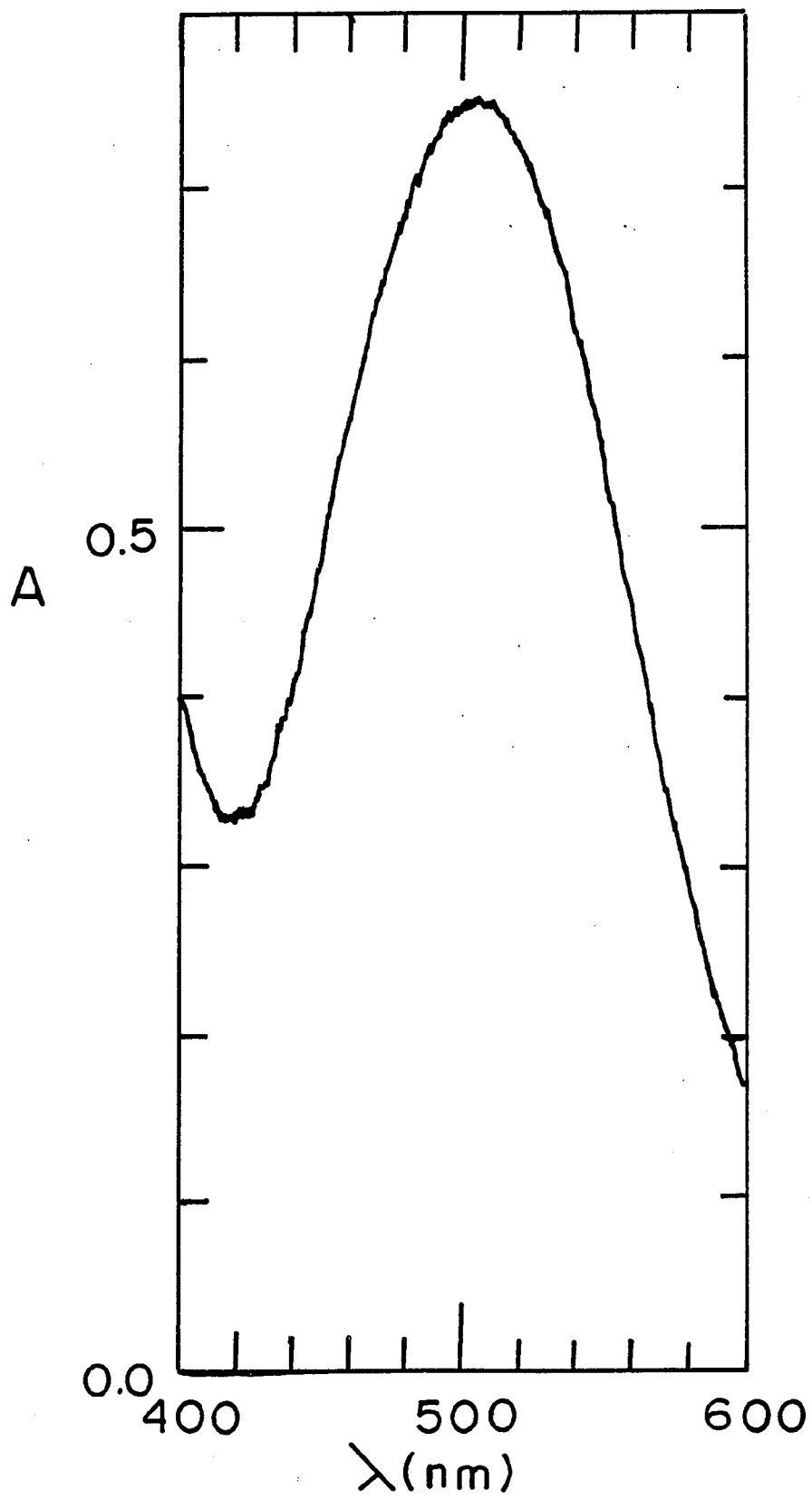


methane sulfonic anhydride were added. Once they were dissolved, which took about a minute or two, 0.0837g of trifluoromethane-sulfonatopentaammine ruthenium(III) were added. The reaction takes two hours at 60° C. Again the temperature was kept constant using an oil bath. This reaction is monitored with the aid of cyclic voltammetry as I mentioned before. In this case the half wave potential shifted from -0.013v to 0.467v vs N.H.E. After two hours the product was allowed to come to room temperature. The bimetallic product was isolated by adding 2 ml of acetone and 20 ml of diethyl ether. Then the complex was recrystallized by dissolution in a minimum amount of water and addition of 10 ml aqueous trifluoromethane sulfonic acid until the total concentration was about 4M. The average yield after the recrystallization step is about 50%. The analytical results are $\text{RuCoC}_{16}\text{H}_4\text{N}_{10}\text{F}_{18}\text{S}_6\text{O}_{20}$: calc. C,13.86%; H,2.89%; N,10.11% Found (MicAnal, Tucson,Az)C,14.55%; H,2.77%; N,10.63%.

μ -1,4-dicyano-[2.2.2]bicyclooctanepentaammineruthenium(III)-
aquotetraamminecobalt(III)trifluoromethanesulfonate

The synthetic procedure for μ -1,4-dicyano[2.2.2]-bicyclooctanepentaammineruthenium(III)aquotetraamminecobalt(III)trifluoromethanesulfonate involves the same steps as described above for the μ -1,4-dicyano[2.2.2]bicyclooctanepentaammineruthenium(III)diaquotriamminecobalt(III) species. The typical amounts used were 0.100 gram of cobalt starting material in one M double distilled dried sulfolane in the presence of 40 λ of trifluoromethanesulfonic anhydride. The visible absorption spectrum shift is from 510 cm^{-1} to 490 cm^{-1} (Figure). The yield was 67%. The next step was also the same as described above. I used 0.100g of aquotetraammine μ -1,4-dicyano-[2.2.2]-bicyclooctanecobalt(III)trifluoromethanesulfonate in two ml of sulfane in the presence of 25 λ of $(\text{CF}_3\text{SO}_2)_0$. The reaction took two hours at 60 $^\circ$ C. and the yield was 88% before recrystallization and about 47% after recrystallization. The analytical results are: $\text{RuCoC}_{16}\text{H}_{41}\text{N}_{11}\text{F}_{18}\text{S}_6\text{O}_{19}$: calc. C,13.88%; H,2.96%; N,11.13. Found (MicAnal Tucson, Az) C,13,71%; H,2.72%; N,11.30.

Figure 19. The visible absorption spectrum of 1,4-dicyano-[2.2.2]-bicyclooctaneaquotetraamminecobalt(III)-trifluoromethanesulfonate in acidic aqueous solution.



μ -trans-1,4-dicyanocyclohexanepentaammineruthenium(III)-
diaquotriamminecobalt(III) trifluoromethanesulfonate

The synthetic procedure for μ -1,4-dicyanocyclohexane-pentaammineruthenium(III)diaquotriamminecobalt(III) trifluoromethanesulfonate involves the steps as described for the previous bimetallic complexes. Typical amounts used were 0.400g of $\text{Co}(\text{NH}_3)_3(\text{H}_2\text{O})_2\text{Cl}(\text{CF}_3\text{SO}_3\text{SO}_3)_2$ and 0.1118g of μ -1,4-dicyanocyclohexane in 4.0 ml of double distilled dried sulfolane in the presence of 160 λ of trifluoromethanesulfonic anhydride. The visible absorption spectrum at the end of 15 minutes shows a peak at 510 nm. The yield was 72%. The next step is as described above. In a typical preparation of this species, I used 0.300g of diaquotriamminedicyanocyclohexanecobalt(III)-trifluoromethanesulfonate and 0.2602g of $\text{Ru}(\text{NH}_3)_5(\text{CF}_3\text{SO}_3)(\text{CF}_3\text{SO}_3)_2$ in 6 ml of double distilled dried sulfolane in the presence of 80 λ of trifluoromethanesulfonic anhydride. The reaction took two hours at 60° C. and the yield after recrystallization was about 45%. The analytical results are $\text{RuCoC}_{14}\text{H}_{38}\text{N}_{10}\text{F}_{18}\text{S}_6\text{O}_{20}$: Cal. C, 12.36%; H, 2.79%; N, 10.30%, Found (MicAnal Tucson Az) C, 12.76%; H, 2.80%; N, 11.21%.

μ -trans-1,4-dicyanocyclohexanepentaammineruthenium(III)-
aquotetraamminecobalt(III) trifluoromethanesulfonate

The synthetic procedure for the μ -1,4-dicyanocyclohexanepentaammineruthenium(III) aquotetraamminecobalt(III)-trifluoromethanesulfonate involves the steps described for the previous bimetallic complexes. In a typical preparation, 0.400g of $\text{Co}(\text{NH}_3)_4(\text{H}_2\text{O})\text{Cl} (\text{CF}_3\text{SO}_3)_2$ and 0.116g of μ -1,4-dicyanocyclohexane in 4.0 ml of double distilled dried sulfolane in the presence of 160 λ of trifluoromethanesulfonic anhydride. The visible absorption spectrum at the end of 15 minutes shows a peak at 490 cm^{-1} . The yield was 73%. In the next step, as 0.200g of trans-1,4-dicyanocyclohexane aquotetraamminecobalt(III)-trifluoromethanesulfonate and 0.174g of trifluoromethanesulfonato-pentaammineruthenium(III) trifluoromethanesulfonate were combined in 4 ml of double distilled sulfolane in the presence of 55 λ of trifluoromethanesulfonic anhydride. The reaction took 2 hours at 60 $^\circ$ C. The yield after crystallization was about 45%.

μ -1,4-dicyano-[2.2.2]-bicyclooctane-bis(pentaammineruthenium(III)) trifluoromethanesulfonate

The synthetic procedure for the 1,4-dicyano[2.2.2] - bicyclooctane-bis(pentaammineruthenium(III) trifluoromethanesulfonate involves the single addition of two moles of the metal complex to one mole of the ligand and the bimetallic complex is formed in one synthetic step since both metal ends are the same. In a typical synthesis, 0.100g of trifluoromethanesulfonatopentaammineruthenium(III) and 0.01265g of 1,4-dicyano[2.2.2]bicyclooctane in 2.0 ml of double distilled dried sulfone in the presence of 30% of trifluoromethanesulfonic anhydride. The reaction required two hours at 60° C. It was monitored with the aid of cyclic voltammetry. The yield was about 49%. The analytical results are $\text{Ru}_2\text{C}_{16}\text{H}_{42}\text{N}_{12}\text{F}_{18}\text{S}_6\text{O}_{18}$: calc. C,13,50%; H,2.95%; N,11,81% Found (MicAnal Tucson, Az) C,13,55%; H,2.73%; N,11.34%. Visible-uv spectrum peaks 298 nm, $\epsilon=1367 \text{ M}^{-1}\text{cm}^{-1}$ (Figure 20). Infrared spectrum CN stretch 2300 cm^{-1} (Figures 21 and 22). A cyclic voltammogram of μ -1,4-dicyano[2.2.2]bicyclooctane-bis(pentaammineruthenium(III) trifluoromethanesulfonate can be seen in Figure 23.

Figure 20. The visible absorption spectrum of a $6.0 \times 10^{-4} \text{M}$ solution of μ -1,4-dicyano-[2.2.2]-bicyclooctane-bis(pentaammineruthenium(III)trifluoromethane sulfonate (1.00 cm cuvette with a 1.00cm H₂O blank).

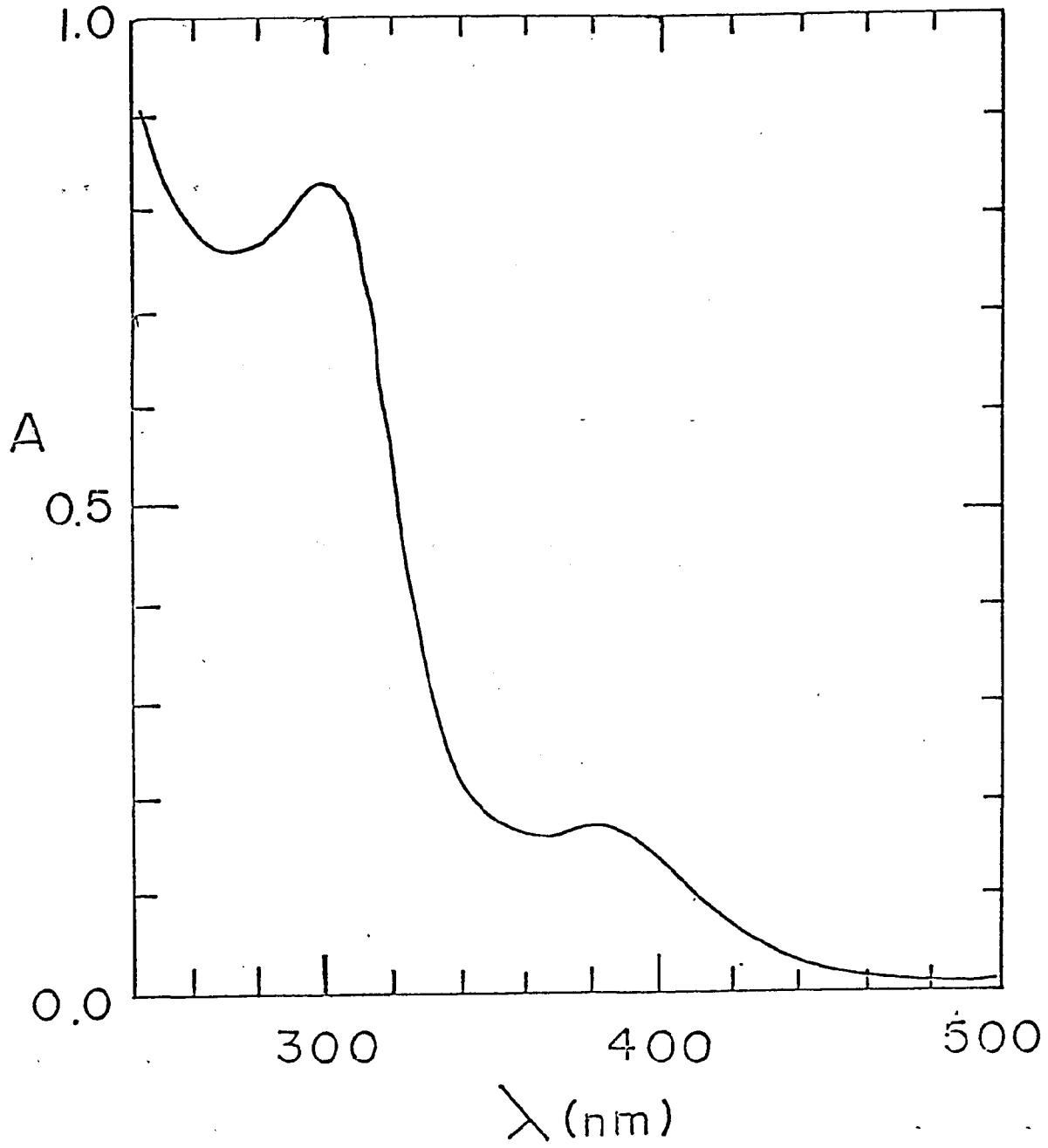
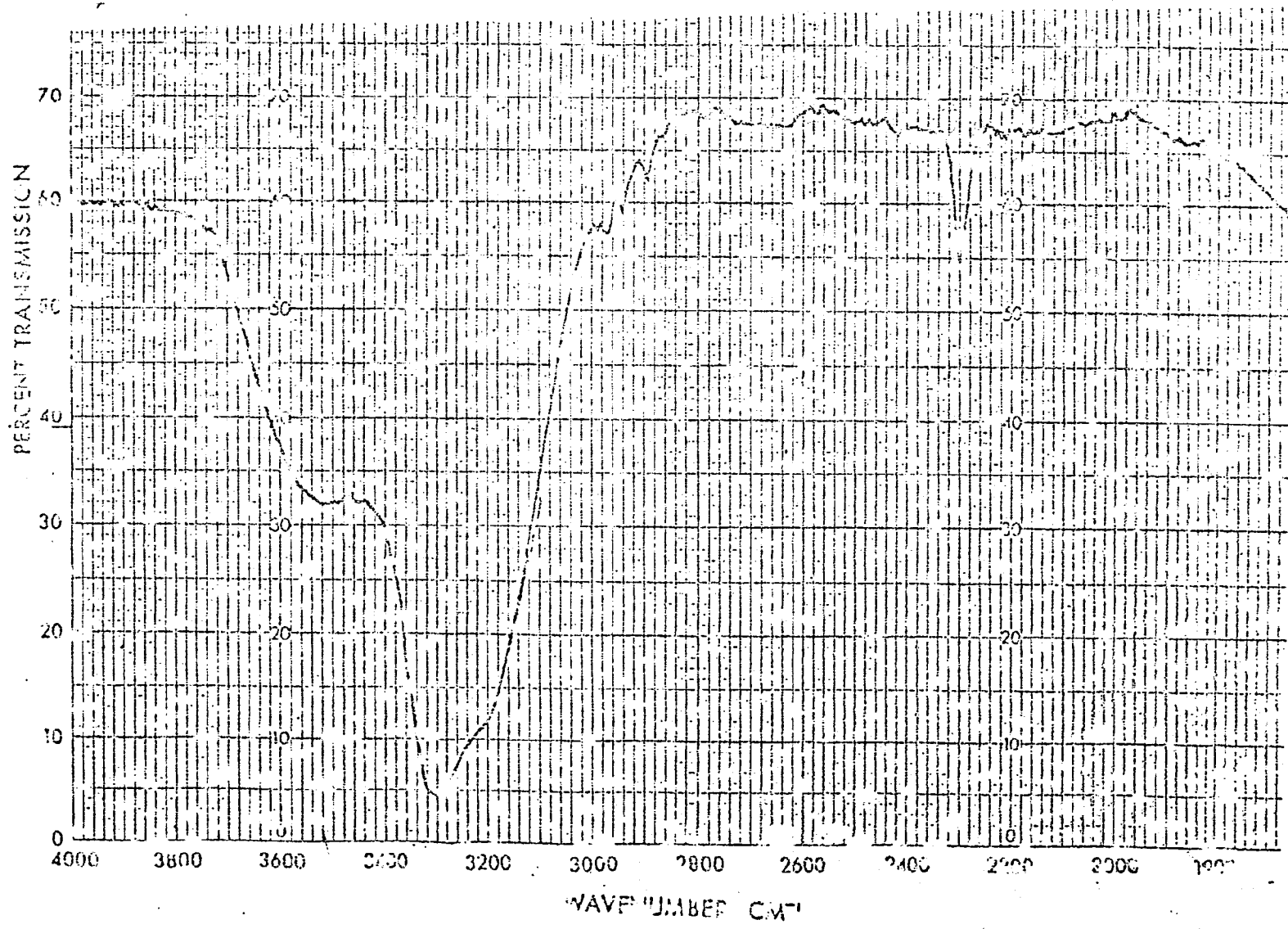


Figure 21. The infrared spectrum of μ -1,4-dicyano-[2.2.2]-bicyclooctane-bis(pentaammineruthenium(III)trifluoromethane sulfonate in a KBr pellet, from 4000 to 1900 cm^{-1} . The peak assigned to the CN stretch is at 2300 cm^{-1} .



104

Figure 22. The infrared spectrum of μ -1,4-dicyano-[2.2.2]-bicyclooctane-bis(pentaammineruthenium(III) trifluoromethane sulfonate in a KBr pellet, from 1300 to 400 cm^{-1} .

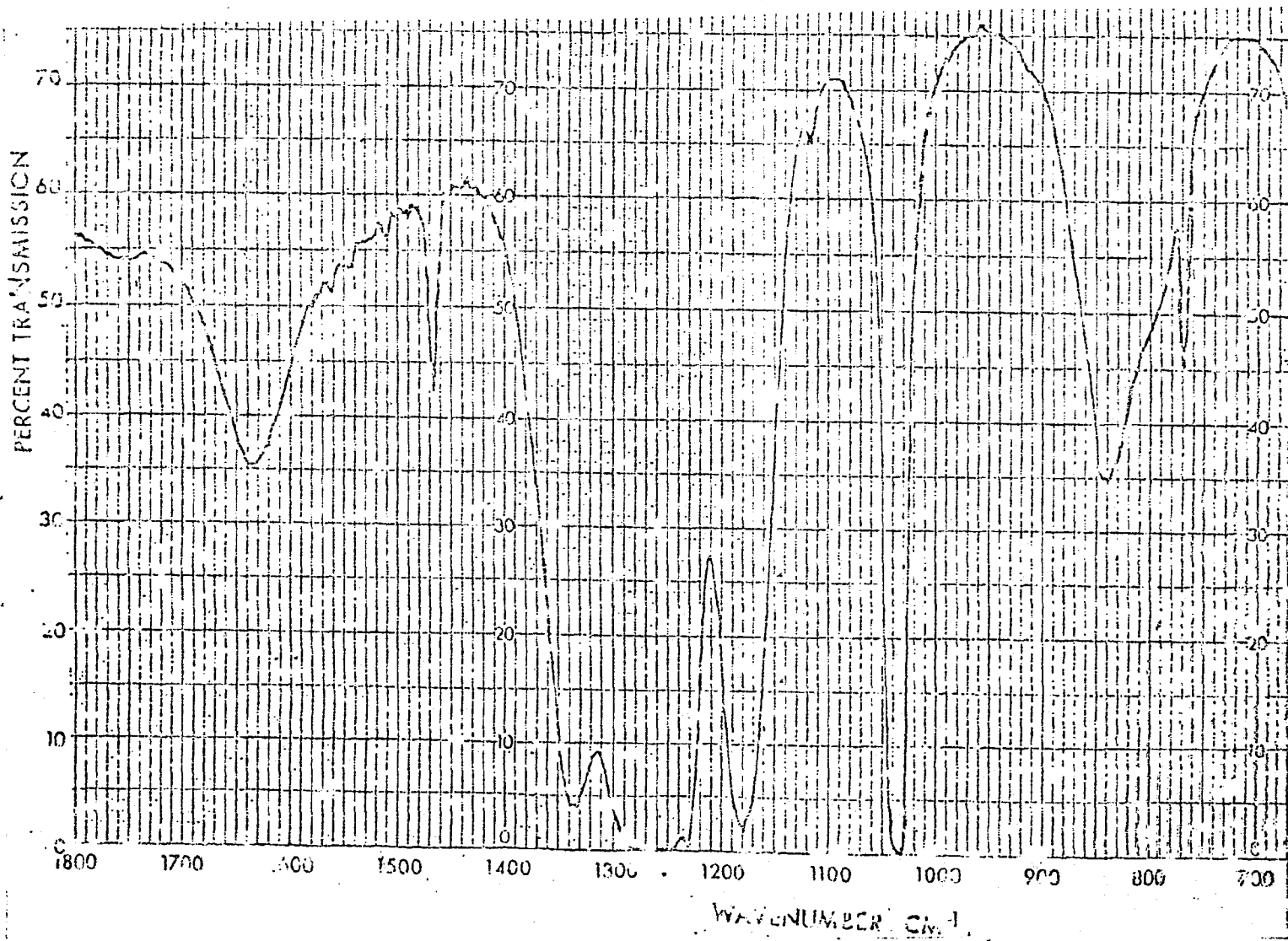
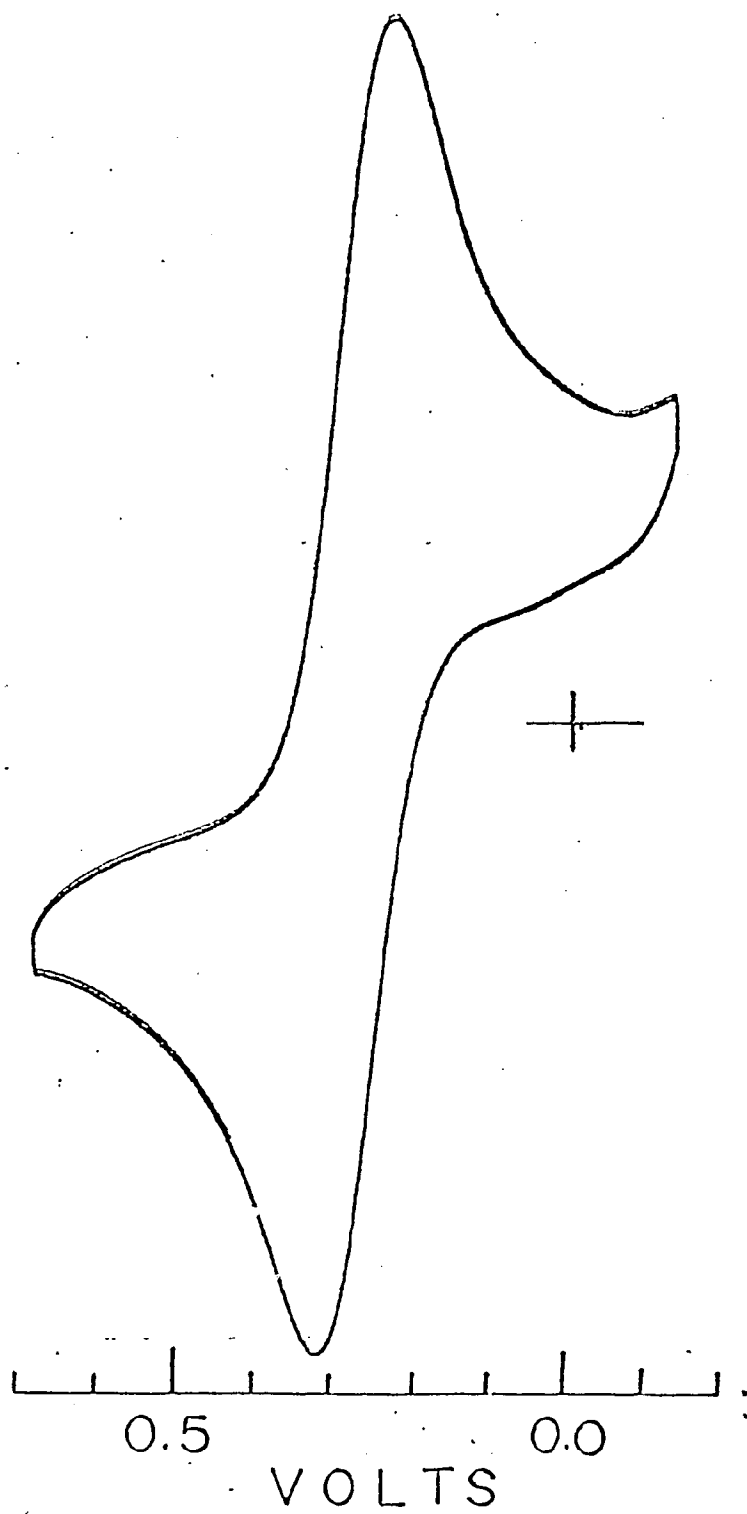


Figure 23. The cyclic voltammogram of μ -1,4-dicyano-[2.2.2]-bicyclooctane-bis(pentaammineruthenium(III) trifluoromethanesulfonate) in dimethylformamide with 0.10M tetrabutylammonium perchlorate. The working and auxiliary electrodes were platinum wires and the reference electrode was Ag/AgCl.



3. Kinetics of Complex Formation

The kinetic characterization of the formation of nitrile and halide complexes of trifluoromethanesulfonatopentaamine-ruthenium(III) was done in acidic double distilled sulfolane (0.01M in trifluoromethanesulfonic acid monohydrate) at 37°C. The ruthenium concentration used was millimolar. All the reactions were done having the ligand in pseudo-first-order excess. Solutions were allowed to equilibrate in the thermostatted cuvette holder of the spectrophotometer before the reactions were initiated. The changes in concentration were monitored continuously at a single wavelength. Data were analyzed by using least-squares fitting programs available with the Prophet computing system (53). The kinetic characterization of each of the different ruthenium(III) compounds studied was done the same way as described above except for the formation of the 4-phenylpyridine complex. In this case the formation was monitored differently because the spectral changes in the visible-u.v. region upon complexation are small. Aliquots of the reaction mixture were removed periodically and the complex was reduced to give the characteristic spectrum of the pentaammine -4-phenyl-pyridineruthenium(II) complex. The procedure was as follows: a millimolar solution of trifluoromethanesulfonatopentaammineruthenium(III) trifluoromethanesulfonate in tetramethylene sulfone with no added acid was deaerated in a 10 ml bubbler flask on an argon line. The ligand, 4-phenylpyridine (twice recrystallized from methanol),

was dissolved in tetramethylene sulfone and deaerated in a separate 10 ml bubbler flask. When the two solutions had been mixed, the progress of the reaction was monitored by reducing an aliquot of the reaction mixture with hexaammine-ruthenium(II) (produced from hexaammineruthenium(II) trifluoromethanesulfonate in acetone over amalgamated zinc) and recording the visible absorption spectrum. The temperature of the reaction mixture was maintained at 48° C. (to facilitate handling of the tetramethylene sulfone solutions which can solidify at room temperature) using an oil bath.

4. Kinetics of Complex Decomposition by Hydrolysis

The complexes used for the study of the acid hydrolysis of organonitriles bound to ruthenium(III) were synthesized the following way. The starting ruthenium complex was the trifluoromethanesulfonatopentaammineruthenium(II) trifluoromethanesulfonate (whose synthesis was described previously). This complex was combined with an excess of the ligand in sulfolane in the presence of trifluoromethanesulfonic anhydride. The anhydride removes any trace amounts of water. The reaction mixture was heated for about 15 minutes at 60°C and then cooled to room temperature. Each product was isolated by adding an equal volume of acetone and diethyl ether in an amount about 20 times the original volume. The product was quickly dissolved in a minimum amount of water, filtered and recovered by precipitation with 5 M trifluoromethanesulfonic acid. The products were identified by their visible-u.v. spectra (52). The trifluoromethanesulfonate reagents described previously in this chapter.

5. Instrumentation

a. Visible-u.v. and Infrared Spectra

Kinetic runs were recorded on both with thermostatted Cary 14 or Beckman DU-8 spectrophotometers. The Visible-u.v. spectra for the complexes were recorded on either Cary 14 or Beckman DU-8 spectrophotometers. Infrared spectra were recorded on a Beckman 4240 recording spectrophotometer (range: 4000-250 cm^{-1}). The KBr disc method was used for all spectra.

b. Cyclic Voltammetry

The apparatus used for recording cyclic voltammograms consisted of a Bisanalytical CV-1A Cyclic Voltammetry Unit. The working electrode was a coiled platinum wire, a second platinum wire was used as an auxiliary electrode and a silver/silver chloride electrode was used as the reference. The solvent was dimethylformamide and the electrolyte was 0.1M tetrabutylammoniumperchlorate (recrystallized). Voltammograms were recorded on an Houston Omnigraphic 2000 x-y recorder. The half wave potentials, $E_{1/2}$, were calculated from the arithmetic average of the peak potentials. Measured potentials were converted to the N.H.E. scale by adding +0.207v to the measured $E_{1/2}$ values. Reversible $E_{1/2}$'s are obtained with these complexes.

6. APPARATUS

a. Inert gas train

An all-glass inert gas train was used to deaerate reactant mixtures for kinetic studies and for some synthetic work. Four branches leading from a common glass line each terminated in a standard socket joint. Gas flow to each branch was controlled with a teflon-in-glass Fisher and Porter Angle Needle Valve (bore range 0-4 mm). Argon (Presto - Sales, New York) used to provide inert atmosphere, was first passed through two chromous scrubbers and then into the glass line. The only non-glass portion of the train was tygon tubing connecting the latter scrubber to the glass line. Solutions requiring deaeration were contained in Erlenmeyer flasks adapted for this purpose by attaching an L-shaped gas inlet tube near the base of the flask. The other end of the tube terminated in a ball joint that was clamped to a socket of the inert gas line. The top of the Erlenmeyer was protected by a loose fitting thimble-shaped glass insert. The glass insert had a 1-2mm hole at its lowest point for withdrawal of the deaerated solutions by means of a syringe. The greater density of argon over air was relied upon to prevent oxygen from entering the system. These adapted Erlenmeyer flasks are referred to throughout as bubbling flasks.

b. Syringes

Glass, gas tight syringes with Teflon plungers (Hamilton Company) were used for most work. All syringes used to handle deoxygenated solutions were deaerated by flushing them with Argon and then rinsing the syringe with two small portions of the solution itself.

c. Chromous scrubbing towers

The chromous solutions was prepared by dissolving chromium(III)perchlorate (G.F.Smith) in perchloric acid to make a final solution 0.2M in total chromium and 0.5M in HClO_4 . The zinc amalgam for the towers was prepared by the method of Stone and Hume (53). In a typical preparation, 4.7 grams of HgCl_2 (Fisher) were dissolved in 75 ml of H_2O . About 70 grams of $\text{Zn}(0)$ (Mossy, Baker) were rinsed three times with water and then added to 4M HClO_4 . The mercuric solution was poured into the vigorously reacting HClO_4 - $\text{Zn}(0)$ mixture and stirred. Bubbling ceased within one minute and stirring was continued until all Hg was removed from solution. (Only white $\text{Zn}(\text{OH})_2$ precipitated upon adjusting the pH of an aliquot to 10 with 50 percent NaOH solution.) The solution was then decanted and the zinc was rinsed approximately six times with house distilled water.

C. Results and Discussion

1. Synthesis

A very important objective of this project was to develop a synthesis for mixed bimetallic complexes which avoided ruthenium(II) as an intermediate. This has been accomplished with the aid of Sargeson's and coworkers' idea of using labile trifluoromethanesulfonate complexes as intermediates (59).

We tried several different ways of making the bimetallic complexes which did not work before we developed the method mentioned here for making the bimetallic complexes. One method that did not work involved using a drying agent such as P_2O_5 to remove the water ligand from chloroaquotetraamminecobalt(III) and adding the desired ligand. The problem with this approach was that P_2O_5 also removed the chloro ligand, therefore, we obtained a mixture of cobalt complexes. Some of the product had one nitrile ligand bound and some contained two cyano ligands. Another method that we tried was to try to make the trifluoromethanesulfonatoaquotetraamminecobalt(III) trifluoromethanesulfonate and then add the ligand. However this method did not work either. It appears that the anhydrous HCF_3SO_3 used to remove the chloride ligand removes the water ligand. Again I obtained a mixture of products. Some that had one nitrile ligand and others with two nitrile ligands

attached. The method that works involves starting with chloroaquatetraamminecobalt(III) and adding the ligand in the presence of trifluoromethanesulfonic anhydride. The anhydride removes only the chloride, which is then replaced by the cyano group of the ligand. Once the ligand is bound to one end to the cobalt complex, the other end can be bound to ruthenium by adding trifluoromethanesulfonatopentaamine-ruthenium(III)trifluoromethanesulfonate. The very labile trifluoromethanesulfonato ligand is replaced by the cyano group that is free to bind.

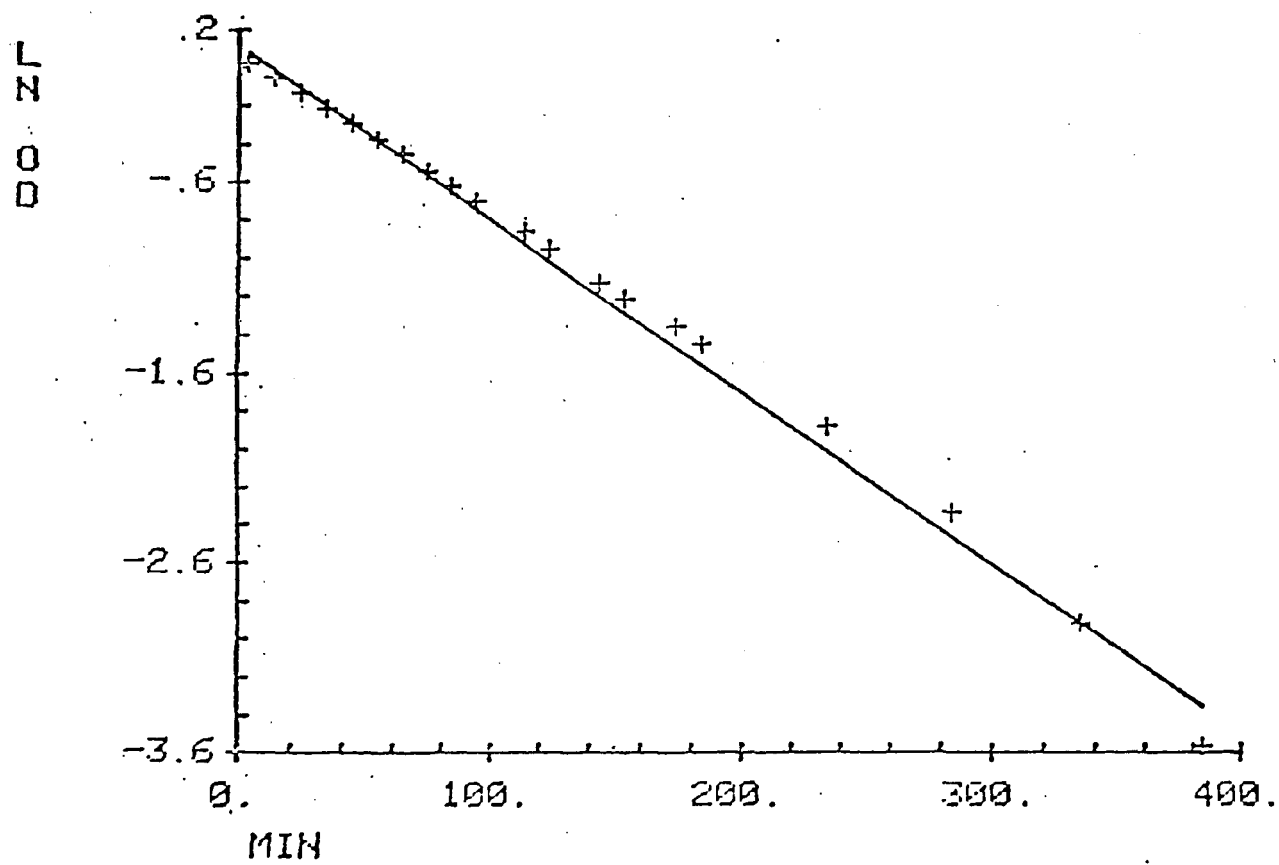
2. Formation Kinetics

Table 1 shows observed rate constant values for the formation of acetonitritopentaammineruthenium(III) trifluoromethanesulfonate in double distilled dried sulfolane at 37°C. The acetonitrile was present in pseudo-first-order excess. The change of absorbance with time shows the reaction to be 1st order in pentaammineruthenium(III). Each individual reaction gave a fit of observed vs calculated optical density values with a correlation coefficient better than 0.99. A typical fit and associated parameters for the statistics are shown on (Figures 24a and 24b). The plot of rate constants as a function of $\text{Ru}(\text{NH}_3)_5(\text{CF}_3\text{SO}_3)^{2+}$ concentration demonstrates the reaction is also 1st order in acetonitrile. Likewise, reactions with all the ligands we've studied are also first order in ruthenium(III) concentration and in the ligand concentration.

Table I summarizes some kinetic data we have obtained for reactions of trifluoromethanesulfonatopentaammineruthenium (III) in tetramethylene sulfane solutions. The formation of 4-phenylpyridine has a rate constant of $0.19\text{M}^{-1}\text{s}^{-1}$ at 48°C.

Figure 25 shows the temperature dependence of the formation of 1-cyanoadamantane complex. The plot is given mainly to demonstrate that these reactions have a linear temperature dependence in the region studied. For this reaction the enthalpy of activation is 14.9kcal/mole and

Figure 24a. The fit for a typical kinetics run for the formation of acetonitrilopentaammineruthenium(III) from trifluoromethanesulfonatopentaammine-ruthenium(III) and acetonitrile in acidic sulfolane solution.



+ (OBSERVED VALUES)
— (FITTED VALUES)

Figure 24b. The table of parameters generated by the Prophet
computing system for the kinetics run of
Figure 24a.

LINEAR FIT TO:

COLUMN 1 VS COLUMN 4 OF STCK92

NUMBER OF DATA POINTS = 20

CORRELATION COEFFICIENT $R = -.9970806$ R-SQUARED = .9941698

STANDARD DEVIATION OF REGRESSION = .07637089

PARAMETER TABLE

PARAMETER	FITTED VALUE	STANDARD DEVIATION	T-VALUE	SIG. LEV.
INTERCEPT	.1120848	.0273079	4.104484	.0007
SLOPE	-.009012119	.0001626681	-55.40189	.0001

ANALYSIS OF VARIANCE TABLE

SOURCE	SUM OF SQUARES	D.F.	MEAN SQUARE	F VALUE	SIG. LEV.
REGRESSION	17.90214	1.	17.90214	3069.369	.0001
RESIDUAL	.1049852	18.	.005832513		

Figure 25. A plot of the observed first-order rate constant for formation of 1-adamantylcarbonitrilopentaamine-ruthenium(III) trifluoromethanesulfonate as a function of temperature.

$k,$
 $M^{-1} \text{min}^{-1}$
 $\times 10^2$

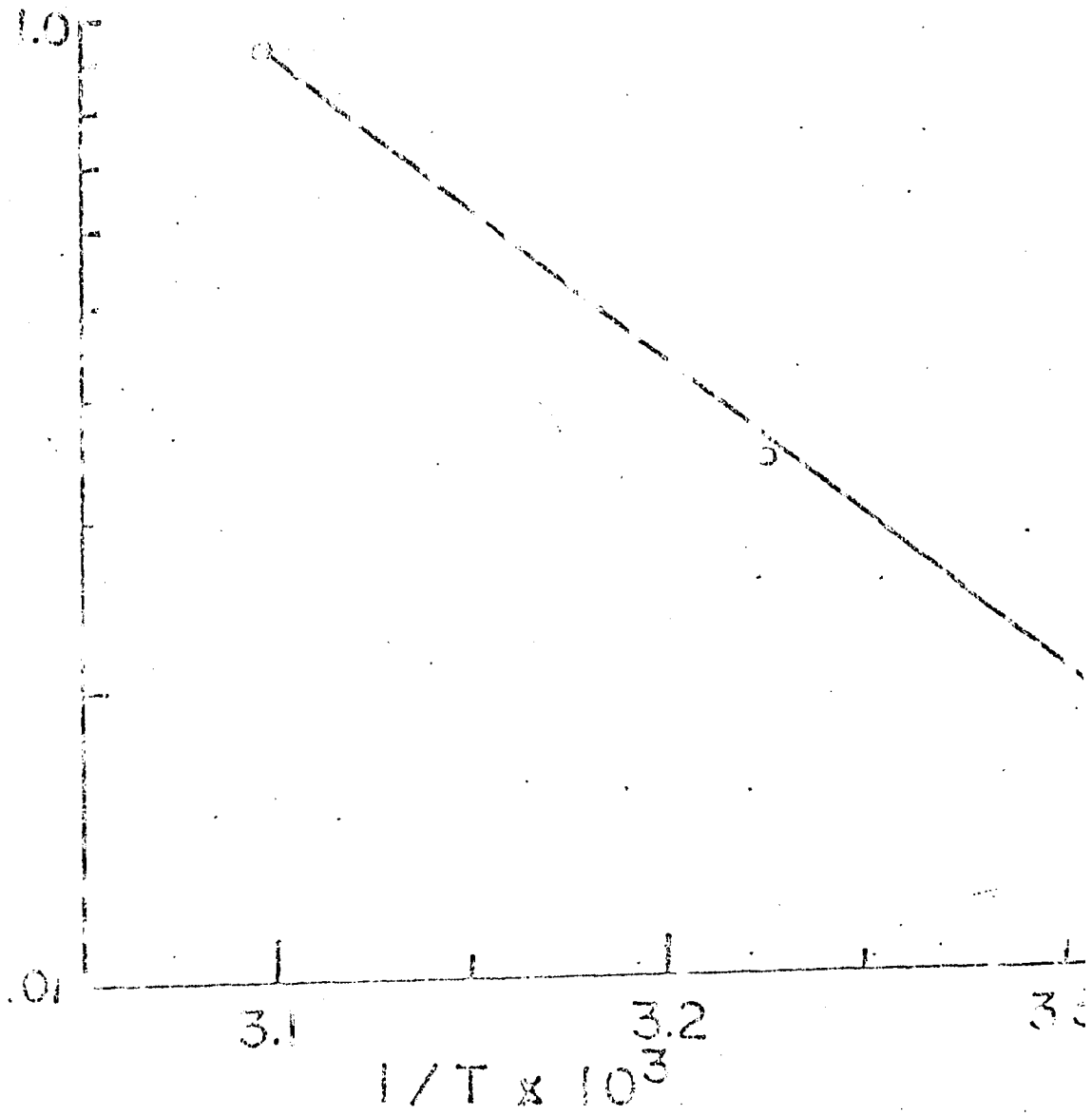


TABLE I

Rate Constants For Formation Of Complexes From

 $[\text{Eu}(\text{NH}_3)_5(\text{CF}_3\text{SO}_3)](\text{CF}_3\text{SO}_3)_2$ in Sulfolane

Temp., °C	Concentr., M	$k_{\text{obs}} \text{ s}^{-1} \times 10^2$	$k_{\text{2nd}} \text{ M}^{-1} \text{ s}^{-1}$
<u>CH₃CN</u>			
25	0.25	0.47	1.9×10^{-2}
25	0.25	0.49	2.0×10^{-2}
37	0.125	0.58	4.6×10^{-2}
37	0.125	0.74	5.9×10^{-2}
37	0.25	1.44	5.7×10^{-2}
37	0.25	1.52	6.1×10^{-2}
37	0.25	1.71	5.8×10^{-2}
37	0.25	2.40	9.6×10^{-2}
37	0.50	3.35	6.8×10^{-2}
37	1.00	5.97	6.0×10^{-2}
<u>adamantylcarbonitrile</u>			
28.6	0.125	0.227	1.8×10^{-2}
37	0.125	0.404	3.2×10^{-2}
50	0.125	1.17	9.4×10^{-2}
<u>Br⁻</u>			
30	0.0050	4.20	8.4
30	0.0050	2.93	5.9
30	0.020	13.9	7.0
30	0.020	13.4	6.7
30	0.040	20.7	7.2
30	0.040	28.1	7.0
40	0.0050	4.54	9.1
40	0.0050	5.15	10.0
50	0.0050	8.17	16.3
50	0.0050	8.44	16.9

the entropy of activation is - 5.7e.u., which are consistent with a dissociative interchange mechanism. A feature of the interchange mechanism is a five-coordinate intermediate. In a dissociative interchange mechanism, the key factor is the disengagement of the ligand and there is relatively small influence of the entering group on kinetics. The activation parameters for reaction of bromide ion are:
 $\Delta H^\ddagger = 8 \text{kcal/mole}$ and $\Delta S^\ddagger = -16 \text{cal/mole degree}$. These activation parameters are reasonable if ion-pairing dominates the reaction rate.

A comparison of the rate constant for acetonitrile, 1-adamantylcarbonitrile, and 4-phenylpyridine shows that these neutral ligands react at similar rates under comparable conditions, consistent with a dissociative interchange mechanism. The reaction with Br^- is considerably faster, likely as a result of favorable ion pair formation as might be expected if ion pairing precedes substitution.

The reaction with iodide ion is very much faster than the others studied. For example, at concentrations of 0.01M or even less, the reaction was complete on mixing. This reaction is too much faster than that of bromide ion to be accounted for by the same substitution mechanism. The very rapid reaction of iodide ion with the trifluoromethanesulfonato-ruthenium(III) complex is not unprecedented. Richardson and Taube have reported that the anation of trans-aquotetraammine-isonicotinamidoruthenium(III) by iodide ion proceeds via a rate law:

$$d \ln [\text{Ru(III)H}_2\text{O}] = k_a [\text{I}^-]^{5/2} [\text{I}_3^-]^{1/2} + k_a [\text{I}^-]^2$$
 and that the rate is much faster than those for the anation by bromide ion and chloride ion, which follow kinetics that are each first-order in anion concentration (12). Richardson and Taube interpret the rate law in terms of a reduction of Ru(III) by I^- to Ru(II) and subsequent rapid substitution (the k_a term) and a presubstitution electron transfer not involving the production of free iodine (the k_b term). Previously Marchant, Matsubara and Ford noted that substitution of I^- for SO_4^{2-} in $\text{trans-Ru(NH}_3)_4(\text{py})\text{SO}_4^+$ did not require addition of a reducing agent, in contrast to reactions involving Cl^- or Br^- (55). They also attributed their results to the ability of I^- to reduce Ru(II) to produce a labile Ru(II) intermediates (55). Unfortunately, catalytic substitution of $\text{Ru(NH}_3)_5(\text{CF}_3\text{SO}_3)^{2+}$ in the presence of I^- does not appear to be useful synthetically because the I^- coordinates preferentially in the presence of other potential ligands (ie in the presence of excess CH_3CN , $[\text{Ru(NH}_3)_5\text{I}]^{2+}$ is formed predominantly).

$[\text{Ru(NH}_3)_5(\text{CF}_3\text{SO}_3)]^{2+}$ can be readily made is stable for months when stored in a dessicator over P_2O_5 . This is a useful intermediate for the direct preparation of a variety of Ru(III) complexes.

The rates of formation of complexes using trifluoromethanepentaammineruthenium(III) that we have found are

several orders magnitude factor than those reported for other pentaammineruthenium(III) precursors. The well-behaved nature of the kinetics of formation for complexes using the trifluoromethanesulfonate complex in sulfolane should make it possible to study the reaction mechanism of Ru(III) complexes more thoroughly than has been possible.

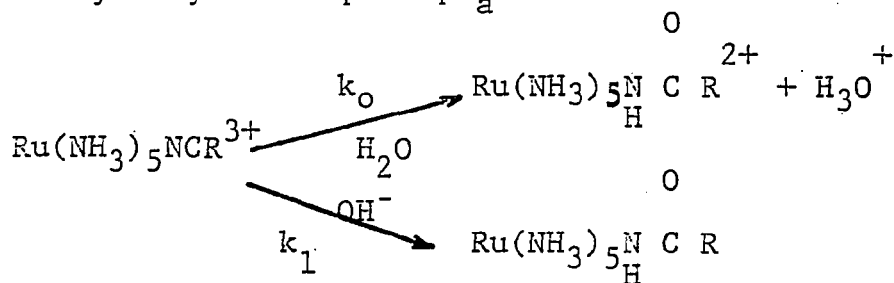
3. Kinetics of Nitrile Hydrolysis

The results of the kinetic studies of the decomposition reactions of organonitrile complexes of Ru(III) in 0.0005M aqueous trifluoromethanesulfonic acid are given in the table II. The acid hydrolysis reactions studied were those of pentaammineruthenium(III) complexes of acetonitrile, benzonitrile and 1-adamantylcarbonitrile. Previous work indicated no base-independent hydrolysis path. In our work we have found there is a base independent hydrolysis path. Since the lowest concentration of hydroxide used in previous studies was 10^{-6} M, it is not unreasonable that the acid hydrolysis path for Ru(III) organonitrile complexes was not previously detected. The rate law for the hydrolysis of ruthenium(III) organonitrile complexes we have found is:

$$-d \ln [\text{Ru}(\text{NH}_3)_5\text{NCR}]^{3+} / dt = k_0 + k_1 [\text{OH}^-]$$

As can be seen in table II, the hydrolysis of ruthenium(III)organonitriles is acid and ionic strength independent. As is evident from these tables, we varied the acid concentration by 100-fold and the rate was the same, 4×10^{-5} /sec. Then we varied the ionic strength by 5-fold and the rate was the same, 4×10^{-5} /sec. The acid hydrolysis of the pentaammineruthenium(III) complexes of different nitriles showed similar hydrolysis rates of about 10^{-5} /sec, with only slight variations for different ligands - these results are sufficiently general that we can use it to predict

other nitrile rates. The purpose of studying the effect of changes in acid concentration and ionic strength was to demonstrate that the reaction in acidic solutions does not involve hydroxide ion as the attacking nucleophile. The independence of the rate constant on acid concentrations and ionic strength indicate the attack of an uncharged nucleophile the water molecule. Table IV shows the absorption maxima and extinction coefficients for amide complexes of pentaammineruthenium(III). The u.v.-visible spectral changes are pronounced and are characteristic of the conversion of the nitrile to the amide (57,58). We find the same spectral changes for the acetonitrile and benzonitrile complexes as previously reported and the changes for the 1-adamantylcarbonitrile complexes is very similar to that for the acetonitrile complex. In the experiment at an acid concentration of the protonated amide complex, consistent with the pK_a of 2.00 previously reported by Zanella and Ford (52). The rate constant to produce this product is the same as that for the unprotonated coordinated amide (produced at 1.0×10^{-3} and 5.0×10^{-3} M acid) as expected for protonation as a rapid step subsequent to hydrolysis. The reaction sequence for organonitrile hydrolysis at $pH \gg pK_a$ is:



All the runs were done in duplicate for the three different compounds at the three different temperature. The data were calculated using Prophet 65. All these reactions show excellent first-order behavior (typical correlation coefficients of 0.999 and standard deviation of individual data points of less than 0.001 absorbance units). The next plot shown (Figure 26) is the acid hydrolysis of acetonitrile complex at 25^o C. This is a typical plot I obtained by letting Prophet fit absorbance vs time data.

The activation parameters for the acid hydrolysis path of the ruthenium(III) organonitrile complexes shown in table V are similar to one another. There does appear to be a significant compensation of more favorable ΔH^\ddagger values by less favorable ΔS^\ddagger values, as expected for reactions with the same mechanism, especially in cases where bond formation is important.

The relative rates for the benzonitrile, acetonitrile and 1-adamantylcarbonitrile reactions (table II) are consistent with the idea previously advanced for the base hydrolysis reactions (51,52), ie. that the metal atom catalyzes hydrolysis by withdrawing electron density from the nitrile group when the nucleophile attacks and that substituents on the nitrile group can retard the reaction by donating electron density. As previously found for the base hydrolysis reactions, the acid hydrolysis of organonitriles coordinated to Co(III) and Ru(II) appears to be much slower.

With regard to their use for the study of electron transfer reactions, the organonitrile complexes of ruthenium(III) are sufficiently stable toward hydrolysis. The rate of hydrolysis of the ruthenium(III)-nitrile moiety can be predicted quite readily and the extent of the reaction can be monitored readily from the visible absorption spectrum of the complex. The half-lives of such reactions at 25° C are sufficiently long to allow sample preparation without unacceptable loss of concentration of the desired nitrile complex. Upon reduction to Ru(II), the hydrolysis is greatly retarded (by a factor of at least 10^6 for the base hydrolysis path and hydrolysis by a base-independent path has not been detected at all), posing no significant limitations to the study of the reactions of bimetallic complexes composed of ruthenium(II) and cobalt(III).

Figure 26. A typical plot of the optical density vs. time for the acid hydrolysis reaction of acetonitrilopentaammineruthenium(III) trifluoromethanesulfonate in aqueous trifluoromethanesulfonic acid (0.005M) at 25° C. The solid line is calculated for first-order dependence with an observed rate constant of $1.24 \times 10^{-5} \text{ s}^{-1}$.

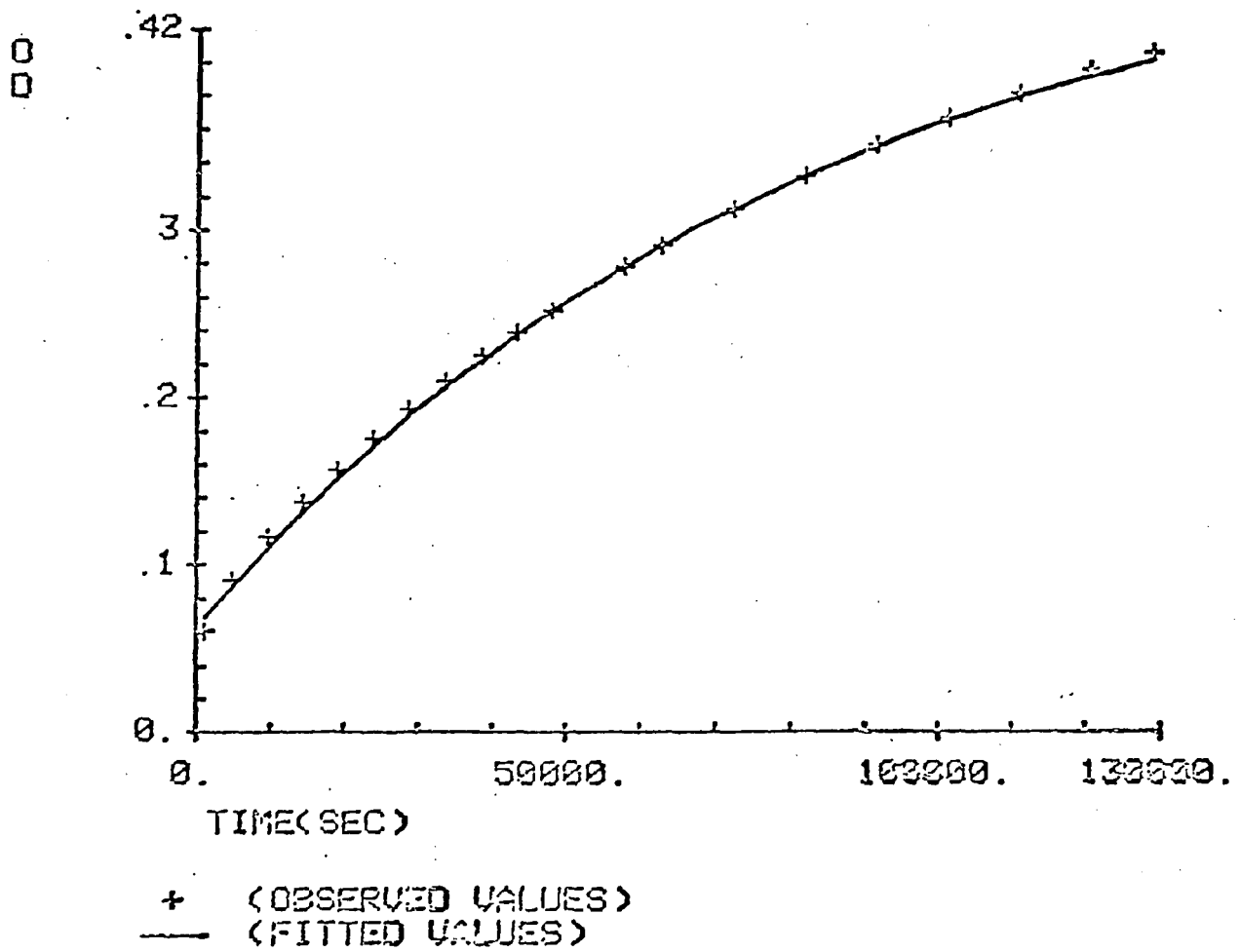


TABLE II Kinetic Results for the Acid Hydrolysis of Organonitrile Complexes of Ru(III) in 0.005 M Aqueous Trifluoromethanesulfonic Acid

<u>Complex</u>	<u>Temperature (°C)</u>	<u>Rate Constant (s⁻¹)</u>
Ru(NH ₃) ₅ NCCH ₃ ³⁺	25.0	(1.24 ± 0.02) × 10 ⁻⁵
	37.0	(4.85 ± 0.22) × 10 ⁻⁵
	50.0	(1.83 ± 0.13) × 10 ⁻⁴
Ru(NH ₃) ₅ NCC ₆ H ₅ ³⁺	25.0	(3.39 ± 0.05) × 10 ⁻⁵
	37.0	(1.24 ± 0.01) × 10 ⁻⁴
	50.0	(4.39 ± 0.08) × 10 ⁻⁴
Ru(NH ₃) ₅ NC adamantane ³⁺	25.0	(7.20 ± 0.15) × 10 ⁻⁶
	37.0	(2.90 ± 0.02) × 10 ⁻⁵
	50.0	(1.25 ± 0.03) × 10 ⁻⁴

TABLE III. Kinetic Results for Acid Hydrolysis of $[\text{Ru}(\text{NH}_3)_5\text{NCCH}_3]^{3+}$ at Various Acid Concentrations and Ionic Strengths^a.

<u>Acid Concentration (M)</u>	<u>Rate Constant (s^{-1})</u>	<u>Ionic Strength (M)</u>	<u>Rate Constant (s^{-1})</u>
1.0×10^{-3}	4.15×10^{-5}	0.0267	4.23×10^{-5}
5.0×10^{-3}	4.13×10^{-5}	0.0517	4.22×10^{-5}
100×10^{-3}	4.31×10^{-5}	0.103	4.22×10^{-5}

a. at 37.0°C

TABLE IV. Absorption Maxima and Extinction Coefficients for Amido Complexes of Pentaammineruthenium (III)

<u>Complex</u>	<u>λ_{max} (nm)</u>	<u>ϵ (cm^{-1})</u>
$\text{Ru}(\text{NH}_3)_5(\text{CH}_3\text{CONH})^{2+}$	383	3.5×10^{3a}
	249	2.3×10^{3a}
$\text{Ru}(\text{NH}_3)_5(\text{CH}_3\text{CONH}_2)^{3+}$	322	1.6×10^{3a}
$\text{Ru}(\text{NH}_3)_5(\text{C}_6\text{H}_5\text{CONH})^{2+}$	393	4.0×10^{3a}
	314	3.7×10^{3a}
$\text{Ru}(\text{NH}_3)_5(\text{C}_{10}\text{H}_{15}\text{CONH})^{2+}$	388	3.6×10^3
	276	2.4×10^3

a. Reference 2.

TABLE V. Activation Parameters for the Acid Hydrolysis of Pentaammineruthenium (III) Organonitrile Complexes

<u>Complex.</u>	ΔS^\ddagger (Kcal/mol)	ΔS^\ddagger (e.u.)	ΔG^\ddagger (298°, kcal/mol)
$\text{Ru}(\text{NH}_3)_5\text{NCCH}_3^{3+}$	20.4 ± 0.1	-12.5 ± 0.1	24.1
$\text{Ru}(\text{NH}_3)_5\text{NCC}_6\text{H}_5^{3+}$	19.0 ± 0.2	-15.2 ± 0.3	23.5
$\text{Ru}(\text{NH}_3)_5\text{NCadamantane}^{3+}$	21.2 ± 0.3	-10.9 ± 0.3	24.4

Literature Cited

1. Chance, B., in "Tunneling in Biological Systems", Chance, B., ed., 1979, Academic Press, New York, pp 483-58.
2. Moorke, J.R. and Beitz, Jr., in "Tunneling in Biological Systems", Chance, B., ed., 1979, Academic Press, New York, 1979, pp. 269-280.
3. Hopfield, J.J., Proc. Natl. Acad. Sci. USA, 1974, 71, 3640.
4. Chien, J.C.W. J. of Phys. Chem. 1978, 82, 2158.
5. Miller, J.R. "Tunneling in Biological Systems", Chance B.; ed.; 1979, Academic Press: New York, (1979); p 95.
6. Vandeskooi, Mary; Ercinska, M., Eur. J. of Biochem., 1975, 60, 199.
7. Mead, C.A. "In Tunneling Phenomena in Solids" (Burstein, E. and Lundquist, S., eds.,) 1969, Plenum, New York, pp. 127-134.
8. Furtin, S.L.; McGill, T.C.; Mead, C.A. Phys. Rev., 1971, 83, 3369.
9. Weismann, S.I., J. Amer. Chem. Soc., 1958, 80, 6462.
10. Voevodskie, V.V.; Solodovnikov. S.P.; Chibrikin, V.M., Dokl Akad Nauk SSSR, 1959, 129, 1082.
11. Basolo, F.; Pearson, R.G., "Mechanisms of Inorganic Reactions", 2nd Ed., 1967, John Wiley and Sons, New York.
12. Taube, H., Advan. Inorg. Chem. Radiochem., 1, 1.
13. Marcus, R.A., J. Phys. Chem., 1979, 83, 204.

14. Marcus, R.A., Sutin, N., Inorg. Chem., 1975, 14, 2136.
15. Marcus, R.A., J. Phys. Chem., 1956, 24, 966.
16. Hush, N.A., Prog. Inorg. Chem., 1967, 8, 391.
17. Meyer, T.J., Accts. Chem. Res., 1978, 11, 94.
18. Wherland, S.; Cary, H. in "Biological Aspects of Inorganic Chemistry", David Dolphin, ed. 1982, John Wiley and Sons, New York, pp 290-368.
19. Bennett, L.I., Prog. Inorg. Chem., 1973, 18, 1.
20. Wilkins, R.G., "The Study of Kinetics and Mechanism of Reactions of Transition Metal Complexes", 1974, Allyn and Bacon, Boston.
21. Sutin, N., "Inorganic Biochemistry", G.L. Eichorn, ed., 1975, Elsevier, New York, p. 611.
22. Forster, T., "Naturwissenschaften", 1946, 33, 166.
23. Jortner, J., J. Chem. Phys., 1976, 64, 4860.
24. Katz, J.J.; Choi, S.I.; Rice, S.A.; Jortner, J., J. Chem. Phys., 39, 1683.
25. Kreitman, M.M.; Hamaker, F., J. Chem. Phys., 1967, 45, 2396.
26. Isied, S.; Taube, H., J. Am. Chem. Soc., 1973, 95, 8198.
27. Endicott, J.; Lillie, J.; Kosgaj, J.M.p Ranaswamy, B.S.; Schmonsees, W.G.; Simic, M.G.; Glic, M.D.; Rillema, D.P., J. Am. Chem. Soc., 1977, 99, 429.
28. Glick, M.P.; Schmonsees, W.G.; Endicott, J.J., J. Am. Chem. Soc., 1974, 96, 5661.

29. Anderes, B.; Collins, S.; Lavalley, D.K., 1982, Abstract INOR-15, 184th meeting of A.C.S., Kansas City, Mo. and submitted for publication.
30. Lavalley, D.K., Anderes, B., Inorganic Chemistry, in press (1983).
31. Calcaterra, J.T.; Closs, G.L.; Miller, J.R., J. Amer. Chem. Soc., 1983, 105, 672.
32. Isied, S.S.; Wonosila, G.; Atherton, S., J. Am. Chem. Soc., 1982, 104, 7569
33. Zawacky, S.K.S.; Taube, H., J. Am. Chem. Soc., 1981, 103, 3379.
34. a) Jordan, R.B.; Sargeson, A.M.; Taube, H., Inorg. Chem., 1966, 5, 1091
b) Buckingham, D.A.; Francis, D.J.; Sargeson, A.M.; J. Amer. Chem. Soc., 1971, 93, 625.
c) Clark, R.E.; Ford, P.C., Inorg. Chem., 1970, 9, 227.
35. Ford, P.C.; Matsubara, T.A. Inorg. Chem., 1976, 15, 1107.
36. Marcus, R.A., Ann. Rev. of Phys. Chem., 1964, 15, 155.
37. Taube, H., 182nd Nat. Meeting of the American Chem. Soc., New York, N.Y. 1982.
38. Endicott, J.F.; Schroeder, R.R.; Chisester, D.H.; Ferrier, D.R., J. Phys. Chem., 1973, 77, 2579.
39. Meyer, T.J.; Taube, H., Inorg. Chem., 1968, 7, 2369.
40. Marcus, R.A.; Siders, P., J. Phys. Chem., 1983, 86, 622.

41. The 4 Å distance is that in excess of the van der Waals radius of the carbon atom of the nitrile group. Since the comparison being made is with intermolecular reactions of Ru(II) and Co(III) complexes with intact first coordination spheres, only the additional distance and not the entire metal-to-metal separation is the relevant value for R.
42. Dixon, N.E.; Jackson, W.G.; Lancaster, J.J.; Lawrance, G.A.; and Sargeson, A.M., Inorg. Chem., 1981, 20, 470.
43. Ford, P.C.; Rudd, De F.P.; Gaunder, R.; Taube, H., J. Am. Chem. Soc., 1968, 90, 1187.
44. Isied, S.S.; Taube, H., J. Am. Chem. Soc., 1973, 95, 8198.
45. Creutz, C.; Taube, H., J. Am. Chem. Soc., 1969, 91, 3988.
46. Diamond, S.E. Tom, G.M.; Taube, H., J. Am. Chem. Soc., 1975, 97, 2661.
47. Ford, P.C., Coor. Chem. Rev., 1970, 5, 75.
48. Broomhead, J.A.; Basolo, F.; Pearson, R.G., Inorg. Chem. 1964, 3, 826.
49. Eliades, T.; Harris, R.O.; Reinsalu, P., Can. J. Chem., 1969, 47, 3823.
50. Swaddle, T., Can. J. Chem., 1977, 55, 3166; Coord. Chem. Rev., 1974, 14, 217 and Inorg. Chem., 1980, 19, 3203.
51. Buckingham, D.A.; Keene, R.R.; Sargeson, A.M., J. Am. Chem. Soc., 1973, 95, 5649.
52. Zanella, A.W.; Ford, P.C., Inorg. Chem., 1975, 14, 42.
53. The PROPHET system is a multisite interactive network with a wide essay of statistical and simulation programs. The Hunter College facility was founded through a generous grant from the N.I.H.

54. Richardson, D.E.; Taube, H., Inorg. Chem., 1979, 18, 549.
55. Marchant, J.A.; Matsubora, T.; Ford, P.C., Inorg. Chem. 1977, 16, 2160.
56. Broomhead, J.A., Kane-Maguire, L., Inorg. Chem., 1968, 7, 2519 .
57. Clarke, R.E.; Ford, P.C., Inorg. Chem., 1970, 9, 222.
58. Coleman, G.N.; Gesler, J.W.; Shirley, F.A.; Kuempel, J.R., Inorg. Chem., 1973, 12, 1036.